MECHANISM OF ALPHAVIRUS RESTRICTION BY THE INTERFERON-INDUCED EXONUCLEASE, ISG20

by

Christopher Michael Weiss

Bachelor of Science, University of Pittsburgh, 2011

Submitted to the Graduate Faculty of

School of Medicine in partial fulfillment

of the requirements for the degree of

Doctor of Philosophy

University of Pittsburgh

2017

UNIVERSITY OF PITTSBURGH

SCHOOL OF MEDICINE

This dissertation was presented

by

Christopher Michael Weiss

It was defended on

June 15, 2017

and approved by

William B. Klimstra, Associate Professor, Microbiology and Molecular Genetics

Carolyn B. Coyne, Associate Professor, Microbiology and Molecular Genetics

Saumendra N. Sarkar, Associate Professor, Microbiology and Molecular Genetics

Yoel Sadovsky, Professor, Microbiology and Molecular Genetics

Patrick H. Thibodeau, Assistant Professor, Microbiology and Molecular Genetics

Dissertation Advisor: William B. Klimstra, Associate Professor, Microbiology and

Molecular Genetics

MECHANISM OF ALPHAVIRUS RESTRICTION BY THE INTERFERON-INDUCED EXONUCLEASE, ISG20

Christopher Michael Weiss

University of Pittsburgh, 2017

MECHANISM OF ALPHAVIRUS RESTRICTION BY THE INTERFERON-INDUCED EXONUCLEASE, ISG20

Christopher Michael Weiss

University of Pittsburgh, 2017

Type I interferon-stimulated genes (ISGs) have critical roles in inhibiting virus replication and dissemination. Despite advances in understanding of the molecular basis of restriction by ISGs, the antiviral mechanisms of many remain unclear. The 20 kDa ISG, ISG20, is a nuclear 3'-5' exonuclease with preference for ssRNA, which has been implicated in the IFN-mediated restriction of several RNA viruses. While the exonuclease activity of ISG20 has been shown to degrade viral RNA *in vitro*, these findings have not been reconciled with proposed effects of ISG20 against RNA viruses that replicate in the cell cytoplasm. In the present study, we utilize a combination of an inducible, overexpression system for murine ISG20 and *Isg20*$^{-/-}$ mice to investigate mechanisms and consequences of ISG20-mediated restriction of alphaviruses. Overexpressed ISG20 primarily localized to Cajal bodies in the nucleus and potently restricted chikungunya virus and Venezuelan equine encephalitis virus replication by inhibiting the translation of infecting genomic RNA. However, degradation of viral RNAs was not observed. Translation inhibition was associated with an ISG20-induced upregulation of over 100 other gene products, many of which possess known antiviral activity. ISG20-responsive gene upregulation correlated with IRF3 activity among other transcription factors. Importantly, ISG20 modulated the production of IFIT1, an ISG that suppresses translation of RNAs possessing the type-0 5' cap structure such as the alphavirus genome. Consistent with this, the replication and virulence of IFIT1-sensitive alphaviruses was significantly increased in *Isg20*$^{-/-}$ compared to congenic wild-type mice. Our findings establish an indirect role for ISG20 in the early restriction of RNA virus replication by altering regulation of other ISGs that inhibit virus translation and possibly other viral activities in the replication cycle.

iv

TABLE OF CONTENTS

LIST OF TABLES

LIST OF FIGURES

PREFACE

This work is dedicated to the life and scientific career of Dr. Kate Ryman, my PhD mentor, whose untimely passing touched all of us who knew her. In the time I was privileged to study under her mentorship, Kate not only taught me how to question everything as a scientist, but also to view even the most discouraging data with curiosity and press on with impunity.

It is also necessary here to recognize the impact of the many individuals in my life who helped shape my educational endeavors and pursuit of a career in science. While I leave many names unmentioned, I would like to thank my parents, Frank and Patti for raising me to shoot for the stars and settle for nothing less. I couldn't have done any of this without you. I would also like to recognize my brother, Robert. You were the best role model a little brother could hope for, and inspired me to always push myself a little harder. Additionally, I would like to thank my wonderful fiancé, Raven, whose unwavering support and editorial input made this work possible. Thank you to all my family and those close to me for shaping me into the individual I am today.

Lastly, I would like to recognize Dr. William Klimstra's outstanding mentorship and the excellent technical assistance provided by all my peers in Dr. Klimstra's laboratory. However, I would like to pay special recognition to our lab manager, Matthew Dunn, our animal husbandry and breeding specialists, Chelsea Maksin and Nicolas Garcia, and Drs. Derek Trobaugh, Christina Gardner and Alan Watson, who provided expertise for various BSL-3 and ABSL-3 techniques throughout my project. Thank you all for your contributions and mentorship.

1.0   INTRODUCTION

Viruses face significant challenges when infecting higher eukaryote hosts. Co-evolution of viruses and their host species has given rise to numerous host factors that act to restrict the replication and spread of the invading virus, while the viruses themselves have developed methods to evade these acquired responses to infection. Two primary systems exist to restrict virus propagation and dissemination and eventually clear the invading organism. The first hurdle faced by an invading pathogen is the innate immune response, which consists of a series of non-specific responses induced by recognition of non-self antigens. These responses may be cellular in nature, such as the killing action of natural killer cells and macrophages, or may be cytokine directed, such as the multi-targeted approach of the interferon response. In addition to these nonspecific responses, which serve to slow the advance of invading pathogens, an adaptive immune response is primed and directed to recognize and clear the invading pathogen utilizing pathogen-specific epitope recognition. These adaptive responses take longer to develop after the initial encounter with a pathogen, but typically establish pools of memory cells that can rapidly expand and clear infection more efficiently in the event of subsequent encounters with a serologically identical pathogen.

1.1   ALPHAVIRUSES

Viruses in the family Togaviridae, genus alphavirus, have members known to infect many Orders of the animal kingdom. Many of these are arthropod-borne viruses (arboviruses), with a natural transmission cycle alternating between a reservoir species and an arthropod vector, typically mosquitoes. Of particular interest, numerous alphaviruses are known to cause disease in humans, either as a transmission-competent or dead-end host. Those alphaviruses known to cause disease in humans are grouped based on their historic geographic distribution, either as Old World or New World strains. While the geographic distribution tended to be restricted to their continent of origin, the continuing globalization and interconnectedness of human populations and vector-adaptive mutations to the viruses themselves has led to a spread of these viruses, particularly chikungunya virus, to a pandemic scale. Thus, it is prudent to group these more accurately under the type of disease caused, either arthritogenic or encephalitogenic. The historic Old World alphaviruses are known to cause arthritic disease, with the prototypic examples being Sindbis virus, chikungunya virus, Ross River virus and Semliki Forest virus. New World alphaviruses instead cause encephalitic disease and include eastern equine encephalitis virus, Venezuelan equine encephalitis virus, and western equine encephalitis virus, all of which are pathogens of interest to the Department of Defense due to the potential for misuse as bioweapons.

1.1.1   Alphavirus Structure

1.1.1.1 Genome Organization

The alphavirus genome (**Figure 1**) consists of a single positive-sense RNA molecule between 11 and 12 kilobases in length (1). The genome is capped with a type-0 7-methylguanosine-ppp cap at

the 5' terminus – that is, it lacks a 2' o-methylation of the terminal ribonucleotide present in most vertebrate RNAs (2-4). The 5'-non-translated Region (NTR) consists of considerable secondary structure and two conserved sequence elements, both facilitating cap-dependent translation of the viral RNA while reducing the exposure of the non-standard mRNA cap structure, and acting as a promoter for RNA synthesis (3, 5, 6). The terminal stem loop also plays a crucial role in evading IFIT1-mediated cap recognition of VEEV, simply by limiting access to the terminal nucleotide overhang (3, 7). Secondary stem-loop structures, which are essential for efficient genomic translation, continue through the entire 5'-NTR and the start of the nonstructural gene coding sequence (8, 9).

The non-structural genes are arranged as a single open reading frame coding for the replicase proteins, nsP1, nsP2, nsP3, and nsP4 in sequential order (10). The alphavirus genome encodes an opal stop codon between nsP3 and nsP4, which requires a read-through event to translate the full nonstructural polyprotein (11-13). Immediately following the nonstructural open reading frame is an approximately 40-60 nucleotide junction coding for a sub-genomic promoter on the negative-sense replicative intermediate RNA (10). Flanking the sub-genomic promoter region is another polyprotein open reading frame that is produced as a 26S RNA late in the replication cycle and consists of the structural gene products, capsid, E3, E2, 6K, and E1 (10).

The 3'-NTR of the alphavirus genome varies significantly in length between individual alphavirus species, as short as 100 nucleotides in VEEV to over 700 nucleotides in some strains of CHIKV, and likewise the secondary structures also vary considerably between viruses (1). A common feature in the 3'-NTR is the presence of additional conserved sequence elements, which are often duplicated and play a major role in virus replication by promoting negative strand

3

synthesis (8, 9, 14). Notably, the NTR secondary structure gives rise to genomic RNA stability and potentially resistance from cellular degradation pathways.
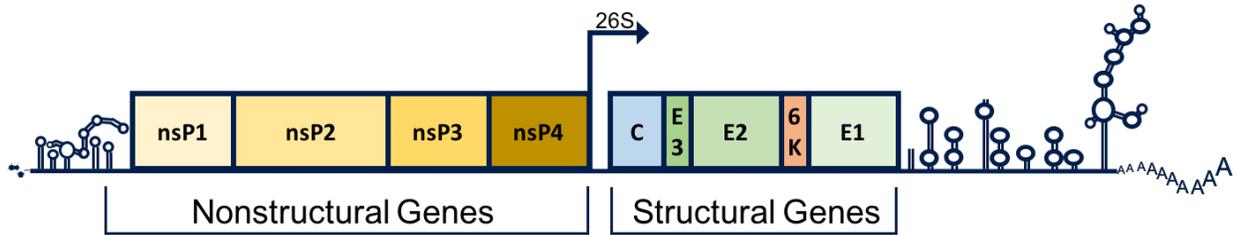
Figure 1: Chikungunya Virus Genome.

Schematic representation of the chikungunya virus genome as a prototypic alphavirus depicts organization of the 49S genomic RNA with the replicative intermediate promoter site for the 26S sub-genomic RNA annotated. Predicted NTR structures, as calculated by mfold v.2 for East/Central/South African clade lineage CHIKV, are included.

1.1.1.2 Gene Products

The alphavirus genome codes for nine in-frame gene products and one additional protein resulting from an inefficient frame shift during translation of the 6K protein sequence. These gene products are characterized as either structural proteins, producing the essential components for the core virion particle and its assembly, or the nonstructural genes involved in replication. The non-structural proteins are produced as a single open reading frame, forming nsP123 or nsP1234, which results from the read-through of an opal stop codon present in most alphavirus genomes (11, 15). The cleavage of the nonstructural proteins by nsP2 is temporally regulated and dependent on the molar concentration of existing cleavage products of the nonstructural polyprotein (16-18). Processing of the structural polyprotein is carried out by a combination of cellular factors as well as an autoproteolysis event carried out by nascent capsid protein (1).

The nonstructural proteins function primarily to form the replicase complex required for RNA genome replication and production of the 26S subgenomic RNA. The alphavirus nsP1 encompasses two known activities, a guanine-7-methyltransferase domain and guanyltransferase

4

domain for capping the positive-strand genomes (19-23). In addition to these known enzymatic activities, nsP1 serves as an anchor for the replicase complex to cellular membranes through a conserved palmitoylated residue (24-27).

The nsP2 protein contains an RNA helicase domain in the N-terminal region, which functions to unwind double-stranded RNA regions during replication and transcription (28-30). Additionally, nsP2 contains RNA triphosphatase activity and has a catalytically-inactive methyltransferase domain that is thought to contribute to cytotoxicity within the host cell (31). Notably, nsP2 contains a cysteine protease domain with a unique fold that recognizes the three cleavage sites for the nonstructural proteins (32-34). The protease specificity is dependent on the molar concentration of the various nonstructural polyprotein intermediates or fully processed proteins (34). Beyond its role in polyprotein processing, nsP2 has also been suggested to act as a transcription factor for the synthesis of the subgenomic RNA (32, 35, 36). Of the nonstructural proteins, nsP2 is the only one to contain nuclear localization signals, and, with certain alphaviruses, up to 50% may be found in the nucleus (37-39). Within the nucleus, nsP2 disrupts macromolecular synthesis as a potent inhibitor of cellular innate antiviral responses (40-45).

The activity of alphavirus nsP3 is not well characterized, though it does play an essential role in minus strand and 26S sub-genomic RNA synthesis (32, 46). A conserved macro domain is present in the N-terminal region of all alphavirus nsP3 proteins, which contains ADP-ribose phosphatase activity (47-51). The C-terminal domain of nsP3 is not well conserved between species, and varies considerably in length (52, 53). One constant feature in this region is the hyperphosphorylation of serine and threonine residues, leading to RNA binding characteristics, which may provide insight into its involvement in RNA synthesis (54, 55). Importantly, the non-conserved regions of nsP3 have played a significant role in developing molecular tools to study

5

the alphaviruses. nsP3 is tolerant to large insertions, allowing for the inclusion of fluorescent and bioluminescent proteins, including enhanced green fluorescent protein and its derivatives, or ATP-independent enzymes like nano-luciferase (56-60). Insertions in the nsP3 protein may last many rounds of replication before reversion and are only mildly attenuating to overall alphavirus growth (56).

RNA-dependent RNA polymerase activity lies within the alphavirus nsP4 (32, 61). Cellular levels of nsP4 are highly regulated during alphavirus replication through the inclusion of an opal stop codon between nsP3 and nsP4 requiring an infrequent read-through event during translation in most alphavirus genomes (11). Additionally, an N-terminal tyrosine residue allows for accelerated degradation kinetics through the N-end rule of the cellular ubiquitin-degradation pathway, leading to a shorter half-life and reduced accumulation of nsP4 as well as functional replicase complex in infected cells (62). This tight regulation of nsP4 concentration is required for efficient virus replication, with alphavirus mutants that express nsP4 more efficiently showing attenuated replication kinetics *in vitro* (63).

The subgenomic message transcribed from the alphavirus genome codes for the five canonical structural proteins and the transframe protein. The capsid protein is the structural component that forms the viral core particle, enclosing the RNA genome. Capsid contains a self-proteolytic activity, and in the New World alphaviruses, is shuttled to the nuclear pore of infected cells (64, 65). New World alphavirus capsid protein has been suggested to play a role in macromolecular synthesis inhibition by blocking the nuclear pores in mammalian cells (43, 66-68). After capsid, the three glycoproteins, E3, E2, and E1, are encoded in that order, with 6K encoded between E2 and E1. The E3 portion of pE2 functions primarily to aid in the folding and trafficking of E2 and the assembly of the glycoprotein spike structures, and is not incorporated in

6

the final virion particle (69-71). The mature E2 acts as the receptor binding protein, and exposes E1 upon cell entry (72-74). E1 serves as the membrane fusion protein, creating a pore through which the capsid is released into a newly infected cell (75-77). The alphavirus 6K protein is essential for proper spike formation on the final virion and likely plays a role in virus budding from infected cells (78-81). The most recently discovered alphavirus protein, the transframe protein, results from a frameshift extension during the translation of 6K and may play an additional role to that of 6K in the assembly of virus particles and virulence *in vivo* (82).

1.1.1.3 Virion Structure

The alphavirus virion is composed of an icosahedral capsid filled with a single copy of the full-length positive-sense ssRNA genome. The capsid particle is surrounded by a host-derived lipid envelope studded with tightly arranged heterotrimers of the alphavirus glycoproteins, E1 and E2, plus trace amounts of 6K and transframe protein (1, 82-87). The capsid is composed of 240 copies of the capsid protein arranged as tetramers and hexamers forming the observed icosahedral particle arrangement with a triangulation number of 4 (88-90).

1.1.2   Alphavirus Transmission/Replication Cycle

Most alphaviruses can be classified in a broader group of viruses called arboviruses, referring to a lifecycle in which the virus propagates through an invertebrate arthropod host, and a natural vertebrate reservoir. An arthropod vector, typically a mosquito species, picks up the virus during a bloodmeal from a viremic vertebrate host. The virus crosses the midgut and replicates in the vector salivary glands to high titer and is transmitted subcutaneously in the infected mosquito's saliva to a naïve host.

Once in a competent host, cellular replication of the alphaviruses begins with receptor recognition and endocytosis of the virus particle (91). Endosomes progress through the lysosomal pathway, triggering an acidification event of the vesicle contents, including the bound virus particle. This acidification event triggers a conformational change in the E1-E2 heterotrimer on the particle surface, exposing a membrane binding motif in the E1 glycoprotein, which allows envelope fusion with the acidified endosome (92). E1 protein homotrimerizes after fusion and forms cation exchange channels, elevating the pH of the cytoplasm in the immediate vicinity of the endosome (76, 93). The nucleocapsid core is released into the cytoplasm where the locally elevated pH facilitates the disassembly of the capsid and release of the positive-sense genome (94-96). Stem-loop structures present in the 5'-NTR of the alphavirus genome prime interactions with cellular cap-dependent translation machinery, and initiate immediate translation of the viral RNA (91).

A polyprotein forming three or four individual non-structural cleavage products, nsP123 and nsP1234, is produced from the genomic RNA from the initial translation event, depending on read-through of an opal stop codon (UGA) present at the end of nsP3 (1, 11-13, 15). The unprocessed polyprotein proceeds with three cleavage events mediated by the protease domain of nsP2 (33, 34, 64). The first event is the cleavage of nsP4 from nsP123, releasing the RNA-dependent RNA-polymerase (RdRp) (16). The nsP4-nsP123 complex is responsible for the replication of the positive-sense genome to a negative-sense replicative intermediate that will serve as a platform for positive strand synthesis and later, structural gene sub-genomic RNA synthesis (16-18, 97-99). Further cleavage of the nsP123 by the nsP2 protease results in a release of the nsP1 methyltransferase/guanyltransferase capping enzyme (16, 18, 100). The complex of nsP1-nsP23-nsP4 starts shifting virus polymerase activity toward production of progeny positive-sense

genomes plus a positive-sense 26S sub-genomic RNA, which codes for the structural components of the alphavirus (16, 18). Finally, trans-acting nsP2 protease cleaves nsP23, resulting in a complete shift away from negative-strand synthesis and strongly drives production of the sub-genomic RNA and progeny full-length genomes (16, 18, 35, 36). This system of cleavage specificity, dependent on the molar concentration of existing cleavage products, allows for the temporal regulation of the RdRp complex and signals the critical timing events of the virus replicative cycle. Additionally, nsP4 has two intrinsic binding sites that recognize the promoter elements for either the full length genome, or the 26S subgenomic RNA, preferentially producing a 5-fold or greater molar excess of the 26S RNA over genomic RNA (101, 102). It is prudent to note that in addition to the viral nonstructural proteins, a number of cellular proteins, including the La antigen and multiple hnRNP proteins, have been implicated in aiding alphavirus replication and transitioning between phases of genome synthesis (103-113).

Late in the replication cycle when RNA production has shifted primarily to the positive strand and sub-genomic RNA products, translation of the structural polyprotein commences. The capsid, pE2 (E3 and E2), 6K, and E1 proteins are produced in a single chain that is first processed by capsid self-cleavage (1). This one-time cleavage event exposes an endoplasmic reticulum (ER) insertion sequence, allowing the rest of the polyprotein to be processed through the cellular export system (114, 115). The pE2, 6K and E1 proteins are all produced as transmembrane proteins in the ER. Cellular processing of the growing peptide chain results in cleavage of pE2 into the soluble E3 and membrane-bound E2, which is incorporated in the mature virus particle (84, 116). At this time, 6K and E3 are also cleaved in the ER maturation pathway (117).

As capsid protein accumulates, the core particle starts to form and incorporates the genomic RNA through the recognition of specific packaging sequences located in the nonstructural gene

region of the positive-sense RNA (118). The newly completed nucleocapsids transit to the cell membrane where capsomeres associate with the C-terminal domain of E2 complexed as heterotrimers made up of glycosylated E1 and E2 on the cell surface (119-121). As budding proceeds, the progeny virion is released as a mature infectious unit.
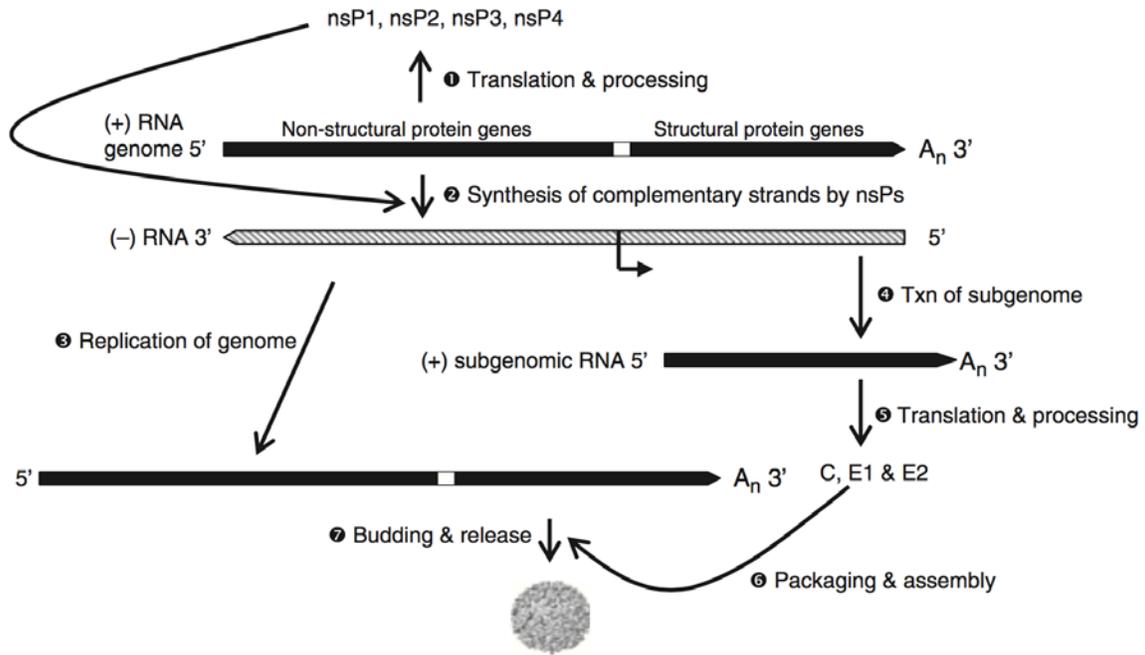
Figure 2: Alphavirus Replication Cycle
Schematic representation of the alphavirus replication cycle from (14). Replicative steps are temporally annotated. Positive sense (black) and antisense (hatched gray) RNA species from each stage are annotated with their respective products.

1.1.3 Reporter-expressing Alphaviruses

Over the years, various molecular tools have been developed to study alphaviruses. The incorporation of a duplicate subgenomic promoter has been widely employed to express a functional transgene or biological reporters including bioluminescent enzymes or various fluorescent molecules (122, 123). The alphavirus nsP3 protein is also amenable to large insertions,

and has been used to successfully express biological reporters (124-126). Recently, our lab has demonstrated that functional reporters may be included in the structural polyprotein through the inclusion of a self-cleaving picornavirus 2A-like peptide sequence from thosea asigna virus (TaV) (56). These TaV reporter viruses retain similar virulence to their unmodified parental viruses, the reporter genes have greater stability than their double promoter counterparts, and are resistant to selective pressure for deletion over several rounds of replication (56). Importantly, the combination of nsP3 and TaV-assisted structural expression of biological reporters allows us to monitor events at distinct stages of the alphavirus replication cycle, with nsP3 transgenes expressed immediately upon initial virus translation, and structural reporters produced after genomic replication has occurred. In addition to the infectious alphavirus reporters, non-replicating mimic RNAs with alphavirus 5' and 3' NTRs flanking a bioluminescent reporter have been used to examine genomic translation in isolation (127, 128). Lastly, replicative events limited to a single round may be studied in detail using replicons, packaged alphavirus RNAs that lack the subgenomic structural genes required for propagation and dissemination (129).

1.1.4   Selection of Alphaviruses for Study

SINV has gained the status of the prototypic alphavirus due to its relative ease of use under biosafety level 2 containment practices. However, SINV does not cause a significant health burden, and typically does not cause disease in humans (130). For this reason, we chose to focus our studies on a selection of both arthritogenic and encephalitogenic alphaviruses with a significant impact on human health. Our chosen arthritogenic alphavirus, CHIKV, has grown to global importance with recent outbreaks in the Indian Ocean territories and the Americas (131-134). While CHIKV is rarely fatal, the associated disease has caused a significant economic burden on

11

afflicted regions. Additionally, we chose to study two representative encephalitogenic alphaviruses, VEEV and EEEV. Both viruses are capable of fatal disease in humans and are high priority pathogens as determined by the United States Department of Defense. While closely genetically related, both VEEV and EEEV follow a different disease course, though each are capable of causing fatal encephalitis in humans and other vertebrates (125, 135, 136). Together, CHIKV, VEEV and EEEV serve as a broad representation of the geographically diverse alphaviruses with global human and veterinary health importance.

1.1.5 Chikungunya virus

CHIKV was first differentiated from concurrent outbreaks of dengue virus in eastern Africa following a 1952-1953 outbreak of the emerging pathogen in Tanganyika, now Tanzania (137-139). At the time of the outbreak, the disease was known locally as "chikungunya," a word stemming from another in the Kimakonde language, "kungunyala," which describes the contorted posture frequently taken by individuals afflicted with the disease as a means to alleviate joint pain associated with virus infection (138). Due to the variable clinical manifestations of dengue virus infection and an apparent overlap in symptoms, there was difficulty assigning the outbreak to the emergence of a hitherto unknown virus. Of note, the new epidemic lacked certain clinical features of dengue such as pain associated with eye movements and there was an unusually high occurrence of chronic flaring joint pain, leading the medical investigators to explore other explanations for the outbreak.

CHIKV is transmitted between primates, including humans, by *Aedes* mosquito species, and primarily relied on *Aedes aegypti* for urban transmission between humans in Africa and Asia (140-146). In 2004, a mutation to the E1 glycoprotein was identified in the East/Central/South

African (ECSA) clade of CHIKV circulating on La Réunion island, which allowed highly competent transmission of CHIKV by the *Aedes albopictus* mosquito, leading to an epidemic of millions of cases in the Indian Ocean territories and eventually Europe (147-151). CHIKV has recently emerged in the western hemisphere with an outbreak starting in the Caribbean in 2013, and spreading to the North and South American mainland shortly thereafter (133, 134, 152). Of note, the outbreak in the Americas was initiated by the Asian clade of CHIKV, and does not demonstrate enhanced vector competence for *Aedes albopictus* (152). However, recently ECSA strains have also been locally detected in Brazil, with potential to acquire similar vector-adaptive mutations as those observed on La Réunion (153).

1.1.5.1 Chikungunya Virus Disease in Humans

CHIKV disease in humans is estimated to be subclinical in 16-18% of cases, presenting no symptoms, but positive serology from regional surveillance programs (131, 132). Onset of CHIKV is abrupt, characterized by high fever, polyarthralgia/polyarthritis, myalgia, general fatigue and headache (154-158). The polyarthralgia occurs symmetrically, and typically afflicts peripheral joints of the wrists, hands and ankles (154, 156). Polyarthritis occurs at a lower frequency – around 40% of total cases – and is most apparent in the hands and feet (154, 156). In addition to the severe muscle and joint manifestations, CHIKV also causes a maculopapular rash of the extremities and sometimes the face in about 50% of those infected (154-157). Other clinical signs of disease include gastrointestinal distress, nausea, vomiting, and diarrhea (154, 156, 158). The debilitating pain associated with CHIKV causes significant disruption in regions with ongoing outbreaks, with more than 60% of individuals incapacitated for all or part of the clinical course of infection (159, 160). While CHIKV rarely causes fatal disease, atypical hemorrhagic and neurological symptoms have occurred in a subset of hospitalized patients, and have resulted in death (154, 157, 158).

Following the acute phase of CHIKV, over half of afflicted individuals report ongoing rheumatic symptoms for a month or longer (160-162). Most frequently, musculoskeletal pain persists with some individuals developing rheumatoid arthritis or chronic inflammatory condition of the peripheral joints (162, 163). Following the 2007 outbreak of CHIKV in Italy, over 60% of follow-up cases reported lasting arthralgia or myalgia a year after primary infection (159). Despite several attempts, a consistent risk factor associated with persistent arthralgia and myalgia has not been identified, though old age and a high CHIKV antibody titer appear to be loosely correlated with disease severity and longevity (164-166).

1.1.5.2 Chikungunya Virus Pathogenesis in Mice

Select wild type adult mouse strains are sensitive to CHIKV infection and can be used for studying arthritogenic disease *in vivo* (167-169). Mice between 3- and 6-weeks in age of the inbred, Jackson Laboratories black-6 genetic background (C57Bl/6J), succumb to CHIKV disease, marked by high serum viremia from 1- to 3-days post infection and virus replication in skin, muscle, and visceral organs between 1 and 5 days (168). Adult mice do not lose weight throughout the course of disease. Notably, mice infected subcutaneously in the footpad experience marked swelling in the infected limb and concurrently demonstrate a pain reflex for the swollen limb (168). Swelling is biphasic, with a small peak around 2-days post infection, and a maximum cross-sectional area achieved around 6- to 7-days post infection (168). CHIKV is detectible in muscle, spleen, and lymph nodes for the duration of the 5-day viremia, and this tissue replication precedes the peak hind limb swelling (168).

CHIKV pathology in the feet is characterized by edema and generalized infiltration of mononuclear cells in the synovial membranes, connective tissues and muscle (168). A generalized breakdown of synovial tissues is observed, while muscle and tendons appear to remain intact with

14

minimal cellular damage (168). Most other tissues appear normal, with mild lesions of infiltrating mononuclear cells in the lymph nodes, spleen and liver (168). Interestingly, mononuclear infiltrates in the connective tissues remain for weeks after other signs of disease have resolved (168). The mononuclear infiltrates observed are mostly monocyte/macrophage lineage cells and NK cells, and a reduction of the overall populations of these cells is sufficient to ameliorate disease, indicating an essential role in CHIKV-induced inflammation and arthritis (168). Furthermore, CHIKV induces a mild inflammatory cytokine response in mice, with some early production of IFN-γ, TNF-α, IL-6 and MCP-1, with virtually no IFN-α/β observed in some studies (168, 169).

Nonfatal CHIKV infection in adult mice may mimic the typical disease course in healthy adult humans, but is not representative of the rare, more severe symptoms associated with CHIKV infection. Additionally, adult mice deficient for various signaling components of the IFN-α/β response, including receptor and signal transducers, exhibit exacerbated, uniformly fatal disease with WT, but not attenuated CHIKV (167, 169). CHIKV is detectible in skin, muscle, and synovial tissues in these animals, with higher rates of replication than observed in WT mice (167, 168). Importantly, these mice progress to neurological disease, similar to the rare severe cases of CHIKV in humans (167). Additionally, neonatal mice younger than 6-days old may be used as a model for fatal CHIKV infection (167). CHIKV replicates in a similar manner in neonates to their adult counterparts, and typically progresses to systemic inflammatory response syndrome (SIRS) or neurological syndrome and death by 12-days post infection (167). Prominent cell targets in all three models of CHIKV infection include mesenchymal lineage cells like fibroblasts, osteoblasts, and myoblasts (167, 168). Monocyte macrophages have also been implicated as a primary target of infection, though their infectivity in vitro remains controversial, owing to the purity of virus preparations, suggesting these cells may not initiate receptor-mediated virus infection (167-170).

15

1.1.6   Venezuelan Equine Encephalitis Virus

A 1938 outbreak of equine encephalomyelitis in Venezuela prompted the identification and characterization of a new virus related to the western and eastern varieties previously described in North America (171, 172). This virus was serologically distinct from the eastern virus that caused an outbreak in Canada and the United States earlier the same year (172). The first human cases of this newly identified disease were described in 1942 for two laboratory workers who had been working with the agent for two months, with no fatalities reported (136). Since this time, numerous large outbreaks of VEEV have occurred throughout South and Central America, involving tens of thousands of equine and human cases (173-177). VEEV is propagated in an enzootic lifecycle between multiple rodent species and mosquitos, occasionally spilling over to equines and humans (174, 178-180). In addition to its natural replication/transmission cycle, VEEV is a pathogen of particular interest due to its previous development as a biological weapon by the United States and Soviet Union (181).

1.1.6.1 Venezuelan Equine Encephalitis Virus Disease in Humans

VEEV is pathogenic in humans, causing a severe acute febrile illness, but rarely fatality (182-185). Only about 1% of human cases result in death, and most fully recover from disease (186). Following a 2- to 5-day incubation period, infected individuals are struck by a sudden febrile illness marked by malaise, chills, and a severe headache (178). This disease may be accompanied by nausea and vomiting or diarrhea, as well as myalgia focused in the upper legs and lower back (186). Rare involvement of the central nervous system (CNS) typically presents as convulsions, somnolence, confusion and photophobia, with some patients progressing to stupor and coma (186).

For most, disease lasts about 4-6 days, followed by a week-long recovery period. However, some patients experience biphasic disease (186).

In fatal cases of VEEV, severe edema is prevalent in the CNS, with congestion and meningitis apparent in most victims (185). Rare hemorrhage and vasculitis may also be observed in the brain (185). Brain tissue doesn't show significant signs of encephalitis in most cases, and inflammatory cell infiltration is mild (185). However, VEEV causes widespread infection in the resident cells of the lymphatic tissues, resulting in high levels of follicle necrosis in lymph nodes, spleen and around the gastrointestinal tract (185). Virus-induced damage is observable in most other tissues, including liver, lungs and kidneys (185). Based on various clinical case studies and the histopathological evidence from fatal cases, VEEV disease is humans is best described as a systemic acute febrile illness with occasional neurological involvement in the CNS.

1.1.6.2 Venezuelan Equine Encephalitis Virus Pathogenesis in Mice

WT VEEV causes a uniformly fatal disease in adult mice that more closely mimics that observed in equines rather than humans (125, 187, 188). Despite the high level of CNS involvement, VEEV infection in mice parallels the systemic disease observed in humans, and may still serve as a model of fatal VEEV. Infected mice rapidly succumb to disease, exhibiting rapid weight loss and acute behavioral changes within 1-day post inoculation (125). Mice become hunched and ataxic early, with obvious piloerection or "ruffling" of fur after one day (125). As disease progresses, CNS involvement becomes evident with mice demonstrating signs of paresis and paralysis, and eventually becoming moribund by 5-days post infection (125). Average survival time is about 5-6 days following subcutaneous inoculation of VEEV (125).

VEEV rapidly replicates in mesenchymal cells and myeloid cells of the draining lymphatics (125, 188). Serum viremia peaks at 12- to 24-hours post infection, seeding infection in

the spleen, and other visceral organs (125, 188). At the time of peak viremia, VEEV strongly induces systemic production of IFN-α/β, which tapers off over the next two days of infection (125). Histopathology reveals VEEV present in the pancreas, liver, spleen, spinal cord and brain at the time of death. VEEV infection in mice also results in a unique lymphotropism, similar to that seen in humans (187). VEEV replicates robustly in monocyte/macrophage cells, leading to its unique disease phenotype among alphaviruses (125).

Adult mice uniformly succumb to encephalitis, with prominent neurological deficits apparent (125, 187, 188). VEEV first reaches the brain between 1- and 3-days post infection, steadily replicating in the CNS (125, 187, 188) (data not shown). Peak titer is observed in the brain around 4-days post infection (125, 188). At this time, virus is present in the hippocampus, thalamus, brainstem and spinal cord, with mild inflammatory cell infiltration evident (187). By day 5, virus can be found in the cerebellum and cerebral cortex and immune infiltration is more apparent (187). At this time, virus begins to decline in the brain and other tissues until the time of death (125, 187, 188). Neuronal decay and sustained inflammation dominate in the brain following peak viral load, and are sustained until the time of death (187).

1.1.7 Eastern Equine Encephalitis Virus

In 1938, an outbreak of a hitherto unknown viral encephalomyelitis among equines in Massachusetts was reported (189). The virus was identified to be an eastern variety of a previously discovered virus from California in 1930 (189). Concurrent to the equine outbreak, several children in the surrounding area fell ill with a viral encephalomyelitis, later identified as the same virus found in horses (189-191). The newly discovered EEEV was noted to have twice the mortality rate of the previously identified strain in this outbreak (190). Since its discovery, EEEV has caused

sporadic outbreaks among horses and humans, with 5 to 25 human cases reported in North America each year (192). EEEV naturally circulates in passerine birds through *Culiseta* species, and is potentially maintained in snakes or other reptiles of endemic regions (193-196). Spillover to humans requires a bridge vector, including *Aedes* and *Coquellitidia* species, which are widely distributed across affected areas of the United States (193, 196, 197).

1.1.7.1 Eastern Equine Encephalitis Virus Disease in Humans

In humans, EEEV is clinically indistinguishable from most acute viral infections early on. A short prodromal phase lasting 5 days on average is typically accompanied by fever, headache, and nausea or vomiting, and is sometimes associated with abdominal pain (198). A longer prodrome is associated with more favorable clinical outcomes in pediatric patients hospitalized with EEEV infection (135). During this period, about 50% of individuals experience generalized malaise and weakness and can have non-focused muscle and joint pain (198). Onset of neurological symptoms is typically abrupt and followed by rapid health deterioration. While neurological signs vary, confusion is most common, with about 25% of patients presenting combinations of somnolence, focal weakness, seizures, and even meningitis (198). Once in the neurological phase of disease, about 90% of patients progress to stupor or become comatose, with the latter lasting several days (198). EEEV is fatal in about 30-70% of cases, and most who recover do so with mild-to-severe long-term neurological impairments (135, 198, 199).

Laboratory results for patients with EEEV reveal elevated white blood cell counts and an infiltration of blood cells in the cerebrospinal fluid (135, 198). This also corresponds to a rise in cerebrospinal fluid protein content (198). Brain imaging on infected patients by MRI or CT reveal abnormal lesions throughout the brain, but most commonly associated with the meninges, cortex, basal ganglia and thalamus (135, 198). Postmortem brain pathology clearly shows signs of

meningoencephalitis with EEEV clearly detectible in the brain, primarily in neuronal cells within the lesions detected by imaging (135).

1.1.7.2 Eastern Equine Encephalitis Virus Pathogenesis in Mice

In adult mice, EEEV disease is characterized by limited viral replication in peripheral tissues followed by the onset of a uniformly fatal neurologic disease (125, 200, 201). Average survival time depends on the dose received, but typically falls between 4- and 6-days post subcutaneous inoculation (125, 200, 201). Mice do not show notable signs of disease for the first 2-3 days of infection, with no prominent weight loss, and normal observed behavior during this period (125). Around the fourth day of infection, health rapidly declines, with rapid weight loss, and behavioral abnormalities including hunching, and reduced motility (125). This rapidly progresses with all mice becoming moribund by 5-days post infection (125, 200, 201).

Following subcutaneous inoculation, EEEV replicates locally in primarily mesenchymal cells, including fibroblasts, osteoblasts, and myocytes (125, 200, 201). Virus is present in the draining lymphatics, but unlike VEEV, does not replicate (125, 200). This restricted cellular tropism is due to the presence of four conserved miRNA binding sites located in the 3'-NTR of EEEV, which prevent replication in macrophages and dendritic cells (127). Functionally, this restriction serves to evade the early IFN-producing immune response and contributes to the high pathogenicity observed with EEEV infection (127). Replication of EEEV in mesenchymal cells continues throughout the course of infection (200). After 18-24 hours, EEEV reaches peak serum viremia, seeding additional sites of replication (125, 200, 201).

Around 24-hours post infection, virus first appears in the brain, with focused regions of replication around the somatosensory cortex (125, 200). EEEV replication in the brain in the first two days of infection is highly variable between mice (200). However, by 3- to 4-days post

20

infection, uniform replication is observed throughout the thalamus, midbrain and cerebral cortex, with virus detectible in most regions (200). This period of peak replication in the brain corresponds to declining viral titers systemically (125, 201). Among the alphaviruses, EEEV is uniquely neurovirulent, owing this phenotype to its ability to bind heparan sulfate, aiding in binding and entry into neuronal cells (202). Damage to brain tissue is evident at the time of death, with significant necrosis observed and mild immune infiltrates of neutrophils and eosinophils (200).

1.2   TYPE I INTERFERON

Host organisms have evolved a complex network of cytokine and cell-based responses to identify and clear microbial infections. Viral and bacterial structures and replicative intermediates can serve as pathogen-associated molecular patterns to trigger a broad, non-specific response aimed at restricting growth of the invading microorganism and priming the cellular innate and adaptive immune responses that eventually clear the infection. The first innate immune cytokine characterized was broadly named interferon (IFN) for its ability to interfere with the growth of influenza A virus, though it was later identified as just one of several cytokines with similar activity (203). There are three known types of IFNs, all class II α-helical cytokines, classified as type I through type III for the receptors they utilize. Both type I and type III consist of multiple members and share a common downstream signaling pathway, while IFN-γ is the only type II IFN. In humans, the functional type I IFNs consist of 13 subtypes of IFN-α, IFN-β, IFN-ε, IFN-κ, and IFN-ω (204). Due to cell-type restrictions of several these cytokines, however, immunological reference to type I IFN specifically refers to the subtypes of IFN-α/β. Unlike IFN-γ, which is produced primarily by T-cells and natural killer (NK) cells, type I IFNs may be induced and signal

in most cell types and act as a rapid first line of defense in both the infected cell and neighboring cells through autocrine and paracrine signal induction (204). Likewise, IFN-λ1, -λ2 and -λ3 signal through a distinct cell surface receptor that is primarily restricted to epithelial cells (205-207).

1.2.1   Interferon Induction in Alphavirus Infection

Host cells constantly sample their environment for pathogen-associated molecular patterns (PAMPs) through the recognition of non-self nucleic acids, proteins, lipids or polysaccharides. Nucleic acid sensing pattern recognition receptors (PRRs) identify RNA in atypical forms and locations such as double-stranded helices and 5'-triphosphate RNA associated with virus replication or localized to endosomes within the cell, as well as DNA present in the cytoplasm or endosomes. Likewise, specific bacterial-associated antigens such as lipopolysaccharide can trigger a separate receptor, TLR4, and activate the production of IFNs. In total, there are ten Toll-like receptors in humans – eleven in mice – named for the original Drosophila homologues. These are complemented by the RIG-I-like receptors (RLR), RIG-I, MDA5 and LGP2, as well as cGAS and other cytoplasmic DNA-sensing molecules that signal through the stimulator of interferon genes (STING).

The receptor that identifies the PAMP determines the specific mediators of IFN induction. In the case of alphavirus replication, double-stranded RNAs (dsRNAs) are present in the cytoplasm at all stages of the replication cycle. Additionally, nascent 5'-triphosphate ssRNA is present and may serve as an additional PAMP for alphavirus infection. These cytoplasmic RNAs are detected by MDA5 and potentially RIG-I, inducing a conformational change and an association with MAVS on the mitochondria (208-210). MAVS activation leads to a cascade of phosphorylation events with TBK1 and IKKε, which in turn activate the interferon regulatory factors, IRF3 and/or

IRF7, depending on the cell type (211-214). Poly-phosphorylated IRF3 dimerizes and translocates to the nucleus, where it assembles on the promoters of IFN-α4/β in non-myeloid cells along with ATF-2, c-Jun, CBP-p300, NF-κB and the RNA Polymerase II transcription machinery (215).

Figure 3: Induction and Signaling of IFN-α/β
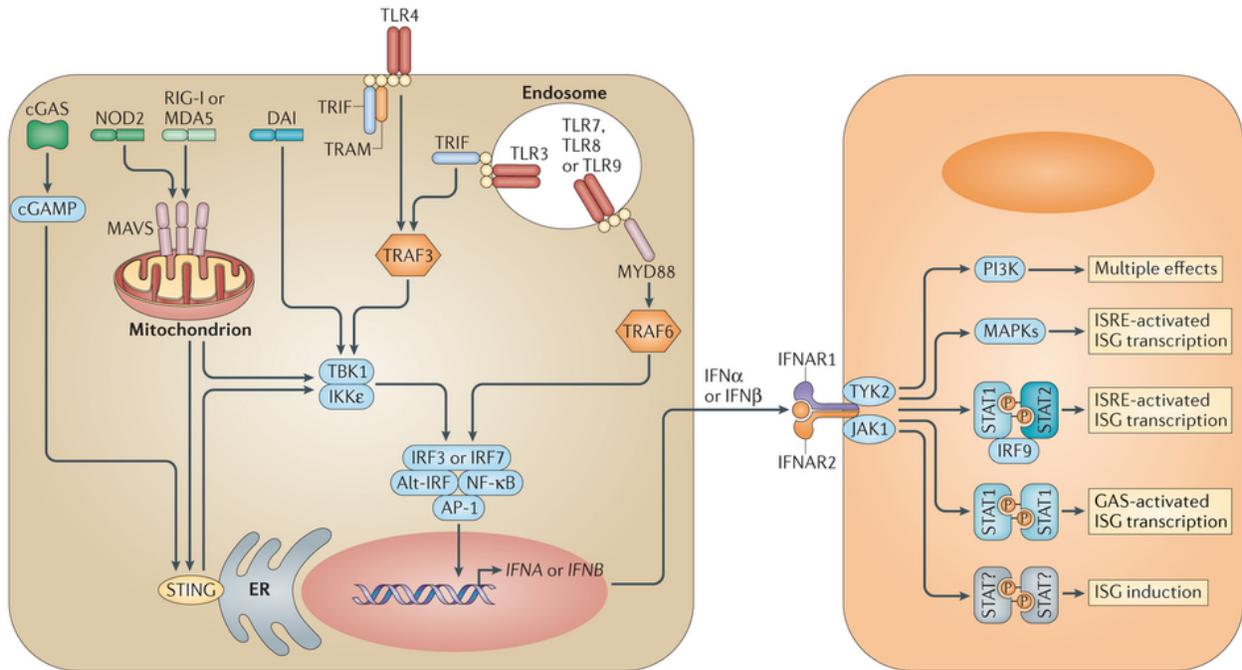
Cellular induction pathways for IFN-α/β production and downstream signaling. IFN produced from stimulated cells may act through paracrine signaling as shown, or autocrine signaling. Reprinted by permission from Macmillan Publishers Ltd: Nature Reviews | Immunology, (216), copyright 2015.

IRF3-mediated activation of IFN-α4/β contributes an initial production of IFN in response to microbial infection. Subsequently, IRF7 is induced by downstream IFN signaling, resulting in a feedback loop where IRF7 is the primary driver of secondary IFN production, that includes several other IFN-α genes (217, 218). While most cell types are capable of producing and responding to IFN-α/β, the largest production of serum IFN is often attributed to a class of cells called plasmacytoid dendritic cells (pDCs) (219). IFN-α/β is induced in pDCs, and other myeloid

cells, through constitutively expressed IRF7, bridged through MyD88 (220). In the case of pDCs, viral components are sampled from the environment and the endosomal dsRNA-sensing receptor TLR7 signals through MyD88 which is pre-associated with IRF7 for rapid signal transduction in these cell types (221-224). However, despite their crucial role in other viral infections, pDCs do not appear to play a major role in the IFN response to alphavirus infection *in vivo* (225, 226).

1.2.1.1 Cytosolic RNA Sensing Pathogen Recognition Receptors

Virus-associated RNAs are a universal identifying characteristic for cells to initially detect infection. As such, eukaryotes have evolved several non-redundant mechanisms for detecting foreign RNA in the cytosol and endocytic vesicles. Within the cytosol, two known functional RLRs, RIG-I and MDA5, act in concert to detect non-self RNA structures and signal the cascade of initial innate immune responses. These proteins are members of the DExD/H box RNA helicases, which also includes the related LGP2 helicase with yet unknown function in antiviral signaling (227-229). RLRs are present at a low resting state, and are upregulated by IFN signaling to increase sensitivity after infection is first identified (227, 230). In addition to the cytosolic RNA sensors, TLR3 detects dsRNA in endocytic vesicles, and TLR7/8 detects ssRNA sequences within endosomes. While the RLRs are ubiquitously expressed in most tissues, the TLR RNA sensors are more restricted in their expression.

Both RIG-I and MDA5 are composed of three distinct functional domains, containing two caspase activation and recruitment domains (CARD), the DExD/H box RNA helicase responsible for binding RNA substrates, and a repression domain at the c-terminus (227-229). Prior to substrate binding, the CARD and repressor domain interact to form a closed conformation of the RLR, preventing binding and signaling with the MAVS adaptor protein (229, 231). The RNA substrate is recognized through a binding event in the repressor domain, releasing the CARDs for

oligomerization and binding with MAVS (209, 232-234). In RIG-I, the repressor activity is regulated intramolecularly. However, MDA5 does not autoregulate its activity, and requires an additional repressive signal, potentially through the related LGP2, which lacks the N-terminal CARD (235).

RIG-I and MDA5 both bind cytoplasmic RNA, but show preference for different structures. RIG-I has been characterized to respond to numerous RNA substrate specificities, including single and double stranded RNA motifs that contain a 5'-triphosphate (235, 236). The 5'-triphosphate appears to be a required motif for most RNA recognition, with reduced signaling activity resulting from diphosphate or monophosphate ends (237, 238). However, RNA degradation products from RNase L, which lack a 5'-triphosphate, but contain a 3'-monophosphate can also induce signaling through RIG-I (239, 240). In addition to the phosphate specificity of RNA substrates, RIG-I also preferentially responds to short RNAs with at least a short double-stranded region or a stretch of poly-uridine sequence interspersed with cytosine residues (235). RIG-I recognition of cytoplasmic dsRNA is not limited to 5'-triphosphate RNA, but may also include type-0 capped RNA species as well (235, 241). In contrast, MDA5 is much more specific to dsRNA and lacks the ability to recognize the negatively charged phosphate moieties that define RIG-I binding (242). Instead, the C-terminal domain recognizes dsRNA motifs with a preference for blunted ends rather than those containing overhangs.

1.2.1.2 IRF3 Activation and Transcriptional Activity

IRF3 is the primary transcription factor associated with the induction of IFN-α4/β following pathogen recognition in non-myeloid cell types. IRF3 contains both nuclear localization and nuclear export signals, with the latter dominating, resulting in a steady-state distribution mostly in the cytoplasm of non-infected cells (243). Upstream signaling events result in TBK1 and IKKϵ

polyphosphorylation of serine residues in the IRF3 C-terminal domain (244-246). Resulting from this polyphosphorylation, IRF3 either homodimerizes or heterodimerizes with activated IRF7, blocking the nuclear export signal, and shuttles to the nucleus where it associates with CBP and p300 (246). In addition to enhancing transcription of IFN genes, IRF3 recognizes specific interferon stimulation response elements within its target promoters, specifically a sequence of GAAANNGAAANN, which is present in both the IFN-α4/β promoters as well as several other IFN stimulated genes (ISGs). One study with a constitutively active mutant of IRF3 has revealed multiple ISGs with known antiviral activity to be upregulated by IRF3, including members of the IFIT family of antiviral proteins, the ubiquitin-like ISG15, 2'-5' OAS, IFI44, and GBP2 (247).

1.2.1.3 Other RNA Pattern Recognition Receptors

In addition to the cytosolic RNA PRRs, IFN can be induced through the activation of TLRs, the cytoplasmic DNA sensor, cGAS, and the cytosolic peptidoglycan NOD-like receptors. In particular, three TLRs may play an important role in viral detection, again through specific binding to RNA. While the membrane-bound TLRs may localize either on the cell surface or within endosomes, the RNA-sensing TLR3/7/8 are all located within endosomes. TLR3 and TLR7 have both been implicated in downstream signaling in the context of alphavirus or alphavirus replicon infections and play a protective role in mice (248, 249). TLR3 detects dsRNA intermediates present in endosomes, while TLR7 and TLR8 show specificity to ssRNA (222-224). TLR3, while ubiquitously expressed in most cell types, exhibits differential signaling between myeloid and non-myeloid lineage cells. In particular, macrophages and dendritic cells, while able to respond to TLR3 ligands, do not induce IRF3 signaling (250). In contrast, TLR7 and TLR8 are the primary

drivers of IFN-α/β production in myeloid cells, particularly pDCs, and are restricted in expression primarily to pDCs, monocyte/macrophages and B-lymphocyte cells (251).

While PRR signaling for IFN production is an important function for this class of molecules, some PRRs may carry out additional antiviral functions for the cell. The IFN-inducible RNA-dependent protein kinase, PKR is activated by binding dsRNA through its N-terminal domain, resulting in auto-phosphorylation and activation (252-256). Instead of inducing an IRF3/IRF7 mediated IFN production like the other RNA PRRs discussed, activated PKR phosphorylates the eukaryotic initiation factor eIF2α, blocking cap-dependent initiation of translation (257). PKR activity may also lead to the activation of NF-κB through phosphorylation of the inhibitory IκB subunit (258-261). Lastly, PKR may play an additional non-redundant role in IFN production in response to some viruses, including some alphaviruses, by stimulating poly-adenylation of IFN mRNAs in the cytoplasm and by independently activating MDA5 (262-264).

Similar to PKR, another cytoplasmic IFN-induced PRR, 2'-5'-oligoadenylate synthetase (OAS), demonstrates a targeted antiviral activity rather than directly stimulating IFN production in response to pathogen detection. OAS binds dsRNA substrates in the cytosol and synthesizes oligomers of 2'-5'-linked adenosine or guanosine (265, 266). These substrates act as a second messenger for the activation of RNase L, a latent endonuclease that may either serve to directly cleave viral RNAs or generate additional stimuli for RIG-I signaling and eventual IFN-α/β production (239, 267). However, the extent of the contribution of the combined mechanisms of PKR and RNase L is in question as mice deficient in both show little enhanced susceptibility to multiple viruses, including alphaviruses (268, 269).

1.2.1.4 Additional Induction Pathways

IFN induction from cytosolic PRRs follows a MAVS-centric signaling pathway. TLR induction of IFN, however, transduces the receptor signal through the adapters TRIF or MyD88 depending on the TLR, and ultimately the cell type in question (270, 271). In the case of RNA-sensing TLRs, TLR3 signals through a recruitment of TRIF and subsequent phosphorylation and activation of the TBK1/IKKε signaling cascade observed with the cytosolic RNA sensors (244, 270, 272). TLR7/8, the primary inducer of IFN in pDCs, recruits MyD88, which phosphorylates IRAK, leading to an association with TRAF6 (271-275). Activated TRAF6 initiates a cascade of signaling events through additional IκB kinases leading to the phosphorylation of the IκB inhibitor of NF-κB (276-281). NF-κB proceeds to initiate the transcription of numerous innate and adaptive immune regulatory factors, including the production of IFN-α/β (282).

1.2.2   Interferon Signaling through JAK/STAT

Most healthy cell types can respond to IFN-α/β signaling. Secreted IFN-α/β binds to the IFN-α receptor complex (IFNAR), a heterodimeric transmembrane cytokine receptor consisting of the IFNAR1 and IFNAR2 subunits, to initiate autocrine or paracrine signaling through the JAK/STAT pathway (283). The cytosolic end of the IFNAR1 subunit is associated with the tyrosine kinase TYK2 and the IFNAR2 subunit with JAK1, which are activated upon ligand biding and result in the phosphorylation of STAT1 and STAT2 (284-287). The two phosphorylated STAT proteins form a heterodimer and recruit cytosolic IRF9 to form the IFN stimulated gene factor 3 (ISGF3) complex (288). The functional ISGF3 complex traverses the nuclear pore where it associates with IFN stimulation response elements (ISRE) within the promoters of target genes to initiate

28

transcription (289, 290). In addition to this canonical signaling pathway, IFN-α/β can activate additional STAT proteins through IFNAR, and may lead to additional pathway activation, including MAPK and mTOR signaling (291-295).

Much like the IFN-α/β signaling cascade, IFN-λ is recognized by a heterodimeric type III IFN receptor complex consisting of the IFN-λ receptor 1 and IL-10 receptor 2 (IFNLR1/IL10R2), which are associated intracellularly with JAK1 and TYK2 (296-298). Within the cell, IFN-λ results in the same signaling cascade through STAT1 and STAT2, leading to ISGF3 complex formation (299). Due to the shared cellular signaling pathway between both IFN-α/β and IFN-λ, a common pattern of ISGs are induced by both cytokines (300, 301). In contrast to the type I and type III IFNs, IFN-γ signals through the heterodimeric IFN-γ receptor subunits 1 and 2 (IFNGR1/IFNGR2) coupled intracellularly with JAK1 and JAK2 (302, 303). Activation results in tyrosine phosphorylation of STAT1, which homodimerizes and translocates to the nucleus (304, 305). IFN-γ JAK/STAT signaling does not involve additional factors, namely IRF9, and enhances transcription of target ISGs through direct interactions between STAT1 and the gamma activation sequence (GAS) in target gene promoters (305, 306).

1.2.2.1 Downregulation of Interferon Signaling

IFN signaling results in the induction of hundreds of IFN-stimulated genes (ISGs), many of which function to restrict microbial infections, and upregulates multiple stress responses that may lead to cell death. As such, IFN signaling is tightly regulated within the cell to avoid overexposure to pro-apoptotic and inflammatory responses. Cytokine signaling responses may be regulated by receptor internalization or direct inhibition of the signaling pathway in activated cells. The mechanisms of IFN signaling control include disruption of ISG transcription through polymerase pausing,

transcript degradation through miRNA expression, and direct protein-mediated interactions with the upstream signaling components (307-310). Activated JAK1 is directly targeted by two proteins of the suppressors of cytokine signaling family, SOCS1 and SOCS3, to prevent additional activation of STAT proteins (311, 312). A specific interaction with phosphotyrosine residues of the catalytic loop of JAK1 initiate binding of SOCS1/3, immediately blocking catalytic activity (312). SOCS proteins have also been implicated in direct binding to IFNAR, blocking the recruitment of STAT to the receptor-associated kinase (313, 314). Other mechanisms have been suggested in SOCS control of IFN induction and signaling, including targeting of TLR signaling adapters for proteasomal degradation to downregulate NF-κB signaling (315).

Another mechanism of desensitization to IFN signaling occurs through the induction of the ISG, USP18. USP18 is an isopeptidase that functions much like a de-ubiquitinating enzyme, but primarily acts to remove the ubiquitin-like ISG15 through a process called deISGylation (316). While USP18 functions to remove ISGylated proteins from the proteasomal degradation pathway, this activity was not required for inhibition of sustained IFN signaling (317). Instead, USP18 employs a similar binding affinity for IFNAR2 as SOCS2 and blocks the receptor interaction with JAK1, silencing downstream signaling events (317-320). Combined, these methods act in concert to temporally regulate IFNAR signaling, and desensitize cells to a prolonged IFN-α/β response.

1.2.2.2 Alphavirus Suppression of Interferon Signaling

Alphaviruses do not uniformly induce IFN-α/β in vivo, and induction is associated with the degree to which each strain is capable of infecting lymphoid tissues (14, 321). Likewise, the alphaviruses differentially resist the antiviral effects of IFN signaling (see **Table 1**). It has been demonstrated that alphaviruses may overcome this effect by inhibiting cell macromolecular synthesis at both the

30

transcriptional and translational levels (40, 44, 68, 322, 323). The alphaviruses appear to accomplish this activity through multiple proteins, including nsP2 and capsid (40, 42, 43, 66, 68). Interestingly, alphavirus resistance to IFN-α/β corresponds to the degree to which their respective proteins can inhibit infected cell macromolecular synthesis in the presence of existing IFN-priming (40). Additionally, specific antagonism of IFN signaling has been demonstrated with both the nsP1 and nsP2 protein directly interfering with JAK/STAT induction (323-327). Together, these activities function to mount some resistance to IFN signaling, and may account for differences in pathogenicity in humans and animal models of infection.

1.3 INTERFERON STIMULATED GENES

The primary result of IFN-α/β activation of the JAK/STAT pathway is the targeted upregulation of ISGs through transcriptional activation. ISGs represent a diverse class of gene products composed of more than 300 known proteins, many of which have antiviral activity by directly targeting specific pathways and functions involved in the virus replication cycle (328, 329). Early studies in the field of ISG research were dominated by the RNA-dependent protein kinase, PKR, or the latent RNA endonuclease, RNaseL and its activator, 2'-5'-OAS (252, 253, 330). These three components represent a substantial pathway for disrupting viral protein translation, and potential degradation of RNA genomes and gene products recognized by regions of dsRNA. Additionally, Mx GTPases were well characterized for their inhibition of influenza virus and several other RNA viruses through direct interactions with their respective nucleocapsid proteins (265, 266, 331-338). While these proteins were thought to produce the majority antiviral effect of IFN signaling, more recent work has identified numerous PKR/RNaseL independent pathways for virus restriction and

the mechanism of action has been a major target of investigation in the field of molecular virology (3, 268, 329, 339-343).

In mouse models, the alphaviruses are differentially susceptible to the ISG effectors of the IFN-α/β response. At one end of the spectrum, SINV induces and is highly susceptible to the effects of IFN-α/β priming, leading to reduced pathogenesis in healthy adult animals (14). EEEV is highly susceptible to IFN-α/β priming, but does not induce a systemic IFN response *in* vivo due to a restriction of cell tropism (14, 125, 127, 344). CHIKV does not induce a strong systemic IFN response in mice and is mildly resistant to the ISG effectors of IFN-α/β (168, 345). VEEV, however, induces a significant systemic IFN response, but is much more resistant to its effects than the other alphaviruses (14, 40, 125). A summary of alphavirus IFN-sensitivity is shown in **Table 1**. Due to the different avoidance/antagonism strategies employed by these viruses, alphaviruses represent a particularly useful repertoire for the mechanistic study of ISGs and the IFN-α/β response.

	INDUCES IFN	IFN PROTECTION FROM CPE
VEEV	++++	+
CHIKV	++	++
SINV	+++	++++
EEEV	+	+++

Table 1: Alphavirus induction and susceptibility to IFN

Relative induction of serum IFN at 24 hours p.i. and relative protection from virus-induced cytopathic effect from IFN-α/β priming is qualitatively compared between members of the alphavirus genus. Data are from (14) and unpublished data.

1.3.1   Anti-alphaviral Interferon Stimulated Genes

The severity and pathogenic outcomes of numerous alphavirus infections are broadly controlled by the IFN-α/β response (14, 167, 168, 323, 344-346). Identifying the individual effectors of the IFN-α/β antiviral state that contribute to disease attenuation and decreased morbidity/mortality is of particular interest (329, 339, 340, 347). In particular, knowledge of the function of innate antiviral responses to alphavirus infection may lead to identification of virus vulnerabilities as well as a better understanding of virus attenuation to aid in the design of rationally designed vaccines (3).

      Previous work studying host-pathogen interactions between ISGs and the prototypic alphavirus, SINV, has demonstrated a vital role for ISGs independent of PKR and RNase L (339). In this study, 44 putative anti-alphaviral ISGs were identified for follow-up assessment. Another study used both VEEV and CHIKV among other viruses to screen pan-tropic antiviral effectors, ultimately identifying multiple upstream signaling components including IRFs and PRRs (329). To date, ten ISGs have been assessed for their antiviral activities against one or more alphaviruses, and represent a wide range of strategies for inhibiting replication and dissemination.

      The zinc-finger antiviral protein (ZAP) was originally discovered in similar screening efforts to identify putative antiviral genes using Moloney murine leukemia virus (348). Follow-up studies using SINV revealed a potent inhibitory effect of ZAP on alphavirus replication (340, 349-351). While the full significance of ZAP as an antiviral effector is still not entirely clear, it appears to bind viral RNA directly, and act as a scaffold for recruiting additional factors in complex with the virus genome (349-351). Interestingly, ZAP antiviral activity has not been observed in flavivirus or enterovirus infection, suggesting some degree of specificity in RNA targets (126).

Multiple ISGs involved in protein processing have been demonstrated to restrict alphaviruses. The endoplasmic reticulum-localized viperin was shown to significantly impact both SINV and CHIKV replication, with CHIKV infection in viperin-null mice resulting in elevated serum viremia and increased disease severity (340, 352). Another protein modifying ISG, ISG15, has an impact on alphavirus replication and associated disease (340, 353, 354). ISG15 is a ubiquitin-like polypeptide that is ligated to target proteins by multiple E3 ligases via ISGylation and may function to either block protein activity or even enhance stability and resistance to degradation (238, 355-359). In addition to its protein modifying activities, ISG15 may play a role in cytokine signaling with downstream antiviral effects, independent of its conjugation to viral or cellular proteins (354). Related to the activity of ISG15, the antiviral E3 ligase, TRIM25, has a similarly potent antiviral activity, and may synergistically act with ZAP (360). TRIM25 in particular, has been shown to function both in ISGylation as well as ubiquitination of the RIG-I CARD, a process necessary for robust downstream signaling (361).

Alphavirus translation is a prominent target of antiviral activity (339). Recent work with members of the poly-(ADP-ribose) polymerase (PARP) family of proteins has elucidated a role in translation inhibition of both VEEV and cellular proteins (362, 363). Additionally, the interferon inducible protein with tetratricopeptide repeats 1 (IFIT1) has been characterized to exhibit prominent anti-alphaviral activity, leading to a mechanistic understanding of how it restricts translation (3, 340, 364).

In addition to ISGs that restrict replication events within the cell, two known ISGs have been demonstrated to restrict the alphavirus entry and egress pathways (365, 366). IFITM3 is a transmembrane ISG that modestly inhibits alphavirus entry by restricting pH-dependent fusion within the endosome following receptor binding and internalization (366). BST-2 restricts virus

egress by tethering budding virions, preventing escape from the infected cell and slowing the progress of alphavirus spread (365). However, WT alphaviruses appear to have mechanisms to overcome this mode of virus restriction, with CHIKV nsP1 specifically binding BST-2 while simultaneously downregulating it's expression at the mRNA level (365).

The effects of two ISG nucleases have been explored in relation to alphavirus infection (340, 367). OAS/RNase L restrict virus replication through the direct endonuclease activity of RNase L on viral RNA. However, as mentioned above, the role of OAS/RNase L is likely not a major component of the anti-alphaviral response, with mice triply deficient in Mx, PKR and RNase L showing no greater disease after alphavirus infection (268), although virus replication in lymphoid tissues draining infection sites was enhanced approximately ten-fold by the absence of PKR (268). Curiously, a nuclear ISG exonuclease, ISG20, was shown to significantly inhibit SINV replication, the mechanism of which is the subject of the current study (340).

1.3.2   Interferon Induced Protein with Tetratricopeptide Repeat Family Proteins

Following the discovery of the interferon, IFIT1 was one of the first effector proteins to be identified (368, 369). IFIT1 is now understood to be part of a family of proteins with related structural elements, including four known members in the human genome and three in mice (370-377). IFIT family proteins are strongly induced by IFN-α/β and weakly induced by IFN-γ, and can be induced directly by alphavirus infection (339, 378). Most IFIT proteins contain 2 ISREs in the promoter, which are recognized by IRF9 in the ISGF3 complex, plus additional IRFs, including IRF3/7 (328, 370, 372, 375, 379). IFN-stimulation is not required for IFIT induction, however, leading to a distinction among ISGs as viral stress-inducible genes (380-382). IFIT1, the best

characterized family member in both humans and mice, is present at extremely low levels at rest in most tissues and is highly induced by IRF3 or the ISGF3 complex (383-386).

IFIT proteins are not enzymatic in nature, and are instead thought to mediate protein-protein and RNA-protein complex formation through their loosely conserved helix-turn-helix domains, termed tetratricopeptide repeats (387). Between human and mouse homologues of the conserved IFIT proteins, sequence similarity is rather degenerate, standing at about 50%, suggesting differences in activity and or mechanism between species (388). It is not surprising then that similar activities between mouse and human IFIT proteins are achieved through different mechanisms – involving separate species-specific protein interactions that ultimately lead to translation suppression (389). Among the known functions of IFIT proteins, translation suppression appears to be a primary conserved activity between species. In mice, this broad activity against host and viral translation is achieved by IFIT1 and IFIT2 independently binding to the eukaryotic initiation factor eIF3c, preventing ternary complex formation for cap-dependent translation (390, 391). This IFIT function has been shown to impede viral translation with HCV, with IFIT1 and IFIT2 localizing to replication sites with HCV RNA (392). Human IFIT1 has also been demonstrated to bind specifically to the E1 helicase of human papillomavirus (HPV), sequestering it to the cytoplasm and away from the nuclear replication factories where it functions (393). Relating to its translation-inhibitory functions, IFIT1 and IFIT2 in humans have also been shown to feedback negatively and suppress interferon signaling through STING and MAVS in most cell types by disrupting protein interactions in the IRF3 signaling cascade (394).

In addition to its well-characterized protein binding activities, IFIT1 was most recently defined as an RNA binding protein, with specificity for 5'-triphosphate-RNA as well as type-0 2'-O-unmethylated capped RNAs (395-397). Interestingly, the recognition of 5'-triphosphate RNA

by the IFIT proteins requires a minimum of IFIT1 and IFIT5 to function in humans, but only IFIT1 in mice (395, 396, 398). The 5'-triphosphate binding activity of the human IFIT complex is sufficient to sequester VSV RNA in the cytosol, leading to reduced virus replication in culture and knockout mice (395, 397). The ability of IFIT1 to recognize type-0 cap structures is important for viruses that lack 2'-O-methylation of the 5' terminal nucleotide associated with the 7-methyl-guanosine cap, including the alphaviruses (3, 396). Indeed, the prototypical alphavirus, SINV, is significantly inhibited by IFIT1 overexpression in mouse cells (340). While this binding is significant, and leads to sequestration of type-0 capped RNAs in the cytosol, some alphaviruses, including VEEV, have evolved an evasion mechanism where the terminal nucleotide is bound in a terminal stem-loop, and thus inaccessible to IFIT1, which preferentially binds to ssRNA only (3, 397, 398). Due to its alphavirus-associated RNA binding properties and translation inhibiting characteristics, IFIT1 is the focus of ongoing rational vaccine development and therapeutic approaches against multiple alphaviruses.

1.3.3   20kDa Interferon Stimulated Gene, ISG20

Based on previous results from our lab, the IFN-stimulated exonuclease, ISG20, is a potent inhibitor of alphavirus replication, and overexpression leads to a disproportionately high restriction of SINV replication *in vitro* (340). The *ISG20*/*Isg20* gene codes for an approximately 20 kDa 3'-5' exonuclease in the DEDD family of nucleases related to the yeast *Rex4* gene (399, 400). The ISG20 active site is composed of three acidic residues arranged in a catalytic triad, coordinating two Mn^{2+} ions at its core (400, 401). *In vitro*, ISG20 exhibits processive degradation kinetics on ssRNA substrates, and has reduced catalytic efficiency on ssDNA substrates (400). Double-stranded regions, including hairpins, on both RNA and DNA substrates greatly reduce ISG20-

mediated target degradation (400). The ISG20 protein consists of only a single catalytic domain, and lacks autonomous regulatory activity to guide substrate specificity or activation state (400, 401). As such, the cellular or viral targets of ISG20 exonuclease activity are not well characterized, and may instead rely on additional cellular factors for recruitment or nonspecific binding.

ISG20 is present at low resting levels in most cell types and is highly induced by both IFN-α/β and IFN-γ, as well as by estrogen receptor signaling (399, 400, 402, 403). The *ISG20* promoter is composed of an ISRE, which perfectly matches the ISGF3 consensus sequence, a gamma activation sequence, an NF-κB binding site, multiple GC stretches that are essential for strong promoter activity in the absence of a traditional TATA-box, and an E-box element that leads to USF-1-mediated constitutive low-level expression (402). The *ISG20* ISRE is also minimally bound by IRF1, which alone is sufficient for transcription complex formation post-treatment with IFN-α/β (402, 403).

ISG20 protein localizes primarily to the nucleus once induced, and is observed in tightly packed nucleolar puncta. This was originally designated as PML nuclear bodies, but later work identified these resident structures as Cajal bodies (CB) (399, 404). ISG20 binds in complex with both Coilin, the main structural component of CB, and SMN (404). In addition to these protein interactions, pull-downs associated with ISG20 revealed a complex with multiple snRNAs, U1, U2 and U3, known to localize to CB for post-transcriptional processing and assembly events (404). Whether these CB components are direct interaction partners for ISG20 or a consequence of its complex assembly is unclear. Interestingly, the primary protein sequence of ISG20 and solved crystal structure reveal no classical nuclear import signal, suggesting a role for an ISG20 binding partner in its nuclear import and retention (401).

1.3.3.1 ISG20 Antiviral Activity

Since its discovery, ISG20 has been shown to directly inhibit the replication of viruses in the families Rhabdoviridae, Picornaviridae, Orthomyxoviridae, Retroviridae, Flaviviridae, Hepadnaviridae, and Togaviridae (339-342, 405-411). The antiviral activities of ISG20 were first demonstrated by Espert et al., highlighting a marked restriction of RNA virus replication with vesicular stomatitis virus (VSV), influenza virus (FLUAV) and encephalomyocarditis virus (EMCV), but not adenovirus, which possesses a DNA genome (405). Due to the previously demonstrated RNase properties of ISG20 and the observed restriction of antiviral activity to viruses with an RNA genome, a paradigm was established in which ISG20 was presumed to be directly targeting viral RNAs for degradation. Interestingly, work from this group also demonstrated for the first time that the ISG20 antiviral activity is dependent on a functional exonuclease, with a mutant of ISG20 exhibiting a dominant negative effect on the downstream effects of IFN against VSV infection (405). Of note, Espert et al. observed significant differences in the restriction phenotype between virus species, with EMCV and FLUAV demonstrating greater resistance to ISG20-mediated antiviral activity (405).

A growing number of microarray and deep sequencing ISG functional studies have implicated ISG20 in the IFN-α/β-mediated restriction of several additional virus infections (339, 342, 412-414). Overexpression in various cell culture and virus-based transgene models have highlighted the importance of ISG20 in controlling virus replication at the cellular and whole organism level. Expression of *ISG20* from the human immunodeficiency virus-1 (HIV-1) genome robustly delayed HIV-1 reverse transcription and replication (406). However, prolonged exposure to ISG20 in this study resulted in escape mutations in the virus genome allowing uncontrolled replication (406). While mutation or deletion of the HIV-1-expressed ISG20 transgene would

result in the same escape phenotype, sequencing of the progeny virus indicated no change to the transgene or its promoter (406). This result is particularly significant, suggesting that ISG20 may inhibit virus replication through a mechanism other than non-specific degradation of viral RNAs.

Our lab has previously reported a greater than two-fold increased survival rate in neonatal SINV challenge where *Isg20* is expressed from a duplicate subgenomic promoter (340). Overexpression of ISG20 in murine embryonic fibroblasts led to a corresponding 100-fold reduction of SINV growth *in vitro* (340). A similarly robust *in vitro* antiviral phenotype was observed against hepatitis C virus (HCV), bovine viral diarrhea virus (BVDV), hepatitis A virus (HAV), yellow fever virus (YFV), West Nile virus (WNV), and dengue virus (DENV) (342, 408, 411). Interestingly, ISG20 overexpression did not restrict replication of the severe acute respiratory syndrome coronavirus (SARS-CoV), an RNA virus (411). Generally though, in studies where ISG20 was compared against similarly upregulated ISGs identified in target screens, ISG20 is consistently among the most potent at restricting viral replication and dissemination (340-342).

While the potency of ISG20 antiviral activity against many RNA viruses is now well-established, relatively little is known about its mechanism of action other than inferences derived from its exonuclease activity. For years, a model of ISG20-directed degradation of viral RNAs persisted (405). This paradigm was first challenged with the observation that HCV RNA is not degraded in the presence of overexpressed ISG20 (411). Furthermore, translation of HCV internal ribosomal entry site (IRES)-containing RNAs was not inhibited by ISG20 (411). Together, these observations suggest that the ISG20 exonuclease is acting on a substrate other than viral RNA for its inhibitory effect. The target of ISG20 exonuclease activity is not without controversy, however. Recent work by Leong et al. with hepatitis B virus (HBV) suggests that RNA intermediates produced during replication are a major target of ISG20 activity, with ISG20 accelerating the decay

of viral intermediates by approximately three-fold at three hours post-treatment with the transcription inhibitor, actinomycin D (410). While at odds with a model where ISG20 does not target viral RNA, this result may be a consequence of the HBV replication cycle where the partially ssDNA genome enters the nucleus and produces virally coded RNAs that serve as replication intermediates. This is in contrast to many other RNA viruses that replicate their genomes exclusively in the cytosol of infected cells. Another explanation for the discrepancy could be the treatment of cells with actinomycin D, which may disrupt ISG20 localization by dissociating CB (415, 416).

In addition to the conflicting ISG20-mediated degradation mechanisms proposed, another recent study suggests that a catalytically functional ISG20 may directly inhibit translation through a steric hindrance mechanism (409). Qu et al. demonstrated that ISG20, but not an exonuclease-deficient mutant, associates with FLUAV nucleoprotein during infection, resulting in a block of viral translation (409). It is not clear however whether this interaction is mediated by protein-protein interactions, or facilitated through an RNA intermediate (409). While this work offers a potential alternative mechanism for ISG20-mediated virus restriction through altered translation kinetics, the predominantly cytoplasmic localization in these overexpression studies raises significant questions regarding the conclusions. This specific FLUAV nucleoprotein interaction also does not account for a more general translation-blocking mechanism for other virus species that do not have nucleoprotein-bound RNA genomes.

1.3.3.2 Cajal Bodies
The sub-nuclear localization of endogenous ISG20 to CB may offer some insight into its mechanism of antiviral activity. CB are complex structures of protein and RNA associated with dozens of individual proteins and guide RNAs plus target RNAs and complexed proteins (417).

These dynamic structures are highly mobile within the nucleus and can travel and associate with various genomic structures (416, 418). CB function is best understood for their role in recruiting and processing small-nuclear RNAs (snRNAs) of the spliceosome (415). Indeed, CB associate around the gene loci for snRNAs and small-nucleolar RNA (snoRNA) targets they post-transcriptionally modify (419-422). The nucleation and mobilization of CB around their target loci is mediated by active Pol II transcription at these sites and requires unprocessed U2 snRNA (415, 416, 423-425).

Over the course of CB-associated maturation, snRNAs pass through the CB multiple times in order to complex with essential proteins and receive post-transcriptional modifications (426, 427). Within the CB, snRNAs are methylated and pseudouridylated at specific residues, guided by the small CB-specific RNAs (scaRNAs), and are loaded in complex with spliceosomal proteins for maturation of the small nuclear ribonucleoprotein particles (snRNPs) (428, 429). In addition to final maturation and assembly of snRNPs, CB function as a non-essential catalyst for re-assembly of these complexes in transcriptionally active cells with rapid spliceosome turnover (430). In addition to their role in processing snRNAs, the CB is also essential for the processing of snoRNAs of the nucleolus, providing hypermethylation and trimming of the 3'-end (431, 432). Of note, CB function in the processing and final maturation of numerous snoRNAs lacking a 7-methyl-guanosine cap structure (432-435). Recent evidence also suggests CB may play a role in telomerase RNA biogenesis in humans (436, 437). However this may not be a well-conserved function across species as mice lack this activity (438).

1.4 HYPOTHESIS

The human alphaviruses are an important genus of RNA viruses with severe pandemic potential and risk of misuse as biological weapons. While the antiviral activities of IFN-α/β have been well documented for many alphaviruses, relatively little is known about the individual effectors that restrict replication and dissemination. Elucidating the molecular mechanisms of ISG antiviral activity is important for a general understanding of innate immune responses, and is particularly pertinent to the study of virus attenuation for rational vaccine design and identification of therapeutic targets. For example, understanding the mechanism of IFIT1 antiviral activity and viral evasion strategies has led to a novel approach to developing attenuated alphavirus vaccine candidates (data not shown). Similar attempts to probe antiviral mechanisms have been made with other ISGs with potent restrictive phenotypes (349-351, 355-359).

Utilizing a systems biology approach, our lab previously sought to identify ISGs with antiviral activity against the canonical alphavirus, SINV (339). This screen yielded 44 genes of interest for follow-up study, and ultimately identified three proteins with highly restrictive phenotypes (339, 340). Two of these genes, IFIT1 and ZAP have been the subject of extensive mechanistic research. With regards to alphavirus infection, IFIT1, an RNA binding protein with the ability to bind type-0 capped RNAs, recognizes an exposed alphavirus 5' cap and sequesters viral RNA away from translation machinery (3). ZAP, another RNA binding protein, acts as a binding platform to assemble a functional antiviral complex with hitherto unknown function (350, 351). The third protein, ISG20, is a nuclear 3'-5' exonuclease whose antiviral activity has been the subject of numerous studies with both RNA and DNA viruses.

While it has been determined that the ISG20 exonuclease activity is essential for its antiviral effect, there is no clear understanding of how ISG20 suppresses viral replication. Work

43

from two groups using viruses with different replication strategies has indicated that ISG20 does and does not directly degrade viral RNAs (410, 411). Further confusing these data, ISG20 primarily localizes to the sub-nuclear Cajal body, a fluid structure involved in the processing of numerous small RNAs and assembly of spliceosomes (404). As such, viral RNAs from genera that replicate solely in the cytosol, including the *Alphaviruses*, would likely not come in direct contact with ISG20 in the context of normal infection. Another mechanism has been proposed, suggesting ISG20 inhibits translation of viral proteins through protein-specific interaction with viral nucleoproteins (409). Such a mechanism, however, would not likely account for the broad antiviral activity of ISG20 observed against numerous virus families.

Questions remain whether ISG20 exhibits uniform antiviral activity against human alphaviruses capable of causing significant disease, and how ISG20 achieves this antiviral activity. Herein, I describe our attempts to answer these questions and elucidate the antiviral activities of ISG20 in context of alphavirus infection with both WT and attenuated alphavirus strains in cell culture and in a recently-developed *Isg20*-deficient mouse model.

- In Chapter 2, I hypothesize that ISG20 achieves its broad antiviral activity through an indirect mechanism, both dependent on its exonuclease function, and independent of direct viral RNA degradation in the cytoplasm.

- In Chapter 3, I hypothesize that alphaviruses, particularly mutants sensitive to other effectors of the type I interferon system, are subject to reduced antiviral restriction in *Isg20*$^{-/-}$ mice compared to WT.

The results of this study will elucidate potential mechanisms of ISG20 antiviral activity against alphaviruses, and demonstrate an approach for utilizing ISG20 for rational strategies of alphavirus attenuation and vaccine design.

44

2.0 ISG20 RESTRICTS ALPHAVIRUS REPLICATION IN VITRO THROUGH AN IRF3-DEPENDENT INDUCTION OF ANTIVIRAL FACTORS

2.1 INTRODUCTION

Innate immune responses provide a first line of defense against many pathogens and act to stimulate adaptive immune responses, which in turn help to clear infections and generate a lasting immunological memory. Stimuli from invading viruses trigger pathogen recognition receptors, which signal infected cells to produce early antiviral effectors and cytokines to alter gene regulation programs in neighboring cells. The most widely studied antiviral innate immune cytokine produced from this process, type I interferon (IFN), signals through its heterodimeric receptor (IFNAR1/IFNAR2) on infected and uninfected cells and activates the IFN-stimulated gene factor 3 complex (ISGF3) to transcribe a targeted set of interferon stimulated genes (ISG). These ISGs control a variety of antimicrobial functions by indirectly or directly limiting replication of the invading pathogen (439).

Alphaviruses are small, single-stranded RNA viruses that are spread via the bite of an arthropod vector. These include the arthritogenic Old World viruses such as chikungunya (CHIKV), Sindbis (SINV) and Ross River (RRV) viruses and the encephalitogenic New World

viruses such as eastern (EEEV) and Venezuelan (VEEV) equine encephalitis viruses. Together, these viruses include widespread emerging pathogens as well as one of the most acutely virulent RNA viruses known. Several studies have revealed a role for individual IFN-α/β upregulated effector proteins in controlling alphavirus infection (3, 329, 339, 340, 354, 366, 440, 441). One contributor to the IFN-α/β antiviral response against alphaviruses that is particularly potent *in vitro* is the 20-kDa exonuclease, interferon stimulated gene 20 (ISG20) (340). ISG20 is a member of the RNA-specific DEXD family of 3'-5' exonucleases and is localized predominantly in the dense, sub-nuclear structures of protein and RNA called Cajal bodies (399, 400, 404). ISG20 has been shown to restrict infection of multiple RNA and DNA viruses (340-342, 405-407, 409-411). Due to the capacity of ISG20 to degrade RNA nonspecifically *in vitro* and its limited effect on DNA viruses, it has been assumed that ISG20 targets viral RNA, resulting in degradation of the viral genome. However, this presumed activity has not been demonstrated in live cells where ISG20 and viral RNA are largely confined to different subcellular locations. The alphavirus genome is replicated entirely in the cytoplasm of infected cells, and would not typically make contact with a nuclear-localized protein.

Here, we describe the antiviral activity of murine ISG20 and its effect on alphavirus replication in an optimized murine cell culture system. Overexpression of ISG20 in fibroblasts potently restricted the replication of multiple alphaviruses through a block in viral translation before replication occurred, but, surprisingly, did not accelerate the degradation of viral RNA. However, the replication-blocking activity was dependent upon the presence of an intact ISG20 exonuclease domain. In the absence of viral infection or IFN gene induction, overexpression of ISG20 but not a nuclease domain mutant, resulted in the induction of multiple genes, many of which have described or predicted antiviral activity. In this *in vitro* system, the induction of

46

antiviral genes was primarily dependent upon IRF3 transcription factor activity. Notably, IFIT1 was consistently among the genes most upregulated by ISG20 overexpression. IFIT1 has been shown to play a prominent role in host cell recognition of non-self RNAs and suppression of viral mRNA translation (3). Notably, an IFIT1-sensitivie mutant of VEEV was significantly more susceptible to ISG20 overexpression activities *in vitro*. Together, the *in vitro* data provided herein suggests a role for ISG20 as an activator of IRF3 and regulator of steady-state antiviral activity against both arthritogenic and encephalitogenic alphaviruses.

2.2   RESULTS

2.2.1   Murine ISG20 Expression Potently Restricts Alphavirus Replication *in vitro*

We first evaluated the antiviral activity of ISG20 against CHIKV and VEEV using a stable, inducible overexpression system. Two separately-derived clonal lines of tetracycline-inducible (tet-off) MEF cells overexpressing C-terminal FLAG-tagged murine ISG20, a homologous mutant of ISG20^{D94G} (ExoII) shown in human ISG20 to disrupt the exonuclease activity through the Exo II domain (400), and enhanced green fluorescent protein (eGFP) or firefly luciferase (fLuc) as non-antiviral controls (340) were generated. We confirmed overexpression of each protein by western blot against the FLAG epitope tag (**Figure 4A**). Cellular localization of ISG20 was consistent with the published literature, forming dense nuclear puncta in confocal micrographs with additional diffuse cytoplasmic localization concentrated around the nuclear envelope (**Figure 5A**). To determine the magnitude of antiviral restriction by ISG20, tet-off cells were induced for 72 hours and infected with WT CHIKV and VEEV, as well as an attenuated mutant, VEEV-G3A,

47

that possesses one of the mutations acquired by the VEEV TC83 vaccine strain during cell adaptation. This mutation alone confers decreased pathogenesis in mice due to a sensitivity to the IFIT1 antiviral effector (3). Overexpression of ISG20 reduced replication by approximately 100-fold by 12 and 24 hours p.i. in both WT CHIKV- and VEEV-infected MEFs (**Figure 4B-C**). However, replication in the presence of the homologous ExoII mutant proceeded uninhibited, similar to eGFP control MEFs. Interestingly, replication of VEEV-G3A was restricted entirely at 6 and 12 hours p.i. by ISG20 overexpression, and was still restricted over 1000-fold by 24 hours p.i. (**Figure 4D**). VEEV-G3A exhibited similar growth kinetics comparing the GFP control and catalytically inactive ISG20 ExoII overexpressing MEFs.
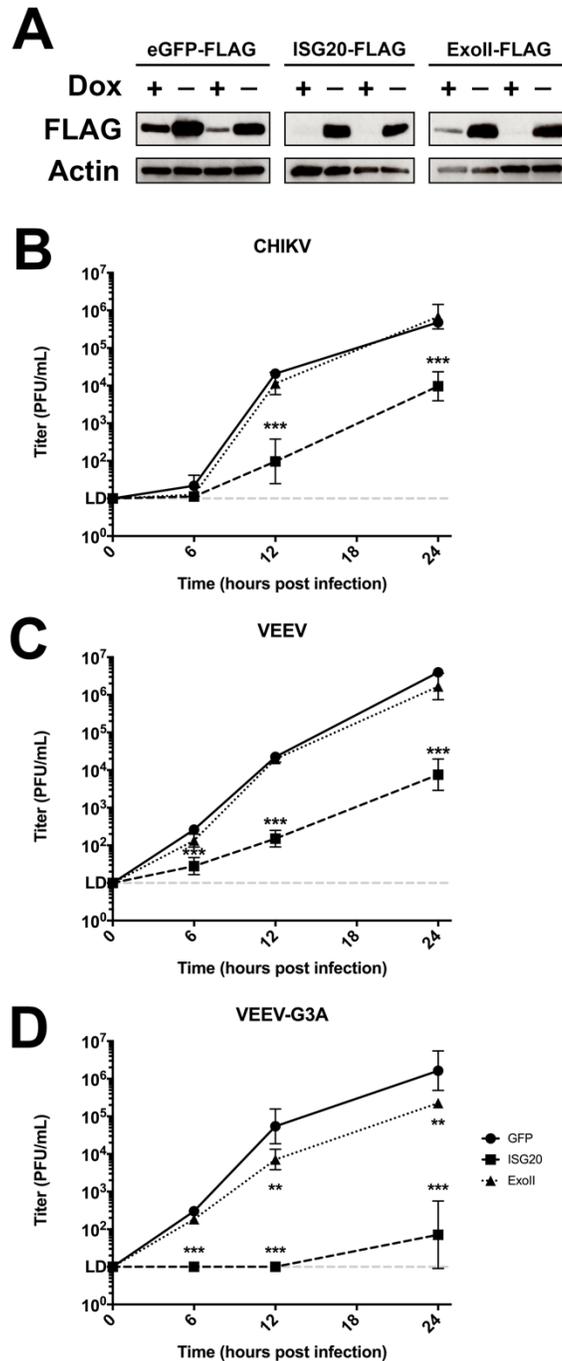
Figure 4: ISG20 Overexpression Restricts Wild-Type and Mutant Alphavirus Replication *in vitro*.

(**A**) Two clones of tet-off MEFs expressing FLAG-tagged eGFP, murine ISG20, or the exonuclease domain mutant murine ISG20^{D94G} (ExoII) were induced for 72 h then immunoblotted for FLAG-tag to demonstrate inducible overexpression. Induced tet-off MEFs were infected with (**B**) WT CHIKV, (**C**) WT VEEV or (**D**) VEEV-G3A (MOI of 0.1). Replicated virus is measured from cell supernatants by BHK-21 plaque assay. * $P < 0.05$, ** $P < 0.01$, *** $P < 0.001$; 2-Way ANOVA with Holm-Sidak post-hoc analysis against eGFP control (n=6).

49

The CHIKV- or VEEV-TaV-GFP reporter viruses were used to determine whether ISG20 restriction was a result of fewer cells initiating infection or a uniform reduction in replication efficiency. Fluorescent microscopy for eGFP revealed both a lower overall number of eGFP-positive cells in both CHIKV and VEEV (**Figure 5B-C**). Again, the ExoII mutant did not exert an inhibitory effect compared to the fLuc control.
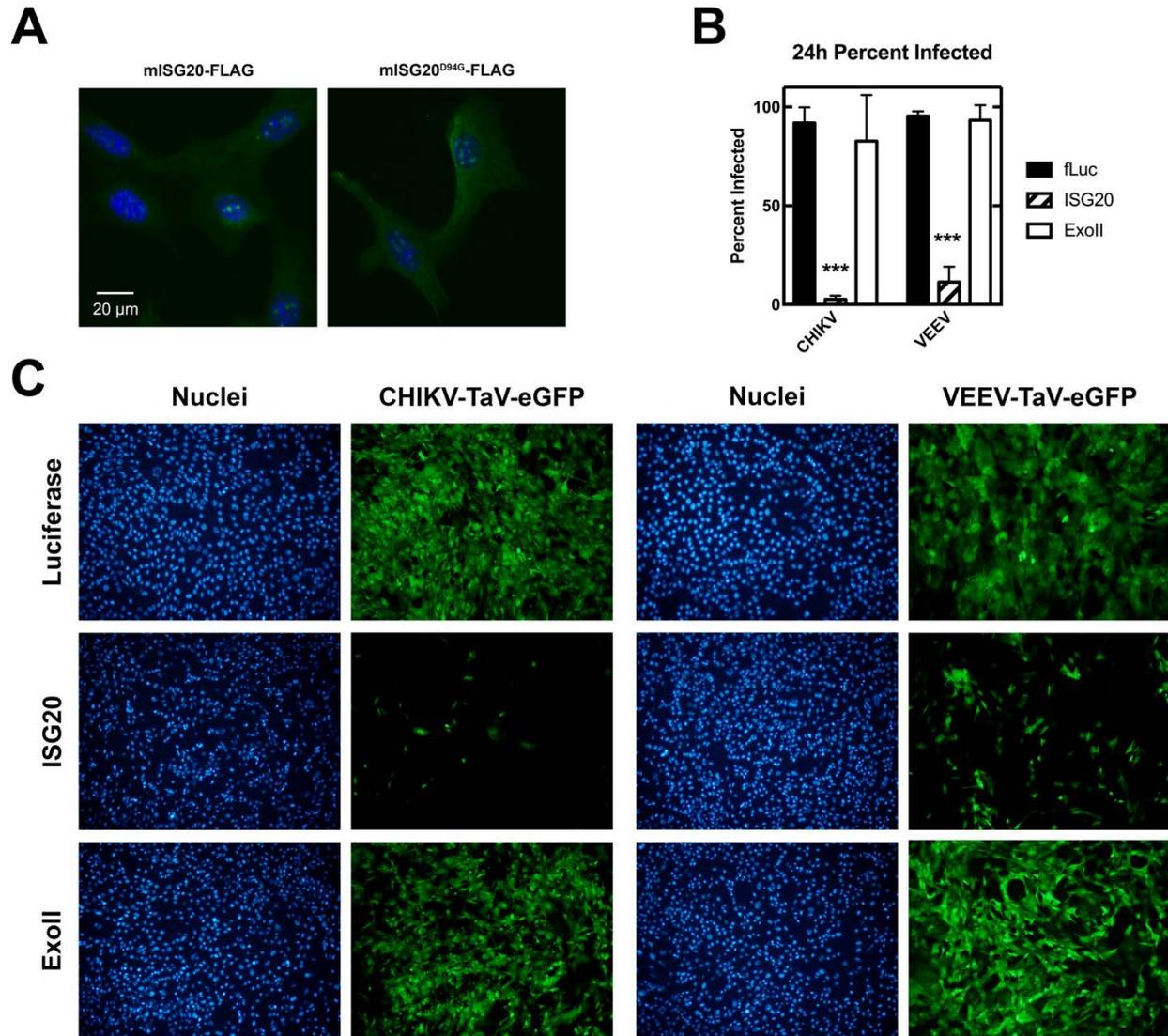
Figure 5: ISG20 Overexpression Reduces the Number of Productively Infected Cells.

(**A**) Tet-off MEFs expressing murine ISG20-FLAG were grown on glass cover slips and induced for 72 h. ISG20 was detected by FITC-conjugate anti-FLAG (M1) monoclonal antibody and localization was determined by confocal microscopy. Images represent an averaged z-stack projection at 100x objective magnification. (**B-C**) Tet-off MEFs expressing the indicated protein were infected with CHIKV-TaV-eGFP or VEEV-TaV-eGFP fluorescent reporter virus (MOI of 1) and imaged by epifluorescence microscopy at 24 h.p.i. *** $P < 0.001$; 2-Way ANOVA with Holm-Sidak post-hoc analysis against eGFP control (n=6)

2.2.2 Exposure to CHIKV does not Change ISG20 Localization

The nuclear localization of ISG20 has been demonstrated in the context of overexpression and IFN treatment of cells, but has not been demonstrated conclusively in the context of viral infection (404). Leong et al. recently published a putative function of ISG20 interacting with FLUAV nucleoprotein, leading to a block in viral translation (410). However, overexpressed ISG20 in their system favored cytoplasmic localization, contrary to the prior literature. Because alphaviruses replicate exclusively in the cytoplasm, it is necessary to determine whether ISG20 remains localized to nuclear puncta, or whether it redistributes in the context of viral infection, potentially associating with alphavirus proteins or RNA in the cytoplasm. Induced MEFs overexpressing eGFP, ISG20 and ExoII were infected for 24 hours with CHIKV-TaV-mCherry and subjected to confocal microscopy for FLAG-tagged ISG20 and virus. ISG20 overexpressing cells did not show significant CHIKV reporter signal at 24 hours p.i. (**Figure 6**), similar to previous data with CHIKV-TaV-eGFP (**Figure 5B**). While these cells were exposed to CHIKV, ISG20 localization remained consistent (**Figure 6**). ExoII MEFs were efficiently infected and show a reduction in total non-viral gene expression as expected, with an observed overall reduction in ExoII expression rather than a specific change in localization from the nucleus to the cytoplasm (**Figure 6**).
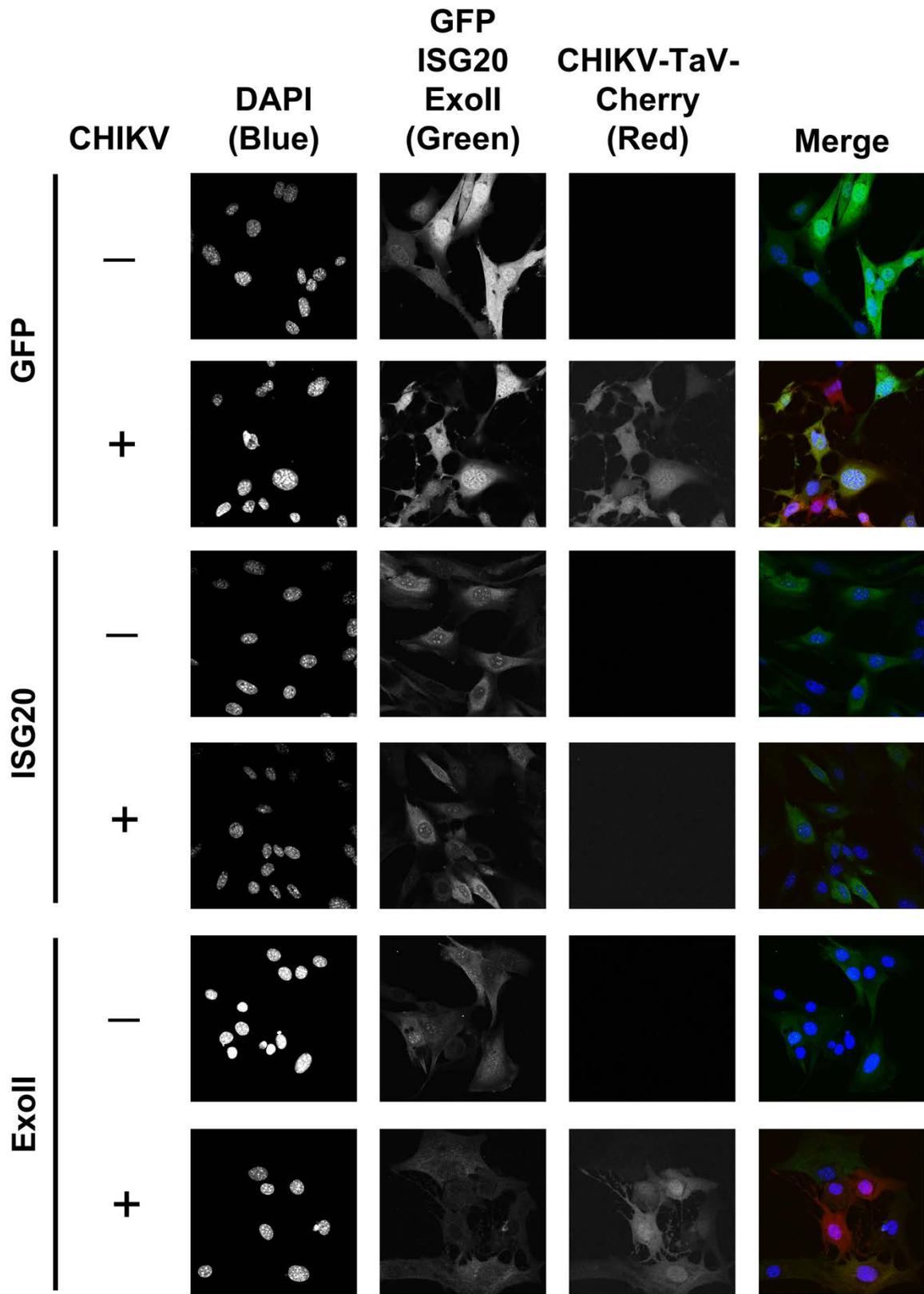
2.2.3   ISG20 Overexpression Leads to a Block in Virus Genome Translation

To narrow down the point of ISG20 intervention in the alphavirus replication cycle, we infected MEFs overexpressing either ISG20 or control proteins with CHIKV- and VEEV-nsP3-nLuc viruses. Reporter signal from these viruses requires translation of the nonstructural polyprotein, an event that requires translation of the full-length genome, and is not indicative of the later subgenomic RNA transcription and translation. The observed reduction of early CHIKV and VEEV non-structural reporter signal by 6-hours p.i. in the presence of ISG20 indicates a block in replication before the translation of the nonstructural polyprotein, one of the earliest stages in alphavirus replication following entry and capsid disassembly (**Figure 7A-B**). Interestingly, both CHIKV and VEEV appear to be similarly inhibited prior to nonstructural protein synthesis, indicating a broad action of ISG20 against members of the *Alphavirus* genus.
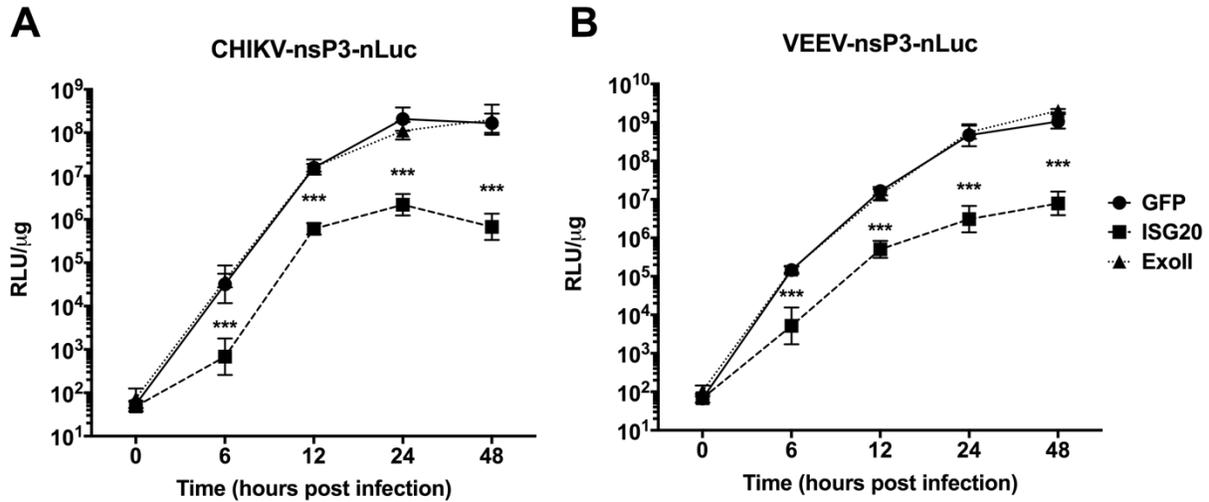
Figure 7: Early Events in Alphavirus Replication are Inhibited by ISG20 Activity.

Tet-off MEFs overexpressing the indicated protein were infected with (**A**) CHIKV-nsP3-nLuc or (**B**) VEEV-nsP3-nLuc non-structural reporter viruses at MOI=0.1 and lysates were collected at the indicated time points. Reporter signal is given as a ratio of relative intensity normalized to cellular protein. *** $P < 0.001$; (**A-B**) two-way ANOVA. (n=6)

Next, we tested whether ISG20 is capable of directly blocking the translation of incoming RNAs using reporters consisting of firefly luciferase flanked by the 5' and 3' non-translated regions from a host RNA, CHIKV or two unique internal ribosomal entry site (IRES) structures (**Figure 8A**) (125). This transfection-based approach removes the steps of binding and entry, allowing for a more direct visualization of initial viral macromolecular synthesis. Transfection of these constructs in MEFs overexpressing eGFP, ISG20 and ExoII revealed a marked decrease in the translation of the CHIKV-mimic reporter as well as the type-0 capped host-mimic reporter in the presence of ISG20 (**Figure 8C**). Notably, this effect was absent in the ExoII overexpressing cells, indicating that translation arrest is not an intrinsic characteristic of ISG20 overexpression, but is instead a specific activity of its functional exonuclease domain. IRES sequences can be utilized by some RNAs to initiate translation without the use of some or all components of the cap-dependent translation machinery (442). The IRES from encephalomyocarditis virus (EMCV)

requires all cap-dependent translation initiation factors to be present in order to initiate translation whereas the IRES used by cricket paralysis virus (CrPV) requires no additional host or viral factors to initiate translation (442). Transfected EMCV and CrPV IRES reporters were unaffected by ISG20, suggesting a targeted block in some cap-dependent translation rather than a global change in protein metabolism (**Figure 8D-E**). Furthermore, the ability of the EMCV IRES to escape translation arrest suggests that ISG20 is not triggering a broad block in cap-dependent translation through disruption of the eIF complex, but instead leads to a targeted recognition of alphavirus RNA elements used for translation initiation. Interestingly, these findings are similar to results obtained when evaluating the effects IFN-α/β treatment on virus reporter translation (128).
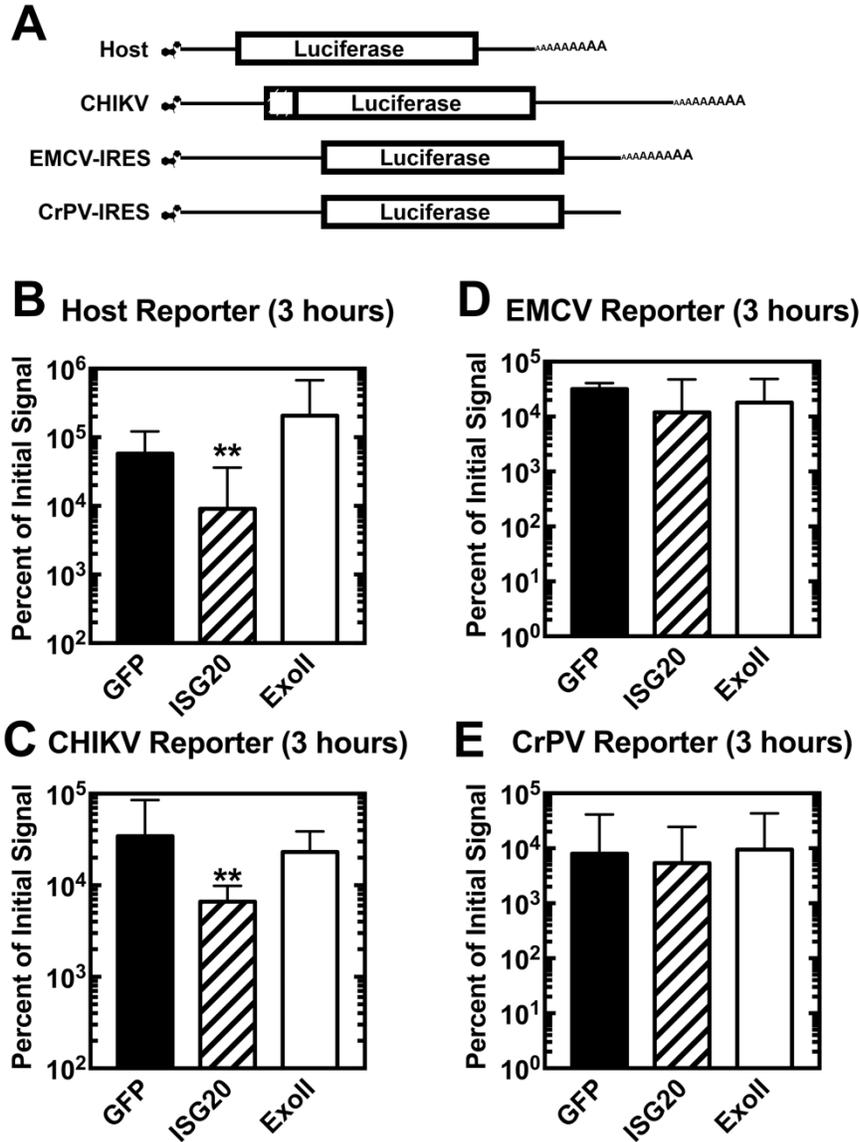
Figure 8: ISG20 Restricts Translation of Type-0 Capped, Non-IRES-Containing RNAs.

(**A**) Schematic representation of type-0 capped and poly-adenylated non-replicating translation reporters. Luciferase gene is flanked by 5' and 3' non-translated regions for the indicated mRNA mimic. (**B-E**) Induced tet-off MEFs overexpressing the indicated protein were electroporated with 7.5 μg of indicated RNA then sampled at the peak of reporter signal, 3 hours. Relative luminescence is given as a percentage of signal at t_0 (30 min post transfection). ** $P < 0.01$; (**B-E**) two-way ANOVA. (n=12)

2.2.4   ISG20 Overexpression Does Not Accelerate Decay of the CHIKV RNA 3'-Terminus

ISG20 was previously characterized as a 3'-5' exoribonuclease capable of degrading non-specific RNA targets in a processive manner *in vitro* (400). Testing the effects of ISG20 overexpression on degradation of viral RNA requires introduction of RNA into the cell cytoplasm, in the context where RNA replication is inhibited such that only the introduced RNA is detected. Cycloheximide, a potent global inhibitor of translation, was shown to block translation of the CHIKV non-structural polyprotein and sufficiently inhibit virus replication to decouple this effect (**Figure 9A**). Induced tet-off MEFs overexpressing ISG20, ExoII, or control eGFP, were then infected with WT CHIKV (MOI=5), and treated with cycloheximide in the inoculum and culture media. Primers for qRT-PCR were designed to target the 3' terminus of CHIKV to detect the earliest signs of 3'-5' degradation within the 3' non-translated region, as would be expected from the characterized exonuclease activity of ISG20. qPCR analysis revealed a very gradual loss of CHIKV 3'-terminus signal over time in each of the tet-off MEFs, with no significantly acceleration in RNA decay from ISG20 overexpression (**Figure 9B**). Therefore, overexpression of ISG20 does not appear to accelerate the decay of viral RNA per its catalytic activity *in vitro*, suggesting an alternative pathway for translation suppression.
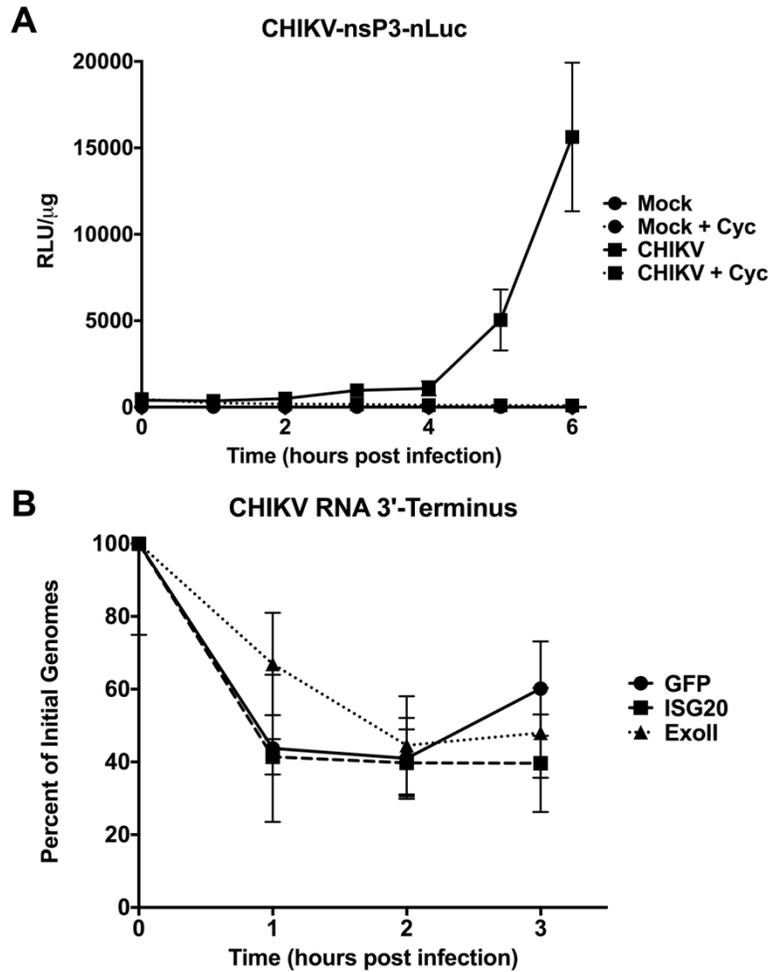
Figure 9: ISG20 Overexpression does not Accelerate Decay of CHIKV Viral RNA.

(**A**) MEFs were infected with CHIKV-nsP3-nLuc then treated with 0 or 10 μM cycloheximide to block translation, and ultimately replication, of CHIKV viral RNA. (**B**) MEFs were infected with WT CHIKV (La Réunion) then treated with 10 μM cycloheximide. RNA was collected at the indicated time p.i. and analyzed by qRT-PCR for the CHIKV 3' terminus. RNA degradation is represented as a percentage of signal at t=0 hr. Not significant; (**A-B**) two-way ANOVA. (n=6)

Additionally, we examined whether virus RNA was functionally inhibited through irreversible modification, including degradation, by exposure to overexpressed ISG20 (**Figure 10**). In this case, non-replicating translation reporter RNA, which is highly repressed in ISG20 expressing cells, was transfected into control or ISG20-expressing cells, harvested after 3 hours along with total cellular RNA and then re-transfected into control cells. RNA harvested from

control or ISG20-expressing cells exhibited similar translation activity after re-transfection, suggesting no functional differences (**Figure 10B**).
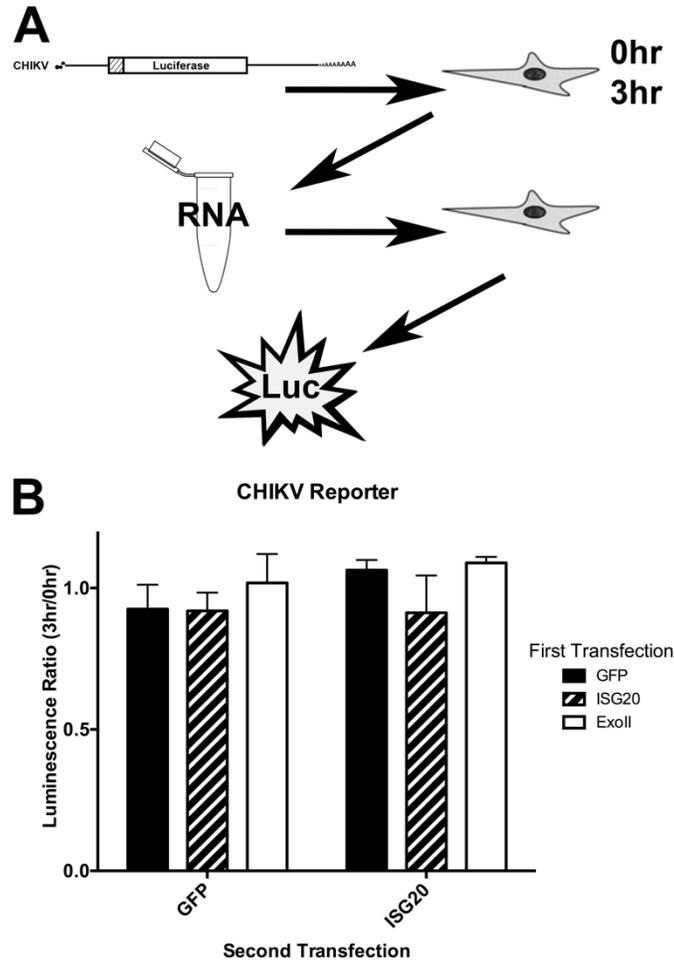
Figure 10: Integrity of Non-replicating RNA is not Altered by Cellular Exposure to ISG20.

(**A**) Schematic representation of the experimental workflow is shown. Tet-off MEFs overexpressing eGFP, ISG20, or ExoII mutant were transfected with 7μg of non-replicating CHIKV-mimic reporter RNA and RNA lysates were taken at 0 and 3 hours post electroporation. RNA was extracted and re-transfected in MEFs overexpressing either eGFP or ISG20 for 3 hours. Lysates were collected in passive lysis buffer and assayed for firefly luciferase reporter activity. (**B**) Luciferase activity from second transfections is given as a ratio of firefly luciferase signal from 3 hour versus 0 hour samples taken from first transfection. Not significant; (**B**) Mann-Whitney test. (n=6)

2.2.5   ISG20 Overexpression Regulates a Focused Gene Expression Response

Previously, we identified an effect of IFN on virus genomic translation mediated by gene upregulation after IFN-α/β treatment associated with production of multiple antiviral gene products (128, 339). Since alphavirus replication and translation reporter activity were both strongly inhibited by ISG20 in the absence of effects on RNA stability, resembling IFN-α/β treatment, we used a transcriptomics approach to determine if the regulation of other antiviral or IFN-induced genes was altered in the ISG20 overexpressing cells.

RNA deep sequencing (RNA-seq) of MEFs overexpressing ISG20 in the absence of infection revealed a unique pattern of gene regulation that was independent of IFN stimulation. The most highly upregulated genes, which exhibited a five-fold or greater induction compared to both control and ExoII mutant cells, tended to have known antiviral activity or were known to be inducible by type I or II IFN (**Figure 11A**). No IFN-α/β, IFN-γ or IFN-λ genes were significantly upregulated by ISG20 overexpression as determined by RNA-seq and qRT-PCR. Among the top gene targets identified were several IFN-inducible proteins with tetratricopeptide repeats (IFIT family) including *Ifit1* and *Ifit3*, as well as multiple IFIT-like genes (**Figure 11B**). Interestingly, not all IFIT family proteins were upregulated, with Ifit2 standing out as an ISG that was not affected by ISG20 overexpression. Additionally, several complete gene families such as the ubiquitin-like *Isg15*, the ISG15 E3-ligase, *Herc6*, and the de-ISGylating *Usp18* were induced (**Figure 11B**). Upregulated genes also of note were multiple IRF and STAT genes, and the viral RNA-sensing helicase *Ddx58* (RIG-I). Network analysis of ISG20 overexpression highlighted a pattern similar to that of viral infection or IFN response without the primary signaling components of type I, II or III IFN or their receptors being induced (**Figure 11A**). In addition to IFN-like

responses, eIF2 signaling, eIF4 signaling and mTOR signaling were increased in response to ISG20 in the cell culture system (**Figure 11A**).
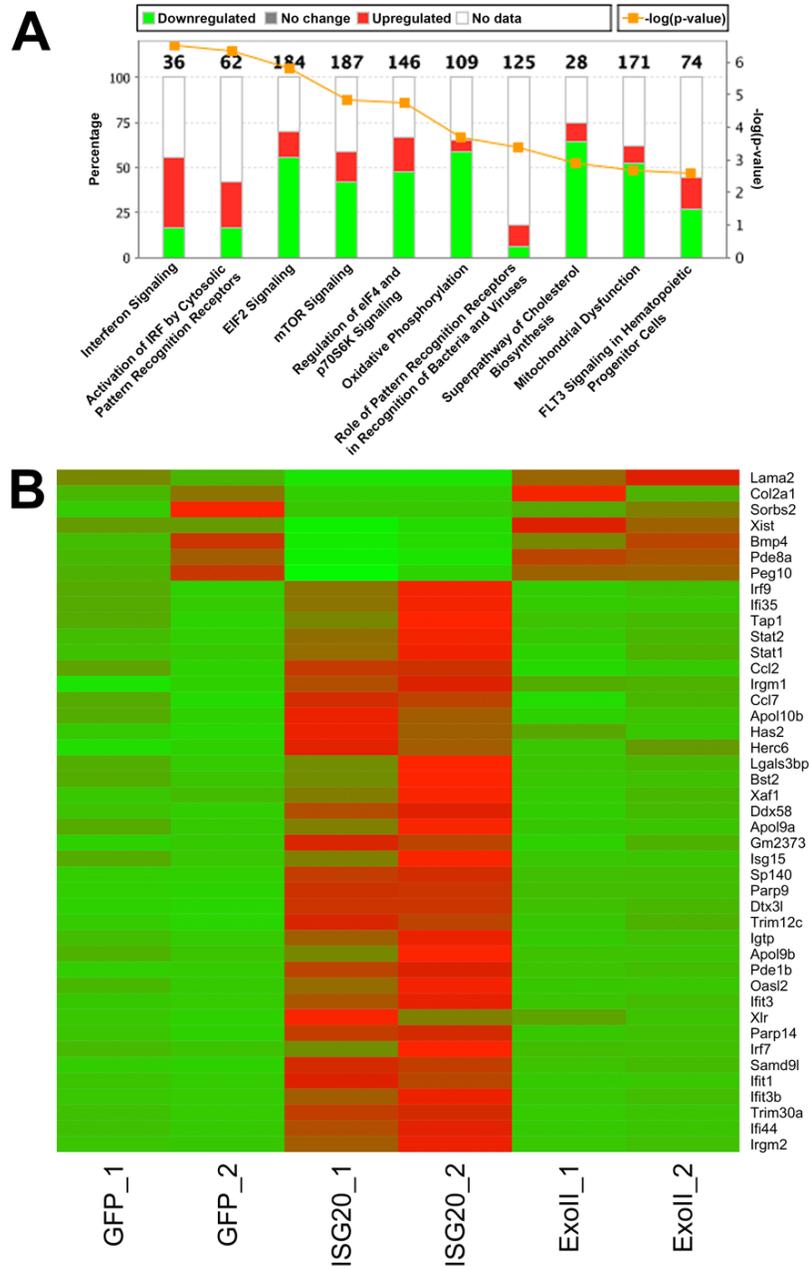
Figure 11: ISG20 Overexpression in the Absence of Infection Results in Targeted Gene Upregulation.

RNA-seq was performed on MEFs expressing eGFP and ISG20. (**A**) Differential gene expression was analyzed and upregulated canonical pathways are shown. (**B**) A heat map of the most significant ISG20-induced genes is shown. Temperature ranges are shown as fragments per kilobase of transcript per million mapped reads (FPKM) from green (low) to red (high). $P < 0.001$; Cuffdiff 2 gene expression model, FDR = 5%. (n=2)

Upregulation of the most significantly induced set of genes from RNA-seq were independently confirmed by qRT-PCR (**Figure 12A**). *Ifit1*, was consistently upregulated approximately ten-fold over basal levels in ISG20 overexpressing cells (**Figure 12A**). This upregulation in mRNA levels led to increased protein expression that was specific to a functional ISG20 protein (**Figure 12B-C**).
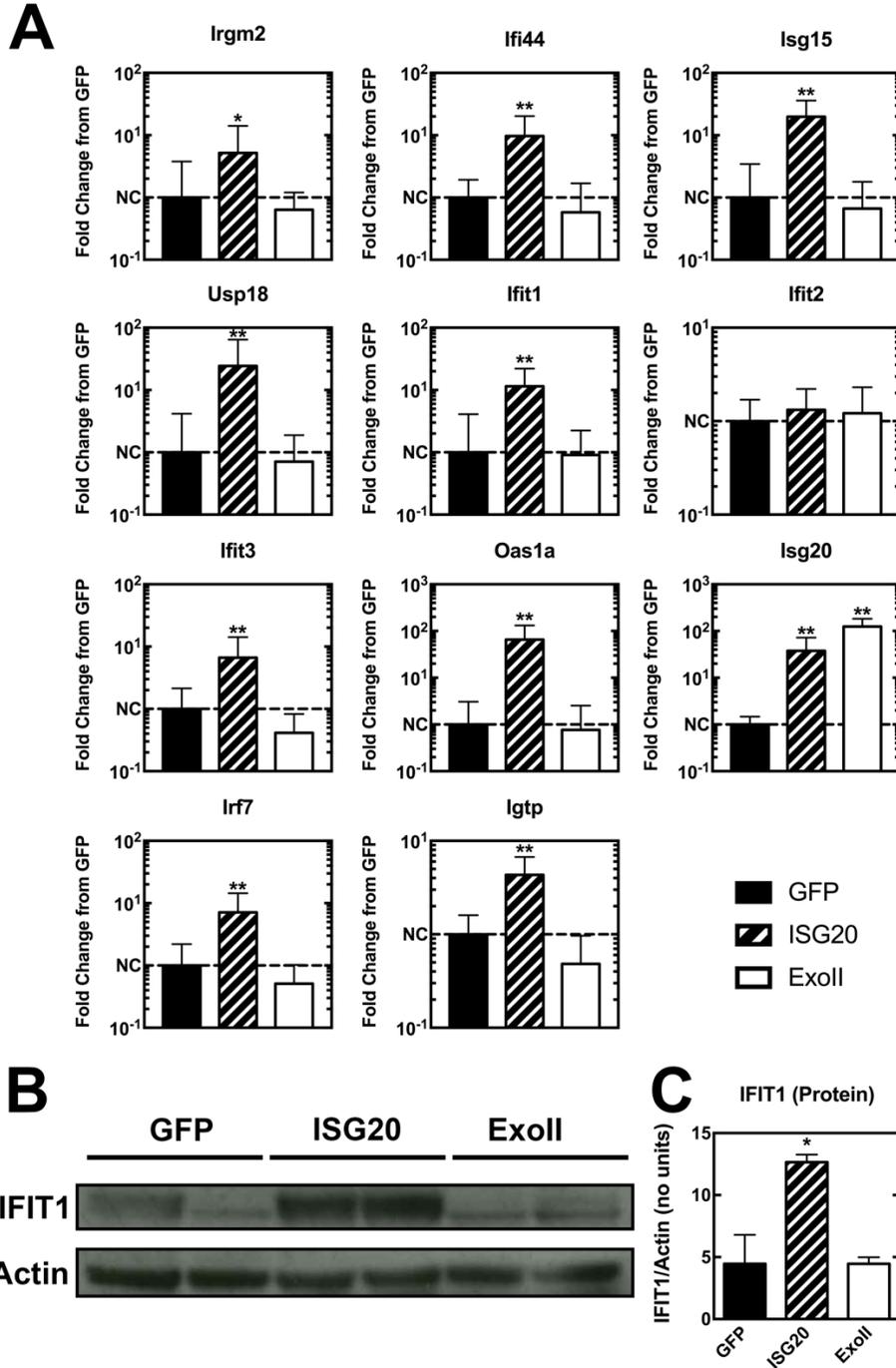
Figure 12: Overexpression of ISG20 Upregulates Antiviral Factors *in vitro*.

Tet-off MEFs expressing eGFP, ISG20, or ExoII mutant were induced for 72 h, and total cellular RNA and protein were collected. (**A**) A selection of genes identified to be induced by ISG20 overexpression through RNA-sequencing were confirmed by qRT-PCR or (**B**) IFIT1 protein induction was confirmed by western blot for two independent clones of each overexpressing cell line and quantified in (**C**). (**A,C**) * $P < 0.05$, ** $P < 0.01$; Mann-Whitney test. (n=6)

2.2.6 ISG20-mediated Gene Induction Profile Involves IRF3

Interestingly, many of the genes unregulated by ISG20 are also upregulated by IRF3 activation (383). Indeed, our pathway analysis of the ISG20-regulated genes implicates IRF3 as a candidate for regulating the ISG20 response (**Table 4**). To elucidate the role of IRF3 activity in mediating ISG20 induction of ISGs, we transfected luciferase plasmids containing the complete IFN-β promoter or its constituent two IRF3-binding elements and one NF-κB-binding element individually into our overexpression MEFs. ISG20 overexpression leads to an increase in luciferase expression in cells transfected with the entire IFN-β promoter as well as cells transfected with the partial promoter containing only the two IRF3 components (**Figure 13A**). Notably, the NF-κB element alone was insufficient to significantly drive ISG20-stimulated promoter activity (**Figure 13A**), consistent with previous findings that NF-κB is a poor stimulator of the IFN-β promoter on its own (443). The stimulation of these promoters in the presence of ISG20 overexpression alone was similar to cells treated with lipid-transfected poly-(I:C) (**Figure 13A**). Expression of the exonuclease-deficient ExoII mutant did not drive promoter activity of the complete IFN-β promoter or its constituent elements, and responded poorly to poly-(I:C) treatment, consistent with previous reports describing a dominant negative effect of ExoII on the antiviral activities of IFN (**Figure 13A**) (405). Furthermore, siRNA knockdown of IRF3 in tet-off MEFs overexpressing ISG20 revealed a significant reduction in ISG20-modulated gene upregulation versus a non-targeting control for multiple gene targets (**Figure 13B**). Together, these findings indicate that IRF3 is largely responsible for the transcription profile observed with ISG20 overexpression. Despite apparent upregulation of IRF3-responsive genes, IFN genes were not among the transcripts upregulated by ISG20 overexpression (**Table 2**). To confirm this, we

assessed functional type I IFN production in induced tet-off MEFs in the presence or absence of poly-(I:C) lipid transfection. ISG20 induction alone was not sufficient to produce secreted IFN, though all MEFs produced similar levels of IFN in response to the TLR3 agonist, poly-(I:C) (**Figure 13C**).
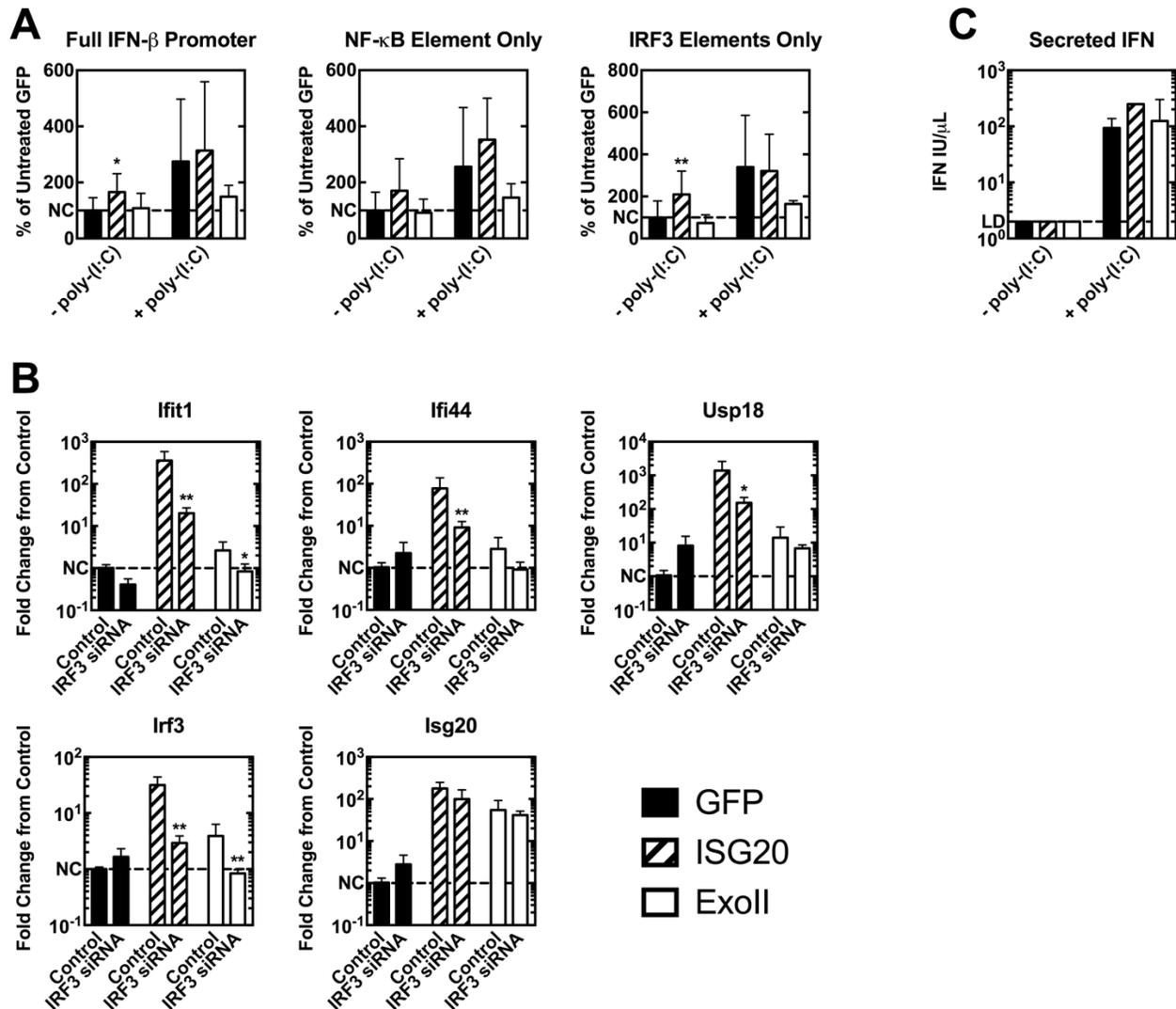
Figure 13: ISG20 Regulates Targeted Gene Expression through IRF3 Activation.

(**A**) MEFs expressing eGFP or ISG20 were induced and transfected with luciferase driven by IFN-β promoter (pβLUX), or the IRF3 responsive elements (PRDI/III) and NF-κB element of the IFN-β promoter (PRDII). Induction is given as a ratio of firefly luciferase expression to SV-40 promoter-driven Renilla luciferase. (**B**) MEFs expressing GFP, ISG20 and ExoII mutant were induced and treated at 24 h with siIRF3 or siRNA scramble for an additional 48 h. Selected genes were assessed by qRT-PCR and induction levels are given as fold-change from scram-treated GFP control. (**C**) IFN was measured in the tet-off MEF cell culture supernatant before and after poly-(I:C) lipid transfection. * $P < 0.05$, ** $P < 0.01$, *** $P < 0.001$; (**A,C**) ANOVA with Dunnett post-hoc analysis (n=6), (**B**) Mann-Whitney test (n=6).

2.3   DISCUSSION

Type I IFN-stimulated genes play multiple roles in detecting and suppressing virus replication. Over 300 gene products can be induced by type I IFN, creating a restrictive environment that may have both general and specific viral- and microbial-family targets. The activity of numerous ISGs has now been elucidated through extensive study of the molecular basis of target restriction, but the antiviral activity of many continues to remain elusive. *ISG20* was first biochemically characterized as an IRF1-induced gene with high homology to DEDD-domain nucleases in the same family as the *S. cerevisiae rex4p* gene (400, 402). An activity of ISG20 demonstrated *in vitro* was non-specific degradation of single-stranded nucleic acid substrates with a preference for ssRNA, showing a 3'-5' exonuclease activity (400).

Antiviral activity for ISG20 in cells has been shown through overexpression for a number of RNA viruses (340-342, 405-407, 409-411), including the prototypical alphavirus, SINV (340). However, these studies did not define the mechanism of ISG20 restriction on RNA virus replication in cells or animals. In the present study, we sought to establish a model system for determining the molecular basis of the restriction by ISG20. Stable overexpression of the dominant murine ISG20 (isoform b), which bears 82% homology to human ISG20, had a significant restrictive influence on CHIKV, VEEV, and VEEV-G3A replication *in vitro*, consistent with earlier findings with SINV (340). Introduction of a homologous glycine mutation at the catalytic aspartic acid D94 in the ExoII exonuclease domain was sufficient to abrogate the antiviral activity of ISG20 *in vitro*, consistent with the published role of ISG20 catalytic activity on its antiviral function.

Recent reports have suggested that ISG20 may be directly involved in viral RNA degradation, accounting for its observed antiviral activities. Findings with hepatitis B virus suggest

that ISG20 restricts viral replication through a direct degradation of viral RNAs and genomic intermediates produced over the course of infection (410, 444). In our cell culture model, the extreme 3' terminus of the CHIKV genome was protected from ISG20-mediated degradation and was further shown to be translation competent following ISG20 exposure in cells, consistent with results obtained with IFN treatment, which induces ISG20 among other cellular nucleases (128). Unlike hepatitis B virus, the alphavirus RNA genome is replicated entirely in the cytoplasm, and would not be potentially exposed to the nuclear puncta containing ISG20. Thus our results more closely mimic previous work demonstrating that RNA from hepatitis C virus, a cytoplasmically-replicating virus, is not degraded by ISG20 during the course of infection (411).

Another study attempting to demonstrate the *in vitro* antiviral activity of ISG20 using influenza A virus suggested that ISG20 directly interacts with viral RNA to block translation, specifically binding to the influenza nucleoprotein to facilitate this activity (409). One caveat to these experiments however is the abnormal distribution of ISG20 observed in their transient overexpression system, favoring an atypical cytoplasmic localization, even in the absence of influenza nucleoprotein. In our *in vitro* model, we observed the punctate, primarily-nuclear localization of ISG20 consistent with previous studies (404). We too observed an ISG20-specific restriction of virus translation, but only in our host- and CHIKV-mimicking, type-0 capped RNAs, consistent with previous findings demonstrating that translation from the HCV IRES is unaffected by ISG20 overexpression (411). Restriction was not observed for reporters containing an internal ribosomal entry site from encephalomyocarditis virus (EMCV) or cricket paralysis virus (CrPV), indicating the block in translation is the result of a cap-dependent mechanism, and not a more general reduction in protein synthesis or RNA degradation. Despite the localization inconsistencies between studies, it is possible that ISG20 may employ multiple mechanisms of translation

restriction dependent upon the virus. In light of recent work with hepatitis B virus demonstrating ISG20 accumulation on particular secondary structures within viral RNAs, ISG20 may in fact contribute to the restriction of nuclear replicating RNA viruses through direct binding or degradation (444). However, the catalytically-inactive ExoII was still capable of binding HBV RNA (444). ExoII did not arrest translation of the alphavirus reporters, suggesting direct RNA-binding by ISG20 is not the primary mechanism of alphavirus translation suppression.

The localization of ISG20 may offer some additional insight as to its mechanism of antiviral action. Despite being a small, soluble protein capable of free diffusion through the nuclear pore complex, ISG20 localizes primarily in the nucleus and interacts with the protein- and RNA-rich Cajal bodies (404). The primary purpose of these structures is the processing and modification of small nuclear RNAs that make up the spliceosome (445, 446), suggesting that ISG20 may influence virus replication through the regulation of additional antiviral effectors rather than directly degrading viral nucleic acids. Our transcriptional analysis of ISG20 overexpressing MEFs revealed more than 100 genes significantly regulated by the ISG20 exonuclease, including two interferon regulatory factors (IRFs), the cytoplasmic viral RNA-detecting helicase RIG-I (*Ddx58*), and members of the interferon-induced protein with tetratricopeptide repeats (IFIT)-family. *Ifit1* upregulation stands out in particular because it has been previously characterized to inhibit translation of type-0 capped RNA in a manner consistent with our findings with ISG20 overexpression.

Our upstream pathway analysis of ISG20-mediated gene regulation strongly implicates the involvement of one or more IRFs in the transcriptional cascade observed following Isf20 overexpression. IRF3 – one such candidate – is a master regulator of both primary IFN-β production and is directly responsible for the induction of multiple virus-stimulated genes (VSGs),

which do not require IFN for transcription (383). IRF3 transcriptional activity on the promoters of IFN-β and VSGs is activated through the recognition of PAMPs in the cytosol and endosomes, ultimately leading to the activation of IRF3 and transcriptional regulation of ISRE-like sequence in target promoters. Our genetic results suggest that the ISG20-mediated antiviral response is facilitated by IRF3 transcriptional activity. Thus, the involvement of IRF3 presents a potential mechanism for ISG20-directed gene transcription, where a potential degradation product of ISG20 catalytic activity is serving to activate the transcriptional activities of IRF3 and perhaps its downstream effectors including IRF7 and IRF9. While the involvement of IFN production does not appear to play a role in ISG20-mediated transcription responses in our cell culture system, this pathway would suggest that ISG20 may also serve as a positive feedback mechanism in the production of IFNs, which may be produced below the limit of detection in our current assays or play a greater functional role as a feedback regulator *in vivo*.

3.0   ISG20 PROTECTS FROM IFIT1-SENSITIVE VIRUS CHALLENGE IN VIVO,

BUT NOT WT ALPHAVIRUS INFECTION

3.1   INTRODUCTION

Antiviral effectors of the IFN-α/β response play a crucial role in the pathogenic outcomes of alphavirus infections in mouse models of disease. Mice lacking signaling components of the IFN-α/β cascade, including STAT1 and the IFN-α/β receptor (IFNAR), succumb to fatal systemic disease from both the arthritogenic and encephalitogenic alphaviruses (127, 167, 169, 344). While numerous ISGs induced by this response have demonstrated anti-alphaviral activity in cell culture models of infection, relatively little work has been done to recapitulate these findings in animal models of disease.

In vitro models for ISG activity often rely on overexpression and RNA-interference knockdown of a single antiviral effector, which may or may not properly represent the physiological expression conditions following IFN-stimulation and ISG induction. Furthermore, several ISGs may act with binding partners that are not concurrently upregulated in single-ISG overexpression studies. While informative on their own, these studies are best complimented by evaluating the effects of individual ISGs in animal models of disease to define a physiologically

71

relevant role for ISG activity *in vivo*. Homozygous knockout mice have been used to study the role of IFIT1 and ISG15 restriction of VEEV and CHIKV respectively, elucidating functional activity for both in the context of innate immune restriction of viral pathogenesis (3, 354).

Study of ISG20 *in vivo* has previously been restricted to tissue specific overexpression or knockdown through hydrodynamic injection of constitutive-expression plasmids or short hairpin RNA (shRNA) (340-342, 405, 406, 409-411, 444). Utilizing *Ifnar1*$^{-/-}$ mice, the authors of one study demonstrated that tissue-specific expression of ISG20 in the absence of other IFN-α/β effectors is sufficient to reduce HBV viral load (410). Subsequently, RNAi knockdown of *Isg20* in WT mouse livers resulted in a concurrent increase in HBV viral load (410). This study, however, does not demonstrate the systemic influence of ISG20, and importantly misses potential regulatory activity associated with ISG20 as a positive feedback mechanism for IFN production.

In the present study, we describe for the first time an *Isg20*$^{-/-}$ mouse model for the study of viral infection. Utilizing a combination of WT CHIKV, VEEV and EEEV and IFIT1-sensitive, attenuated strains of VEEV and EEEV (VEEV-G3A and EEEV-nt4&6), we demonstrate the fundamental importance of ISG20 for a functional innate immune response to alphavirus infection. Our findings indicate a minimal individual contribution by ISG20 in protecting against sub-lethal CHIKV challenge in adult mice, and lethal challenge of neonates. Furthermore, ISG20 does not significantly influence disease course and average survival time for adult mouse models of WT VEEV and EEEV infection. However, *Isg20*$^{-/-}$ mice infected with WT VEEV present neurological symptoms sooner than their WT counterparts. VEEV-G3A and EEEV-nt4&6 are uniformly lethal in *Isg20*$^{-/-}$ mice with <100% mortality observed for both viruses in WT mice. Further characterization of VEEV-G3A pathogenesis in *Isg20*$^{-/-}$ mice revealed a consistent increase in early viral load in both draining lymph nodes and serum, concomitant with reduced early serum

IFN production. Likewise, primary fibroblasts and osteoblasts isolated from *Isg20*^{-/-} mice demonstrate an increased susceptibility to VEEV-G3A infection, regardless of IFN-priming. Together, our results demonstrate that ISG20 critically restricts IFIT1-sensitive, but not WT, alphaviruses *in vivo*, and support a role for ISG20 as a feedback regulator of IFN-α/β and VSG production in response to viral infection.

3.2   RESULTS

3.2.1   ISG20 Does Not Protect Against WT Alphavirus Challenge in Mice

With the robust *in vitro* restriction observed with ISG20 overexpression, we sought to verify our findings in a small animal model of CHIKV infection. Utilizing an adult mouse model for CHIKV musculoskeletal disease (168, 345, 447), 3-week old male mice were infected with 10^3 PFU WT CHIKV (La Réunion) subcutaneously in the left rear footpad and disease was tracked by arthritis manifested as swelling in the infected and contralateral, un-infected footpad. We observed no gross pathological differences in footpad swelling between *Isg20*^{-/-} and B6 mice in response to CHIKV infection (**Figure 14A**). Furthermore, serum, inoculated footpad and popliteal lymph nodes draining the infection site were collected and the level of CHIKV genomic RNA was assessed by qRT-PCR. No significant differences in RNA levels detected between all tissues harvested from *Isg20*^{-/-} and B6 mice (**Figure 14B**) were observed. In addition, no detectible serum IFN-α/β was detectible in infected animals at 24 hours p.i.
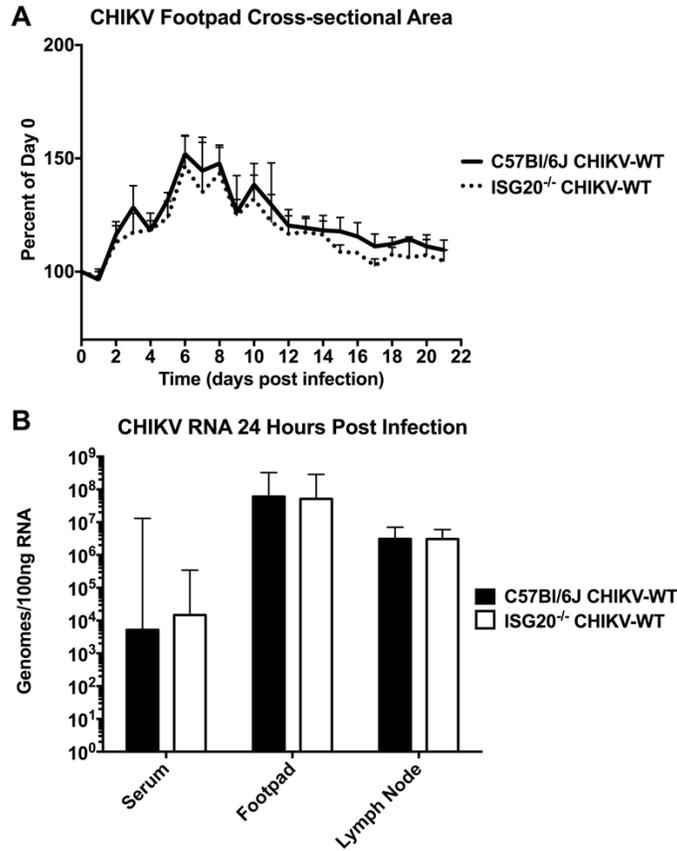
Figure 14: ISG20 does not Protect from CHIKV Disease in Adult Mice.

3-week old male C57Bl/6J and *Isg20*^{-/-} mice were inoculated subcutaneously with 10^3 PFU WT CHIKV (La Réunion) in the left hindlimb footpad. (**A**) Swelling was determined by footpad cross-sectional area measured as an ellipse at 24-hour intervals for 3-weeks p.i. (**B**) CHIKV genomic RNA was measured by strand-specific qPCR at 24-hours post infection in serum, footpad, and popliteal lymph node draining infection. Not significant; (**A**) two-way ANOVA (**B**) Mann-Whitney test.

In addition to the non-lethal adult model of CHIKV infection, neonatal pups lacking a fully developed immune system may be used to assess pathogenic differences of CHIKV between mouse strains through differences in survival time due to an underdeveloped type I interferon response, potentially allowing the effects of a single missing ISG to manifest (167, 448). Homogenized litters of *Isg20*^{-/-} and B6 pups were infected with 10^3 PFU CHIKV subcutaneously in the axial region and housed with a surrogate mother.

Neonates succumbing to disease earlier than 6-days p.i. manifested symptoms indicative of a systemic inflammatory response syndrome-like disease as is observed with Sindbis virus (449). However, after 6 days, neurological symptoms developed in all surviving mice, consisting of severe ataxia progressing to hind limb paralysis. No differences in median survival times or disease manifestations were observed between $Isg20^{-/-}$ and B6 neonates infected with CHIKV, 8.0 +/- 3.7 days and 8.5 +/- 2.1 days respectively (**Figure 15A-B**). Indeed, survival correlated more closely with birth weight than mouse strain across groups (data not shown). These findings indicate that while CHIKV is greatly modulated by ISG20 overexpression *in vitro*, CHIKV restriction in mice does not appear to be prominently influenced by the presence of a functional ISG20 exonuclease.
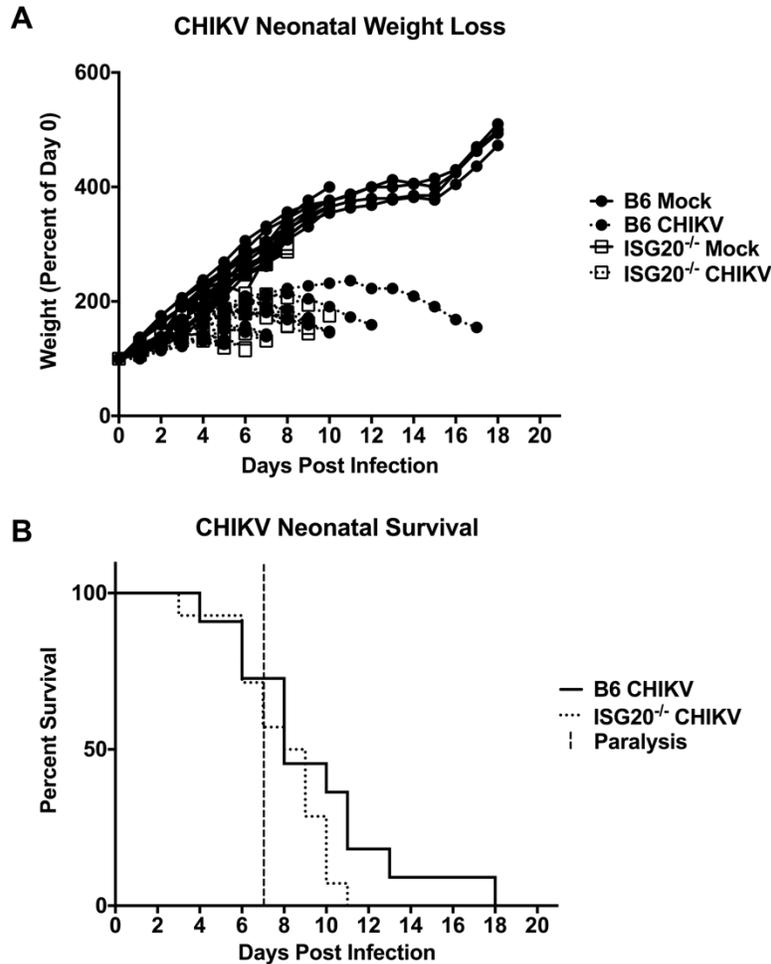
Figure 15: ISG20 is not Protective Against Fatal CHIKV Challenge in Neonatal Mice.

1-day old neonatal mice were infected subcutaneously in the axial region with 10^3 PFU CHIKV WT and monitored for (**A**) weight loss and (**B**) survival. Not significant; (**B**) log-rank test.

Non-fatal disease could be a confounding factor in determining small effects contributed by ISG20. The encephalitigenic alphaviruses, VEEV and EEEV, cause uniformly fatal disease in adult mice, and differences in virulence can be assessed quantitatively through survival and scoring of clinical manifestations. Age matched, adult male mice were infected subcutaneously with 10^3 PFU of either VEEV WT (ZPC738) or EEEV WT (FL93939) in both rear footpads and morbidity and mortality were monitored.

76

VEEV WT-infected *Isg20^{-/-}* mice demonstrated earlier onset of symptoms, while clinical manifestations in B6 mice consistently followed about 24 hours later (**Figure 16C-D** and **Figure 18A**). However, no differences in median survival times were observed for mice infected with VEEV WT, with 5.50 +/- 0 days and 5.75 +/- 0.25 days for B6 and *Isg20^{-/-}* mice respectively (**Figure 16B**). EEEV WT infected mice demonstrated no significant differences in either clinical disease score or median survival time, with animals succumbing to disease by 5.0 +/- 0.5 days and 6.5 +/- 0.7 days for WT and *Isg20^{-/-}* mice respectively (**Figure 17A-D**). With expanded clinical scoring of behavioral changes, VEEV WT infected *Isg20^{-/-}* mice rapidly progress to a level of jumpiness and responsiveness to external stimuli unseen in their WT counterparts, suggestive of changes in visual acuity in these animals (**Figure 18A**). However, no such differences are observed in EEEV WT infected mice (**Figure 18B**).
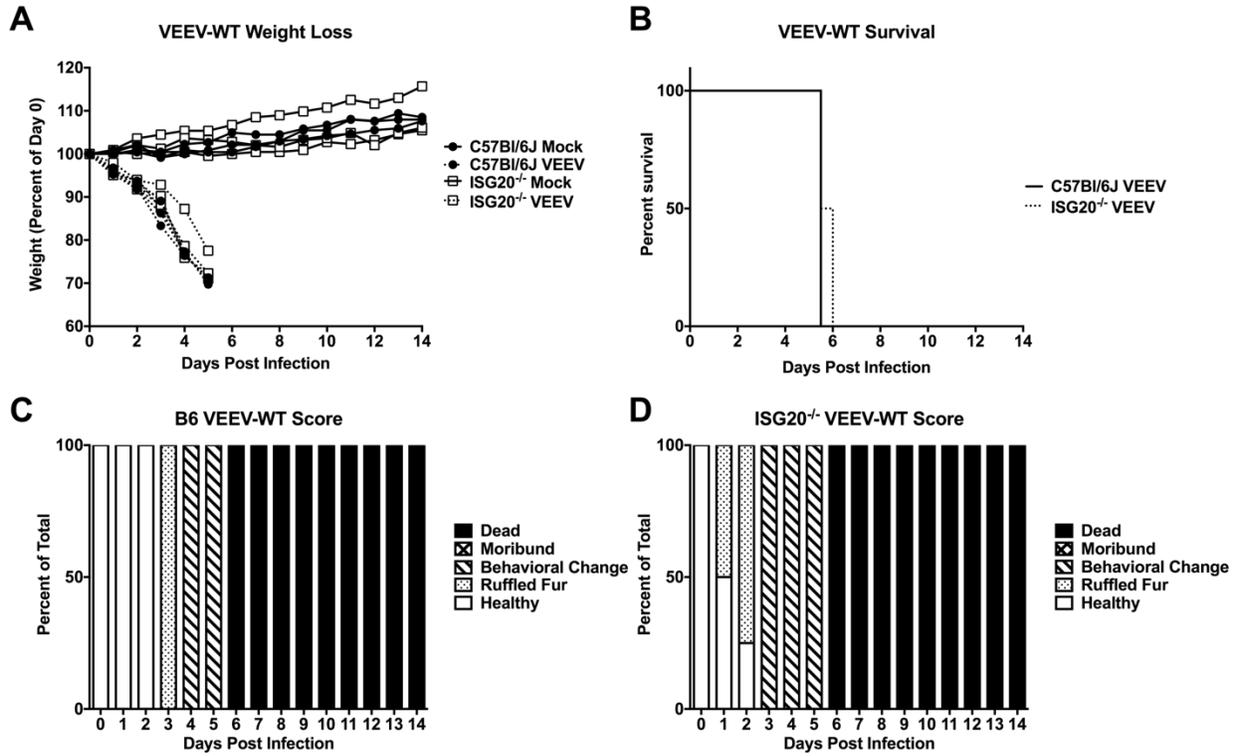
Figure 16: ISG20 is not Protective Against WT VEEV Challenge.

6-week old male C57Bl/6J and *Isg20*^{−/−} mice were inoculated subcutaneously with 10^3 PFU VEEV WT (ZPC738) in each hindlimb footpad and monitored for (**A**) weight loss, (**B**) survival and (**C-D**) clinical disease score. Not significant; (**B**) log-rank test. (n=4)

Figure 17: ISG20 is not Protective Against WT EEEV Challenge.

6-week old male C57Bl/6J and *Isg20*^{-/-} mice were inoculated subcutaneously with 10^3 PFU EEEV WT in each hindlimb footpad and monitored for (**A**) weight loss, (**B**) survival and (**C-D**) clinical disease score. Not significant; (**B**) log-rank test. (n=3)
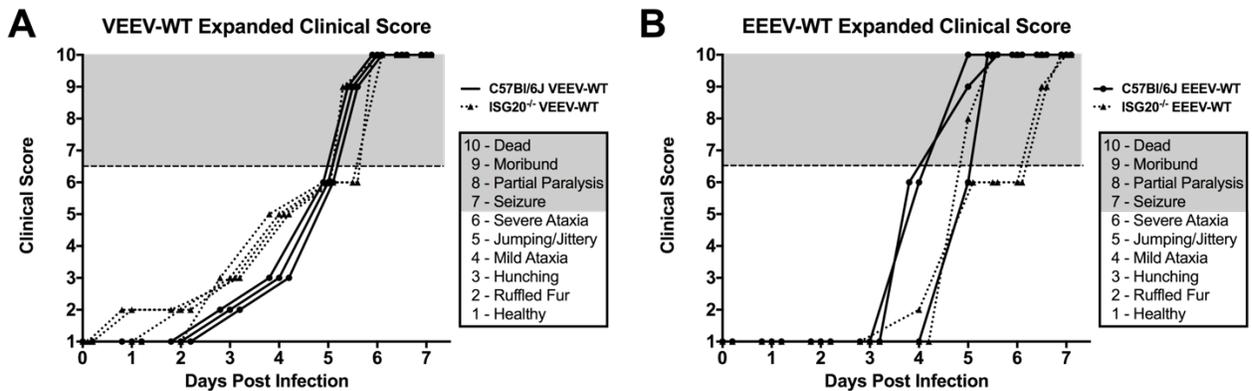
Figure 18: ISG20 Delays WT VEEV Disease Onset.

Expanded clinical scoring criteria are given for (**A**) VEEV WT- and (**B**) EEEV WT-infected mice with specific behavioral changes noted. (n=3-4)

3.2.2 ISG20 Protects Against IFIT1-sensitive Alphaviruses in Mice

Collectively, our *in vitro* overexpression findings suggest a role for ISG20 as a regulator for inducing ISGs as part of the antiviral response. *Ifit1* was highly upregulated by ISG20 overexpression and functions by restricting virus translation. VEEV is an encephalitogenic alphavirus with a well-characterized resistance mechanism to IFIT1 translation restriction present in WT strains (3). A single nucleotide mutation derived from the VEEV TC83 vaccine strain, G3A, disrupts the terminal stem loop structure and reveals a 3-nucleotide overhang for IFIT1 detection of the type-0 alphavirus RNA cap structure (3). Given the enhanced sensitivity of VEEV-G3A to ISG20 overexpression *in vitro*, we explored the impact of IFIT1-sensitivity in *Isg20$^{-/-}$* mice.

Mice infected with VEEV-G3A displayed similar early differences in disease clinical score, with *Isg20$^{-/-}$* mice succumbing to neurological symptoms sooner than B6 (**Figure 19C-D**). Similarly, severe neurological deficits were observed with VEEV-G3A infection in *Isg20$^{-/-}$* mice as with VEEV WT (**Figure 19D**). Interestingly, most B6 mice also demonstrated behavioral abnormalities by 6-days post infection, including hunched posture and ataxia, but about 50% recovered fully by 11-days p.i., with no observed lasting neurological deficits (**Figure 19C**). Additionally, *Isg20$^{-/-}$* mice experienced more rapid weight loss than B6 between replicate experiments (**Figure 19A**). *Isg20$^{-/-}$* mice uniformly succumbed to VEEV disease, while 50% of B6 animals fell ill, but eventually recovered by 12 days p.i. Median survival time for VEEV-G3A was 11.0 +/- 0.5 days and 7.0 +/- 1.4 days in B6 and *Isg20$^{-/-}$* mice respectively (**Figure 19B**).
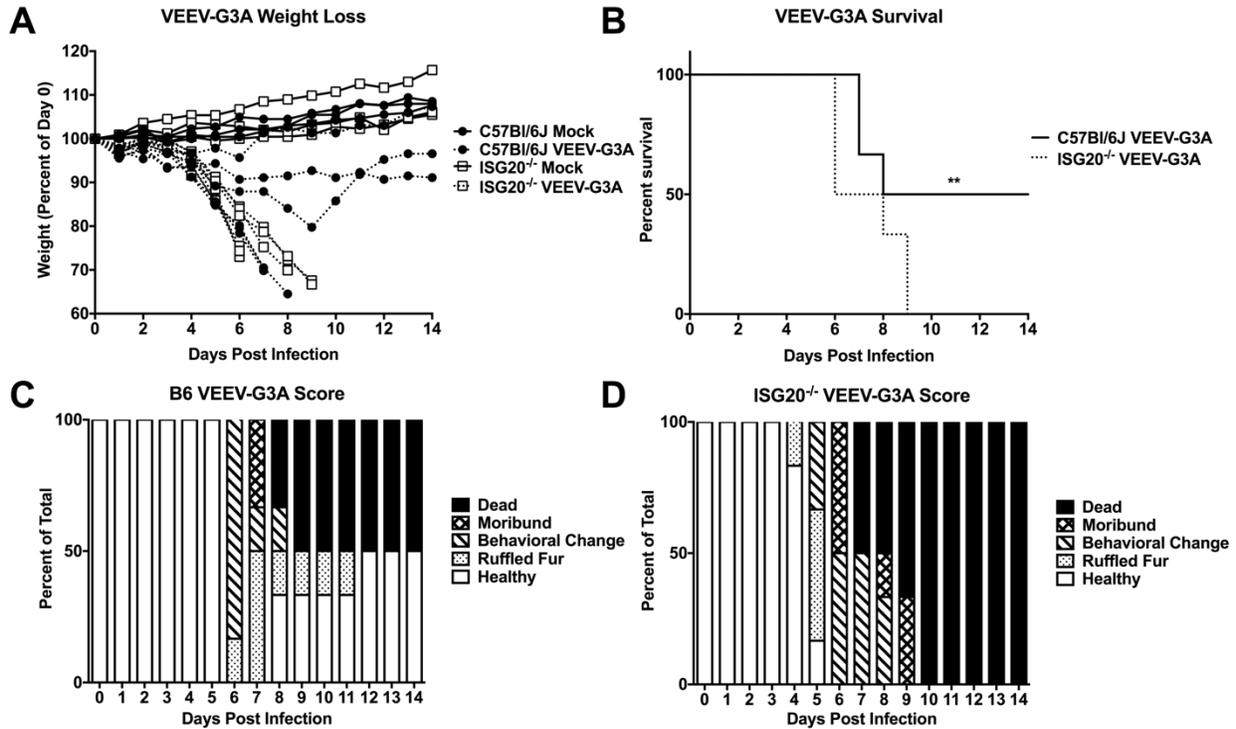
Figure 19: ISG20 Protects from VEEV-G3A Infection.

6-week old male C57Bl/6J and *Isg20*^{-/-} mice were inoculated subcutaneously with 10^3 PFU VEEV-G3A in each hindlimb footpad and monitored for (**A**) weight loss, (**B**) survival and (**C-D**) clinical disease score. ** $P < 0.01$; (**B**) log-rank test. (n=6-7)

The single G3A point mutation in the VEEV 5'-NTR shifts the terminal stem loop positioning, conferring a 3-nucleotide terminal overhang – enough for type-0 cap detection and binding by IFIT1 (3). Using a similar approach, our lab developed a double point mutant, EEEV-G4A/G6A (EEEV-nt4&6), which is similarly predicted to reduce steric hindrance from the 5'-terminal stem loop and exposes the cap structure to IFIT1 (**Figure 20A-B**) (Trobaugh et al., unpublished manuscript). Both B6 and *Isg20*^{-/-} mice infected with EEEV-nt4&6 experienced an approximately 3-day delay in disease onset compared to EEEV WT infection (**Figures 17, 21**). While EEEV WT is rapidly lethal following the onset of symptoms, EEEV-nt4&6 manifests with a brief prodromal phase followed by progressive neurological deficits (**Figure 21C-D**). No differences were observed between B6 and *Isg20*^{-/-} mice in the onset of disease as measured by

81

weight loss (**Figure 21A**) or disease scoring (**Figure 21C-D**). However, *Isg20*^{-/-} mice more rapidly

progressed with EEEV-nt4&6 neurological involvement, with all mice severely ataxic by 9 days

p.i. (**Figure 21C-D**). EEEV-nt4&6 was uniformly lethal in *Isg20*^{-/-} mice, while 16% of B6 animals

survived challenge with no disease (**Figure 21B**). Median survival times for B6 and *Isg20*^{-/-} mice

were 11.0 +/- 1.1 days and 10.0 +/- 0.6 days respectively.
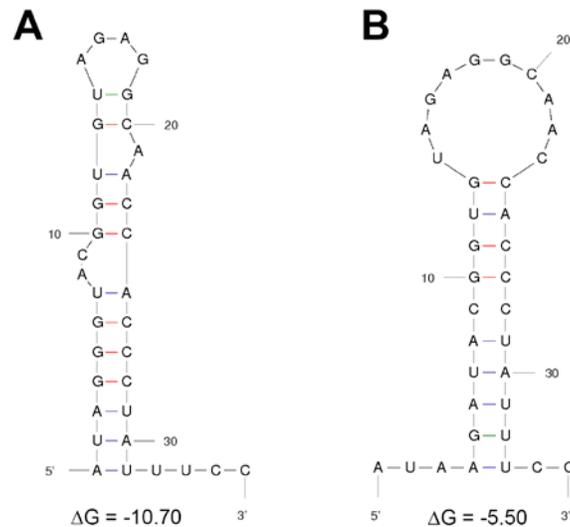
Figure 20: EEEV and EEEV-nt4&6 5'-NTR Fold Predictions

Predicted 5'-terminal stem-loop folds were calculated by mfold (v.2.3 energies). Stem-loop and terminal nucleotide overhangs are shown for (**A**) WT EEEV and (**B**) EEEV-nt4&6 with corresponding Gibbs free energy predictions at 37ºC and physiological conditions.

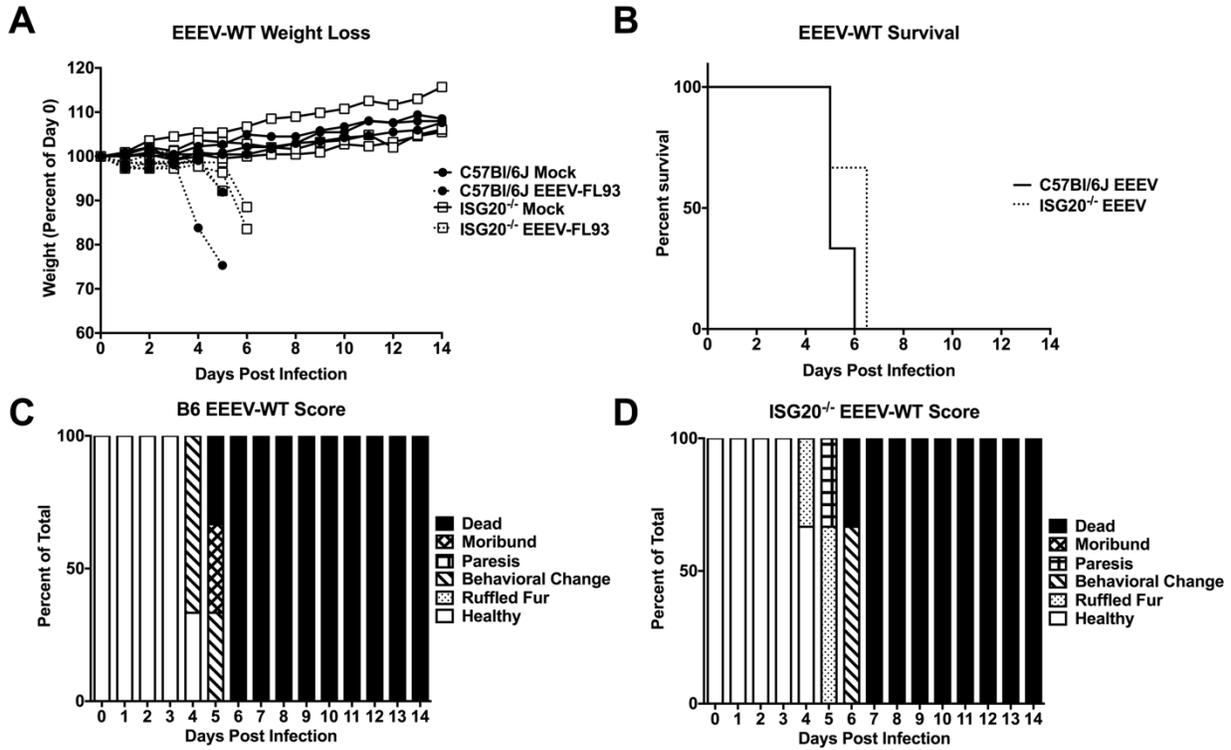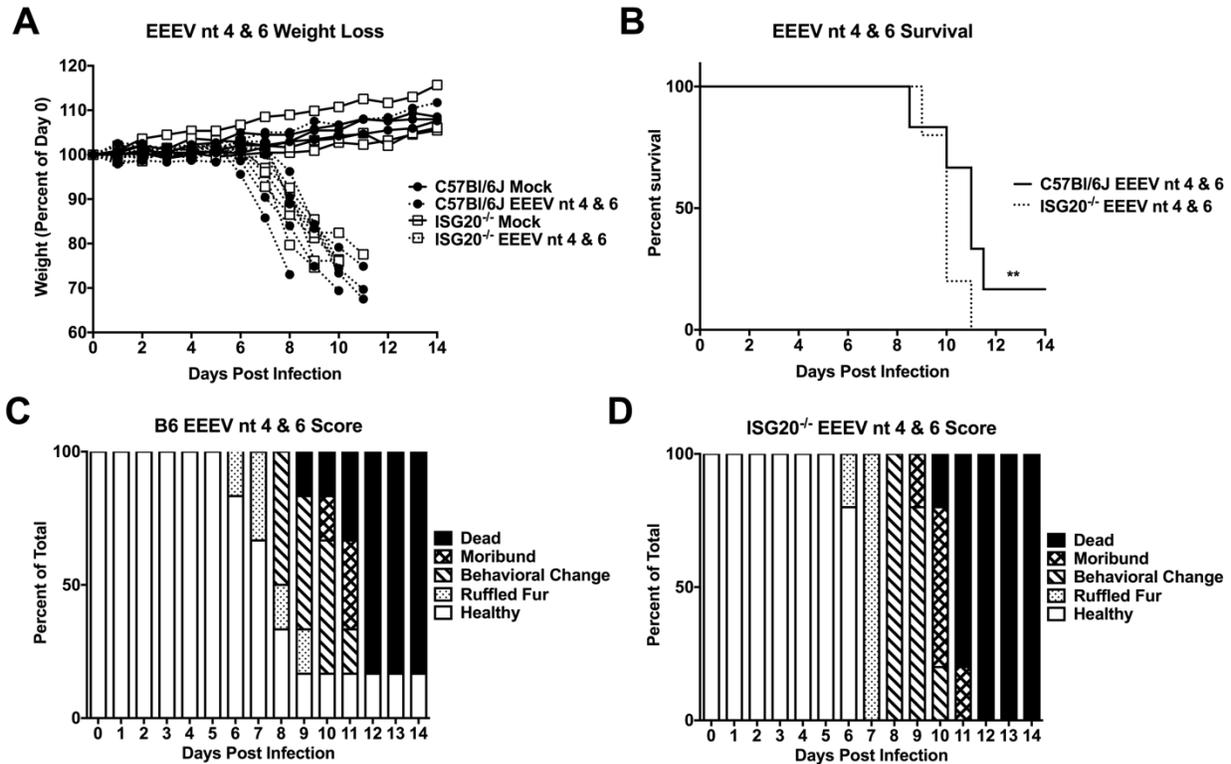**Figure 21: ISG20 Protects from EEEV nt 4&6 Challenge.**
6-week old male C57Bl/6J and *Isg20*^{-/-} mice were inoculated subcutaneously with 10^3 PFU EEEV-nt4&6 in each hindlimb footpad and monitored for (**A**) weight loss, (**B**) survival and (**C-D**) clinical disease score. ** $P < 0.01$; (**B**) log-rank test. (n=6)

Events within the first 24 hours of infection can act as critical determinants of disease outcome as the induction of the type I IFN response slows the spread of disease and helps to prime the adaptive immune response. Thus, VEEV-G3A virus growth was measured at 12 and 24 hours p.i. to determine the extent of virus replication and spread in key tissues and again at five days when neurological symptoms typically appear. At 12 hours p.i., we detected a five-fold increase in serum IFN-α/β levels in B6 mice compared to *Isg20*^{-/-} ($P < 0.01$, **Figure 22E**). However, serum IFN levels in *Isg20*^{-/-} mice increased to similar levels as seen in B6 mice by 24 hours p.i. (**Figure 22E**). Replication in the draining popliteal lymph node (PLN) was found to be significantly elevated in *Isg20*^{-/-} mice compared to B6 mice ($P < 0.01$, **Figure 22A**) at 12 hours p.i. Interestingly,

50% of the B6 mice at 12 hours p.i. did not exhibit detectable lymph node replication (**Figure 22A**); although serum titers were similar between the all mice at this time (**Figure 22C**). By 24 hours p.i., all B6 mice had virus replication in their PLN at which time serum titer was elevated approximately two-fold in *Isg20*^{-/-} mice ($P < 0.05$, **Figure 22C**). By 5 days p.i., VEEV-G3A was undetectable in serum, popliteal lymph node and the spleen in both B6 and *Isg20*^{-/-} mice (**Figure 22A-C**). Virus was detectible at greater than 10^5 PFU in the brain at five days p.i. in both B6 and *Isg20*^{-/-} mice, with the latter reproducibly but not significantly higher (**Figure 22D**). No other significant differences in virus replication were detected in the spleen or the brain at any time point examined. IFN-β mRNA levels were consistently lower in popliteal lymph node and spleen of *Isg20*^{-/-} mice infected with VEEV-G3A, with significantly fewer IFN-β transcripts at five days p.i. in the spleen (**Figure 22F-G**). IFN-β transcript levels in the brain remained consistent between B6 and *Isg20*^{-/-} mice across all time points tested (**Figure 22H**).
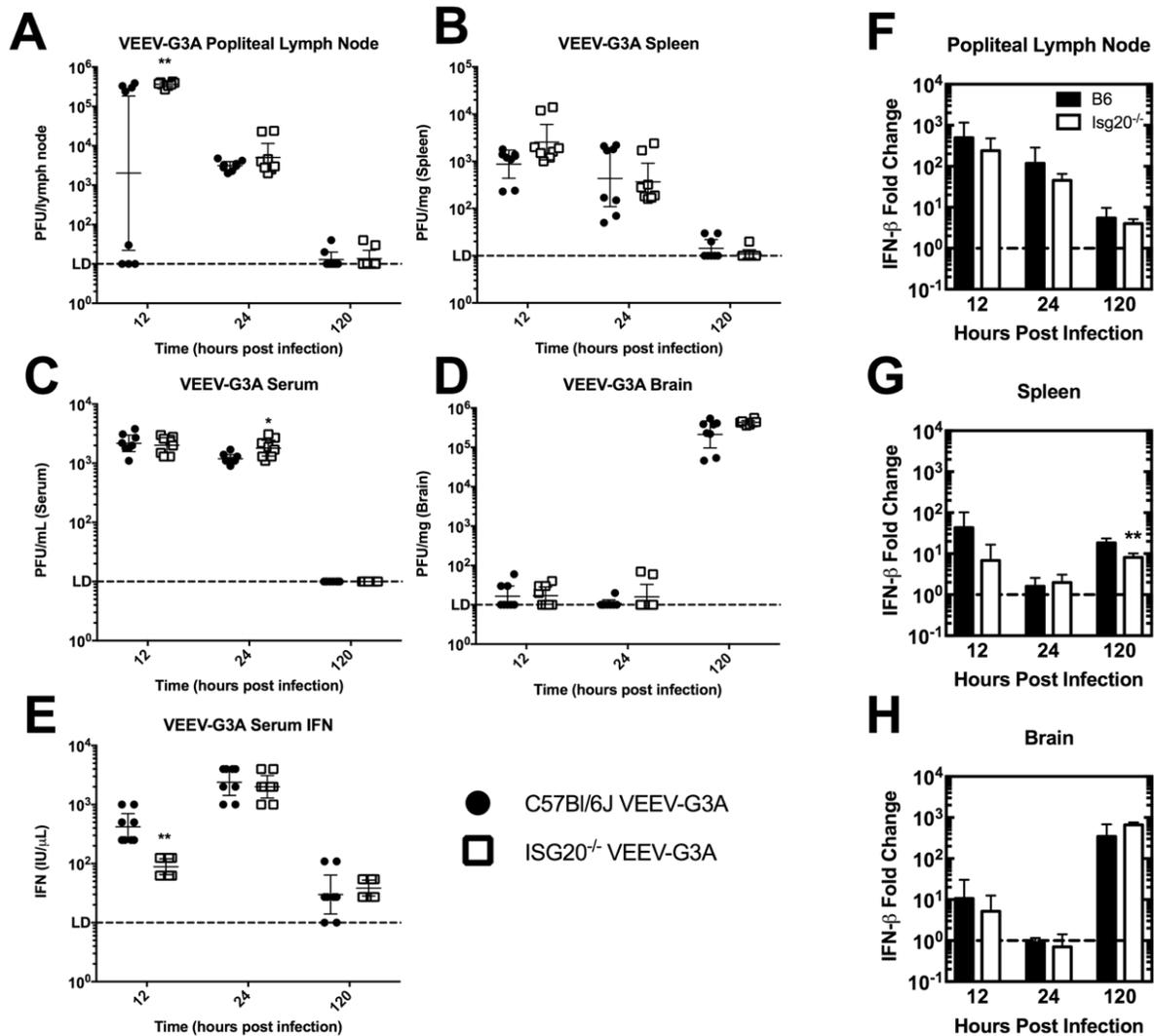
Figure 22: ISG20 Enhances IFN Production and Limits Replication of VEEV-G3A *in vivo*.

6-week old male C57Bl/6J and *Isg20$^{-/-}$* mice were inoculated subcutaneously with 10^3 PFU VEEV-G3A in each hindlimb footpad and tissues or serum were harvested for RNA or live virus extraction at 12 hours, 24 hours, or 5 days p.i. Virus titers were determined for (**A**) popliteal lymph nodes, (**B**) spleen, (**C**) serum, and (**D**) Brain. (**E**) Serum IFN and local IFN-β transcription was determined for (**F**) popliteal lymph node, (**G**) spleen, and (**H**) brain at each time point. * $P < 0.05$, ** $P < 0.01$; (**A-E**) multiple t tests, (**F-H**) Mann-Whitney test. (n=4)

3.2.3 *Isg20$^{-/-}$* Primary Cells are more Susceptible to CHIKV and VEEV Infection

The differences observed in mouse tissue replication suggest that ISG20 may be playing a role in the innate responses of particular cell types, which may influence the overall outcome of infection with IFIT1-sensitive viruses. We first assessed *Isg20* induction in response to both IFN treatment and virus infection. Both CHIKV infection and IFN treatment significantly induced *Isg20* in primary MEFs, but *Isg20* was only induced by IFN in osteoblasts, at reduced levels (**Figure 23A**).

In order to determine cell-specific effects of *Isg20*-deficiency, primary cells were generated from sex- and age-matched B6 and *Isg20$^{-/-}$* mice. Primary MEFs and osteoblasts were infected with CHIKV-LR or VEEV-G3A to measure virus replication in these early primary cell targets of virus infection *ex vivo* (125, 450). In the absence of type I IFN priming, CHIKV replicated to approximately ten-fold higher levels by 24 hours in *Isg20$^{-/-}$* MEFs compared to B6 MEFs ($P <$ 0.01, **Figure 23B**). When MEFs were primed with 10 and 100 IU of IFN-α4/β at a 1:1 ratio for 4 hours, we observed a similar difference in virus replication, with approximately ten-fold greater replication in *Isg20$^{-/-}$* MEFs over B6. In osteoblasts, a minor increase in CHIKV virus replication was seen in *Isg20$^{-/-}$* cells compared to B6 in the absence of IFN priming (**Figure 23C**). However, this difference was not statistically significant. Following IFN priming, CHIKV replicated to similar levels in both *Isg20$^{-/-}$* and B6 osteoblasts demonstrating cell-specific differences in ISG20 antiviral effects (**Figure 23C**).

Similar results were seen in MEFs infected with VEEV-G3A. In *Isg20$^{-/-}$* MEFs, a 100-10,000-fold increase in VEEV-G3A replication was measured compared to B6 MEFs ($P < 0.01$, **Figure 23D**). These differences were maintained in the presence of IFN treatment, where B6 MEFs released no detectable virus at 24 hours p.i. (**Figure 23D**). VEEV-G3A also experienced significant

gains in replication in primary $Isg20^{-/-}$ osteoblasts after IFN treatment, albeit with 5- to 100-fold difference in progeny virus at 24 hours p.i. ($P < 0.01$, **Figure 23E**).

We sought to determine whether observed differences in virus replication can be attributed to differential regulation of ISG20-stimulated genes in primary cells. Using IFIT1 as a representative gene, we see a significant two-fold reduction in induction following low dose (10 IU/mL) IFN priming in $Isg20^{-/-}$ MEFs ($P < 0.05$, **Figure 23F**). This reduction was abolished with high dose (100 IU/mL) IFN treatment (**Figure 23F**). These results are consistent with a model where ISG20 regulates the induction profile of ISGs and VSGs, providing antiviral activity against viruses in spatially separated subcellular compartments.
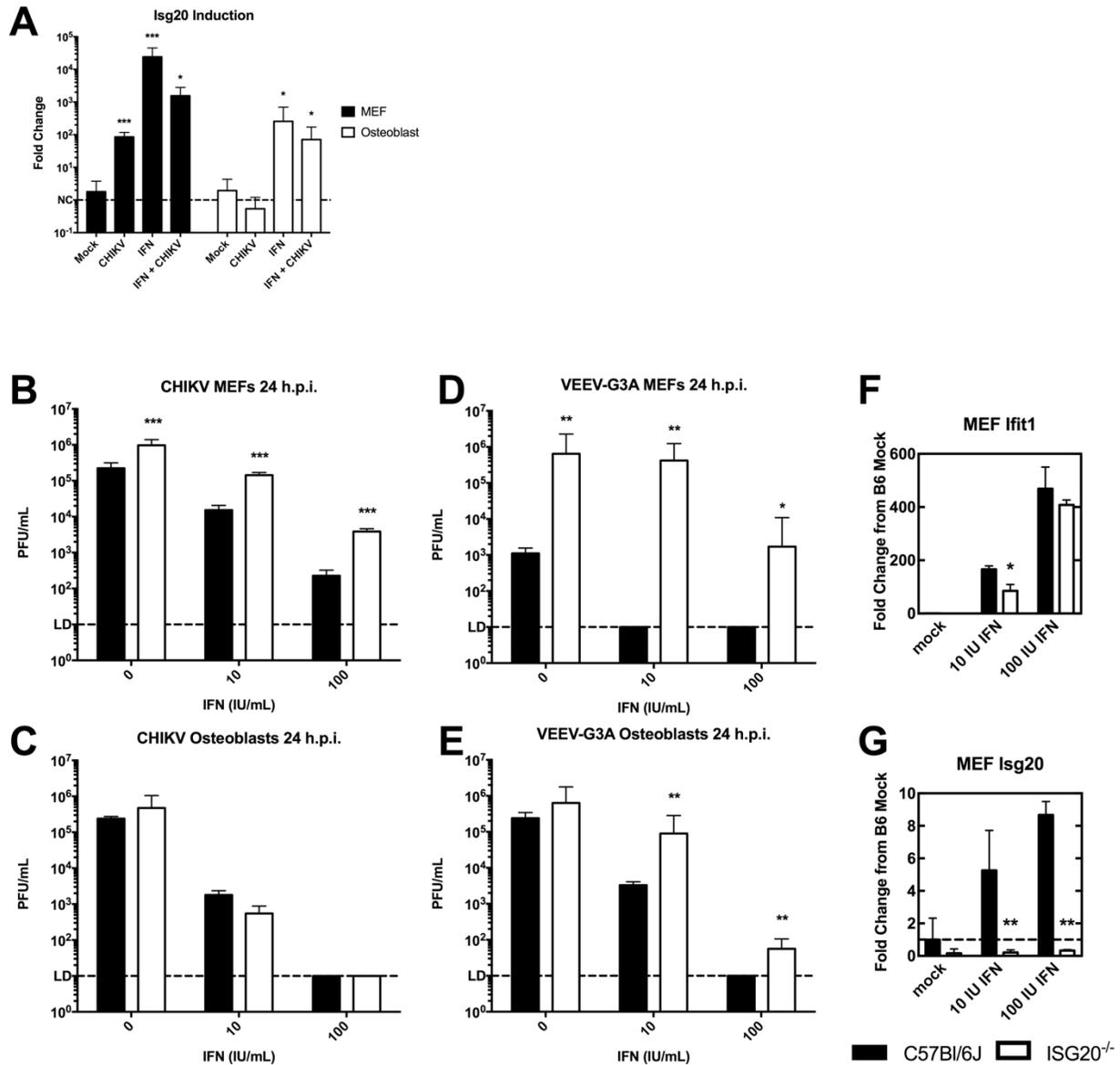
Figure 23: ISG20 Knockout Leads to Increased CHIKV and VEEV-G3A Replication in Primary Cells.

(**A**) *Isg20* induction was measured by qPCR in primary WT MEFs and osteoblasts by either IFN treatment or CHIKV infection. (**B-E**) Primary cells isolated from WT and *Isg20⁻/⁻* mice were assessed for (**B-C**) CHIKV and (**D-E**) VEEV-G3A replication competence with or without IFN priming. (**F-G**) ISG induction was measured by qPCR in uninfected WT and *Isg20⁻/⁻* MEFs with or without IFN priming. * $P < 0.05$, ** $P < 0.01$, *** $P < 0.001$; (**B-E**) ANOVA, (n=6) (**A,F-G**) Mann-Whitney test. (n=6)

3.3   DISCUSSION

Among the alphaviruses, CHIKV is highly susceptible to murine type I IFN responses with this effect being attributed to numerous individual effector proteins (167, 354, 365, 451-453). However, despite sensitivity to murine type I IFN, adult C57Bl/6J mice are susceptible to non-lethal CHIKV disease, and mimic the arthritis phenotype observed in humans (168, 169). Disrupting signaling components of the type I IFN system, including IFNAR and STAT1, significantly increases CHIKV virulence, resulting in uniformly fatal disease in mice (169). Similarly, neonatal mice struggle to mount an effective innate immune response to infection, and are susceptible to fatal disease (167). Our findings with ISG20 overexpression *in vitro* would suggest that *Isg20* deficiency should negatively impact the IFN-mediated antiviral response, leading to increased viral load, altered kinetics of viral spread, or varied pathological outcomes. However, in both non-lethal and lethal mouse challenge models, no differences were observed with CHIKV survival, disease symptoms or viral load.

Both VEEV and EEEV infection are uniformly lethal in mice. VEEV infects rodents as a reservoir host and has evolved ways to circumvent the murine IFN response (14, 40). However, the VEEV-G3A mutant is attenuated in WT mice, but remains virulent in *Ifit1*-null mice (3). WT EEEV is also resistant to IFIT1 and dual G→A point mutations at positions 4 and 6 within the 5'-NTR confer susceptibility to IFIT1 (Trobaugh et al., unpublished manuscript). Our *in vitro* findings indicate that ISG20 functions as a positive feedback regulator of antiviral factors, including IFIT1.

The *Isg20*$^{-/-}$ mouse model revealed no significant difference in WT VEEV or EEEV infection, but trended toward earlier disease onset with WT VEEV infection. However, loss of *Isg20* had a dramatic effect on both VEEV-G3A and EEEV-nt4&6 virulence in mice. Furthermore,

early after infection, *Isg20^{-/-}* mice produced lower levels of IFN-α/β and some tissues (e.g., spleen) exhibited reduced IFN-β transcript levels in response to VEEV-G3A, which is consistent with ISG20 acting as a general stimulator of IRF3 and subsequently type I IFN. However, in ISG20 overexpressing cells, IFN induction was not observed, although the cells were capable of responding to poly I:C transfection with IFN-α/β release. Additionally, a subset of *Isg20^{-/-}* primary cells showed a greatly increased susceptibility to infection, even in the presence of IFN-priming. *Ifit1* stands out as a prominent ISG20-regulated gene and a reduction in IFIT1 production would help explain the phenotypes of both VEEV-G3A and EEEV-nt4&6 in mice. Indeed, *Ifit1* transcription in response to IFN stimulation is impaired in *Isg20^{-/-}* MEFs. Combined with our understanding of IFN-mediated *Isg20* upregulation and downstream ISG20-mediated upregulation of IFIT1 and other antiviral effectors *in vitro*, the mouse model of VEEV-G3A supports a feedback mechanism of ISG20 to help stimulate sustained IFN and ISG production in response to infection. The failure of the overexpressing cells to produce IFN-α/β may instead reflect cell type-dependent differences in the effects of ISG20 or clonal adaptations to downregulate IFN production in response to ISG20. This is supported by primary cells that showed no effect on type I IFN induction levels (data not shown), which would suggest that IFN feedback regulation occurs in an unidentified cell type, possibly myeloid cells.

4.0   CONCLUSIONS

4.1   MODEL OF ISG20 ANTIVIRAL ACTIVITY

The literature surrounding a mechanism for ISG20 antiviral activity is both incomplete and
contradictory. When ISG20 was first characterized, genetic similarities to related DEXD nucleases
and *ex vivo* biochemical analysis identified ISG20 as an IFN-induced 3'-5' exonuclease with
catalytic activity against single-stranded nucleic acids (400). ISG20 demonstrated a preference for
ssRNA over ssDNA substrates, with no apparent sequence preference (400). Subsequently, ISG20
antiviral activity against numerous RNA viruses was demonstrated through overexpression, but it
failed to restrict the few DNA viruses tested, leading to the hypothesis that ISG20 actively targets
and degrades RNA virus genomes and replicative intermediates (340-342, 405, 406, 411). This
was further supported when it was discovered that a catalytically-dead mutant of ISG20 in the
ExoII domain lost its antiviral activity against RNA viruses (405).

ISG20 antiviral activity against RNA viruses is not uniform. For example, VSV was found
to be potently inhibited by ISG20, but EMCV was notably more resistant (405). Further
complicating matters, localization studies with ISG20 identified the sub-nuclear Cajal body as the
primary cellular location for ISG20 (404). This compartmentalization of ISG20 would limit

exposure to many RNA viruses that replicate in the cytoplasm, including many with a known ISG20-restricted phenotype. The first direct evidence against ISG20-mediated virus degradation was demonstrated with HCV infection, where the authors found that ISG20 overexpression did not accelerate the decay of viral RNA at multiple time points post infection (411).

Recently, the debate over ISG20-mediated viral nucleic acid-degradation as a mechanism for antiviral activity was renewed with two studies using HBV as a model (410, 444). HBV is a non-covalently-closed circular DNA virus, which replicates in the nucleus with a retrotranscribed RNA intermediate known as the pre-genome. Both studies demonstrated an accelerated decay of pre-genomic RNA in the presence of ISG20 overexpression, with the most recent demonstrating direct ISG20 binding to the viral RNA (410, 444). Interestingly, ISG20 was found to bind at the base of known stem-loop structures used to initiate virus replication, including one located away from the 3'-terminus (444). This study suggested a sequence-specific, or structure-specific, recognition of specific RNA motifs, facilitating ISG20 binding and degradation of the pre-genomic RNA. Furthermore, the catalytically inactive ExoII ISG20 mutant was capable of binding HBV pre-genomic RNA, and retained residual antiviral activity by obstructing encapsidation (444). The authors of this study proposed the most complete model of ISG20 antiviral activity to date, where ISG20 directly binds structural motifs within HBV and degrades pre-genomic RNA, inhibiting replication and translation of viral proteins, and restricting encapsidation.

While there is growing support for the RNA degradation model, there is currently no evidence that ISG20 degrades RNA in the cytoplasm. Like HCV, the alphaviruses replicate their RNA genome entirely in the cytoplasm. Herein, we have demonstrated that both arthritogenic and encephalitogenic alphaviruses are subject to ISG20-mediated replication restriction. Furthermore, that restriction occurs at the point of early genomic translation of the genome-resident

nonstructural polyprotein. Our ISG20 translation inhibition phenotype depends on ExoII domain-directed exonuclease activity, but does not extend to IRES-containing RNAs, strongly suggesting that ISG20 disrupts translation initiation rather than degrading cytoplasmic RNAs. This is consistent with previous findings with EMCV that showed a reduced ISG20-restriction phenotype compared to other RNA viruses (405). We further demonstrated that ISG20 does not accelerate the decay of the CHIKV 3'-terminus, and does not irreversibly modify synthetic reporter RNAs following prolonged exposure to overexpressed ISG20 in cells. Our results indicate that ISG20 may instead utilize an alternative mechanism for restricting cytoplasmic RNA viruses, including the alphaviruses. It should be noted that a similar translation inhibitory activity was recently demonstrated for ISG20 in the context of FLUAV infection, a nuclear replicating RNA virus (409). However, the proposed mechanism is based on ISG20 binding to the FLUAV nucleoprotein and genomic RNA, much like the direct binding mechanism recently presented for HBV (409, 444).

Despite our evidence suggesting ISG20 does not target viral RNA, an intact exonuclease domain is essential for its antiviral activities against the alphaviruses, which is similar to results published with the D94G ExoII mutant of ISG20 using other cytoplasmic RNA viruses. We have demonstrated that overexpressed ISG20, but not the ExoII mutant, modulates a pattern of gene regulation that closely resembles ISG and VSG induction by type I IFN. Furthermore, we have observed a reduction in select ISG induction by IFN in *Isg20*$^{-/-}$ primary cells compared to WT, strongly suggesting that ISG20 plays a fundamental role in regulating the robust expression of a subset of ISGs in response to low levels of IFN production. Our findings indicate that ISG20-mediated gene regulation is IRF3-dependent, demonstrating a clear pathway for ISG20-mediated antiviral activities that extend beyond the nucleus. Interestingly, in mice, this pathway extended to a significant early upregulation of IFN production, but this effect is not observed in our

overexpression system. We attribute this discrepancy to potential clonal mutations or cell type-specific regulatory activity within our inducible MEFs to circumvent sustained IFN production. While our ISG20 overexpressing MEFs respond to the RIG-I/MDA5 agonist, poly-(I:C), and produce IFN-α/β at similar levels to controls, notable IFN regulatory genes including Usp18 are induced by ISG20 overexpression, representing a possible pathway for the down-regulation of IFN.

In contrast to the robust antiviral effect of ISG20 against WT alphaviruses *in vitro*, we observed little or no difference in the virulence of WT CHIKV, VEEV and EEEV in our mouse models of infection. Basal expression of *Isg20* is minimal in most cell types, but it is strongly induced directly by IRF1 activation or through ISGF3 complex activation following IFN signaling. Likewise, an ISG20-mediated restriction in mice would be strongly dependent on the ability of a given virus to induce IFN. Both CHIKV and EEEV are weak inducers of IFN in mice, resulting in minimal detectible serum IFN within the first 24 hours of infection (14). However, VEEV robustly induces IFN shortly after infection, which is largely attributed to its strong tropism for myeloid cells (14). Thus, it is not surprising that a measurable phenotype was not observed with WT CHIKV and EEEV infection. In contrast, we did observe acute differences in VEEV clinical manifestations between B6 and *Isg20*$^{-/-}$ mice. While clinical differences were observed, survival was ultimately unaffected by *Isg20* knockout.

WT VEEV is resistant to the antiviral activity of IFIT1, owing this resistance to the terminal stem loop structure and positioning of the 5' terminal type-0 cap (3). Our findings *in vitro* suggest that ISG20 induces *Ifit1* among other genes, and is required for robust induction following IFN treatment in primary cells. Focusing on IFIT1 as a potential effector of the ISG20-mediated antiviral response, we assessed the virulence of VEEV-G3A, which is known to be sensitive to

IFIT1 activity *in vitro* and *in vivo* (3). Indeed, IFIT1-sensitivity resulted in a significant difference in VEEV virulence observed between B6 and *Isg20^{-/-}* mice, supporting our model for ISG20 regulation of other antiviral effectors. Furthermore, IFN is strongly induced between 12-24 hours – times at which differences in VEEV-G3A viral load are most apparent in tissues and serum.

Interestingly, IFN was induced at significantly lower levels by VEEV-G3A at 12 hours p.i. in *Isg20^{-/-}* compared to B6 mice. Our model of ISG20-mediated gene induction strongly implicates IRF3 as a signal transducer for downstream gene induction, which would include IFN-β among the targeted genes. While we observed no involvement in IFN induction or signaling in our overexpressed ISG20 model, our *in vivo* findings support a role for ISG20 in the positive feedback of type I IFN production in addition to specific gene induction, presumably through the same IRF3-mediated pathway.

Further supporting the direct involvement of IFIT1 as a mediator of the ISG20 response *in vivo*, virulence of EEEV-nt4&6, which has a similarly engineered susceptibility to IFIT1 as VEEV-G3A, was significantly decreased by ISG20 in mice. Unlike VEEV, EEEV largely evades myeloid cell replication, resulting in much lower levels of IFN induction in mice (125, 127). Consequently, EEEV-nt4&6 is not as sensitive VEEV-G3A to ISG20-mediated restriction in mice. However, EEEV-nt4&6 disease in *Isg20^{-/-}* mice closely resembles that which is observed in *Ifit1^{-/-}* mice (Trobaugh unpublished manuscript). Together, our *in vivo* findings with VEEV-G3A and EEEV-nt4&6 support a role for IFIT1 and a positive feedback regulation of IFN as contributors to the ISG20-mediated antiviral restriction of alphaviruses in animal models of disease.

In conclusion, we propose a model by which induced ISG20 blocks incoming alphavirus genome translation through the modulation of additional antiviral ISGs and a more robust induction of type I IFN. This modulation of the host antiviral environment is achieved through the

95

direct activation of ISGs via IRF3 and, *in vivo*, a positive feedback loop of IFN production (**Figure 24**). Given that ISG20 acts to degrade RNAs in the nucleosome and that the exonuclease domain is required for transcription-stimulating activity, it is tempting to speculate that these degradation products somehow activate the IRF3 pathway, perhaps by stimulating RIG-I or MDA5 RNA binding proteins. Additionally, ISG20 may not be increasing the nuclear translocation of IRF3, but instead may be preventing its deposphorylation or degradation. Such a mechanism would likely involve the down-regulation or inhibition of specific phosphatases and ubiquitin ligases.
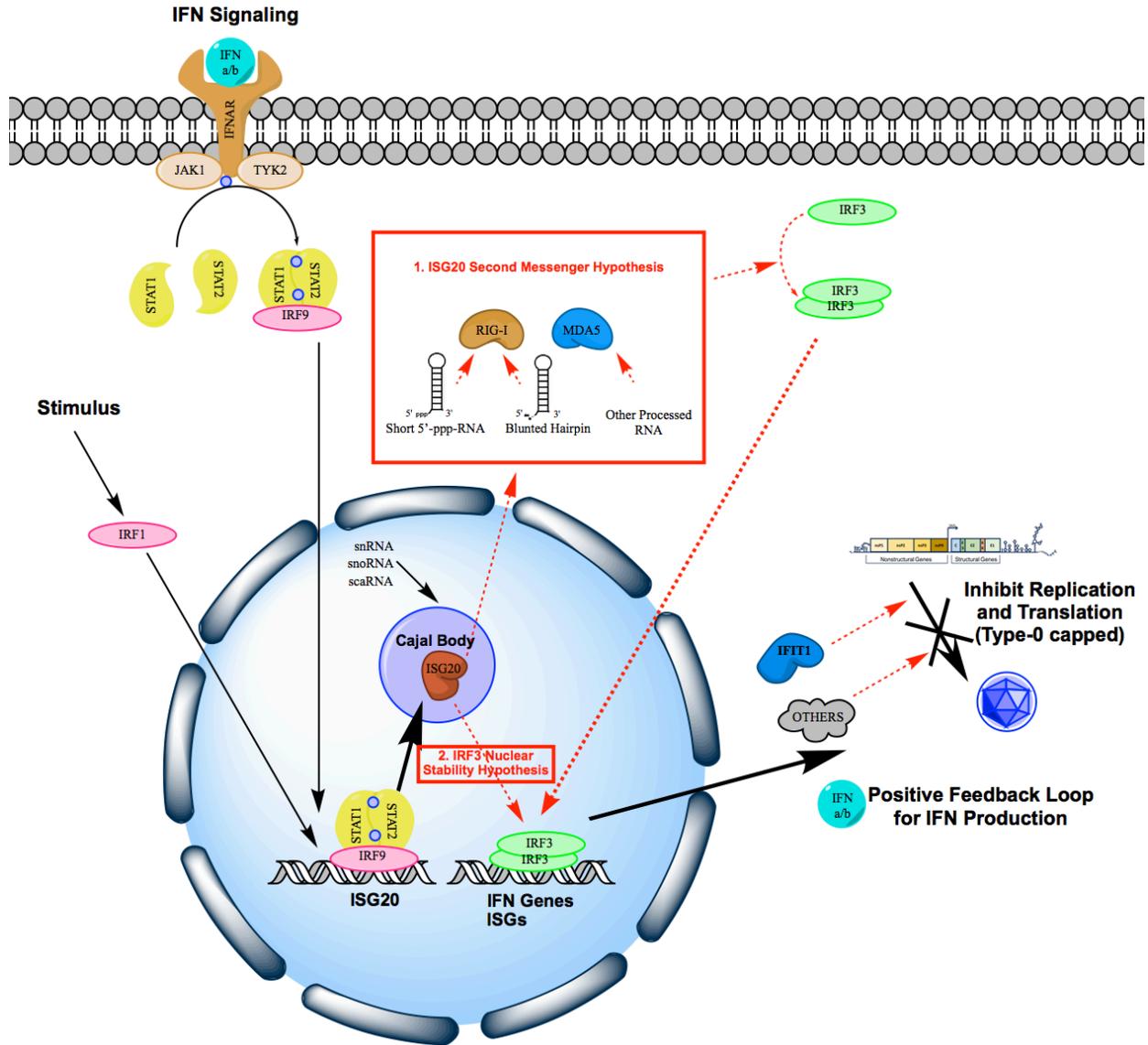
Figure 24: ISG20 Antiviral Model

A model for ISG20-mediated antiviral restriction of alphaviruses is given. Non-bolded black arrows represent published pathway nodes. Bolded black arrows are pathways nodes described in experimental detail herein. Red-dashed nodes are hypothetical and will be the focus of future work.

4.2   SECOND MESSENGER HYPOTHESIS

ISG20 localizes to the sub-nuclear CB structures, and has been shown to co-precipitate in association with the U1 and U2 snRNAs of the spliceosome and U3 snoRNA required for 18S ribosomal RNA (rRNA) processing (404). ISG20 also specifically associates with the survival of motor neurons (SMN) protein within the nucleus, either through direct binding or in complex with the primary CB structural component, coilin (404). SMN acts as a binding platform for the assembly of Sm proteins with their associated uridine-rich snRNAs (454). The snRNAs and associated proteins are then assembled within CBs to form the functional spliceosome machinery responsible for intron removal and splicing of exons (446). Due to its close interaction with CB-associated factors, it is likely that ISG20 is exposed to additional RNA substrates including additional small nuclear RNAs (snRNAs) as well as the small CB-specific RNAs (scaRNAs) and small nucleolar RNAs (snoRNAs) that interact with CB during biogenesis.

The snRNAs, including U1 and U2 are transcribed by RNA polymerase II (Pol-II), and contain a 7-metylguanosine cap structure that is further modified as a 2,2,7-trimethylguanosine cap prior to nuclear import (455). One notable exception to the biogenesis pathway for snRNAs is U6, which is transcribed from RNA polymerase III (Pol-III), and contains a triphosphate motif at the 5'-terminus and 2',3'-cyclic phosphate motif at the 3'-terminus (456, 457). Unlike the Pol-II-transcribed snRNAs, U6 is retained in the nucleus throughout biogenesis and associates with the U4/U6 snRNP (456). The predicted secondary structure of U6 reveals a highly conserved 5'-stem-loop structure including the 5'-terminal triphosphate nucleotide (458). However, 3' secondary structures are fluid, and depend on intramolecular complexes formed between the U4 and U2 snRNAs at different points in the splicing process (458). Thus, it is possible that the lack of 3'-structure in U6 would allow for ISG20-mediated 3'-5'-degradation, producing a truncated hairpin

structure with a 5'-triphosphate and no 5'-terminal overhang. Such a degradation product would be free to diffuse from the associated splicing factors, with potential to interact with the cytosolic RNA sensors RIG-I and MDA5.

RIG-I recognizes primarily 5'-triphosphate dsRNAs as well as type-0 capped dsRNAs lacking 2'-O-methylation (235, 236, 241, 459). RIG-I is not accommodating to 5'-terminal ssRNA overhangs, requiring substrates to be blunt ended, either in complex or as a terminal hairpin structure (241, 459, 460). Our proposed ISG20-directed U6 degradation product would fit the above criteria as an activator of RIG-I. In addition to truncated-U6 as a specific activator of RIG-I, it is conceivable that other degradation products from the RNAs associated with CB and ISG20 could serve as molecular second messengers for the cytoplasmic RNA sensors. Such an activation model would explain the downstream involvement of IRF3 as an ISG20 signal transducer, and is consistent with the requirement of ISG20 nuclease activity for ISG20-regulated gene stimulation and antiviral activity. Indeed, a similar involvement of RIG-I has been demonstrated for another cellular nuclease, RNase L, where cleaved self-RNAs amplify signaling through RIG-I (239). Another cytoplasmic RNA sensor, MDA5, recognizes primarily long, blunt-ended dsRNA without a terminal triphosphate or cap requirement (242). ISG20-mediated trimming of nuclear RNAs in complex, including the snRNAs of the spliceosome, could presumably result in blunt-ended RNA duplexes capable of MDA5 stimulation.

4.3   NUCLEAR STABILITY HYPOTHESIS

IRF3 is distributed throughout the cytoplasm of most cell types at rest. Upon pathogen-associated signal recognition, IRF3 is poly-phosphorylated by TBK1 and IKKε in its C-terminal

transactivation domain, stimulating dimerization and ultimately translocation into the nucleus where it acts as a transcription factor for IFN-β and other target genes (244, 461). IRF3 is inactivated by two distinct mechanisms, proteasomal degradation and PP2A/RACK1 mediated dephosphorylation (462, 463). Disruption of either of these pathways would lead to an aggregation of IRF3 within the nucleus, and prolonged transcription of IRF3-responsive genes.

The exonuclease-deficient ISG20 mutant, ExoII, fails to induce antiviral gene transcription when overexpressed. It is therefore unlikely that ISG20 is regulating either of these pathways through protein-protein interactions. Instead, ISG20 may be regulating either of these through a nucleic acid intermediate. Transcriptional regulation could occur through ISG20-mediated mRNA degradation in the nucleus or perhaps through the regulation of long noncoding RNAs (lncRNA). lncRNAs are capable of regulating clusters of genes in a cis or trans fashion by binding nearby promoter elements to either up- or down-regulate transcription of genes through the rearrangement of histones or recruitment of basal transcription factors (464, 465). Indeed, ISG20 was shown to bind and modify HBV RNA within the nucleus, demonstrating an ability to interact with RNA substrates outside of the CB (444). However, transcriptional down-regulation of PP2A, RACK1 or any of the ubiquitin E3 ligases was not detected by RNA-seq when ISG20 is overexpressed. Likewise, ISG20-mediated protein interactions that inhibit RACK1/PP2A complex formation is unlikely because ExoII, which only differs by a single amino acid in the catalytic site does not result in IRF3 accumulation.

ISG20 interactions with spliceosome and nucleolar RNAs may point to the involvement of splicing or ribosome biogenesis. Splicing occurs as sequence elements in the nascent pre-mRNA transcripts are recognized by the small nuclear ribonucleoprotein particles of the spliceosome (466). A complex forms at the 5' and 3' end of an intron, mediated by specific interactions between

100

the snRNAs of each subunit, and facilitates intron lariat formation and excision (466). Exon selection is mediated by cellular conditions including cis- and trans-acting protein elements that favor which exons are used (466). Changes to the snRNAs of the spliceosome would result in global changes in splicing frequencies, likely decreasing splicing efficiency in cells where ISG20 is overexpressed. While transcript variants were observed between ISG20 overexpressing and control cells, a pattern of global regulation was not apparent, with only 31 gene isoforms consistently regulated (data not shown). Likewise, impacts on ribosome biogenesis would likely have far-reaching consequences for ISG20 overexpressing cells and would likely not manifest as a targeted regulation of IRF3 phosphatases. While two potential approaches to IRF3-dependent gene transcription are possible, our data strongly suggests that ISG20 is not simply stabilizing IRF3 in the nucleus by preventing dephosphorylation and degradation, but rather points to a mechanism of activation and translocation.

4.4   FUTURE DIRECTIONS

Building on the framework of our model, future work should elucidate the extent to which IFIT1 is responsible for ISG20-mediated alphavirus translation inhibition and whether alternative mechanisms are involved. WT alphaviruses are inhibited by overexpressed IFIT1 *in vitro*, but are not more virulent in *Ifit1*$^{-/-}$ mice (3, 340, 364). While translation suppression appears to be the primary mechanism of alphavirus restriction by ISG20, the breadth of antiviral effectors regulated by ISG20 would suggest additional points of intervention are likely involved. Many of the most highly induced genes from ISG20 stimulation have antiviral activity, but the mechanism is unknown. Using the narrow scope of ISG20-induced antiviral effectors, focus should be given to

studying the activity of these gene products. In addition to the ISG20 up-regulated factors, several down-regulated gene transcripts were identified by RNA-seq, including the structural components, collagen and laminin. While the primary focus should be placed on the antiviral effectors induced by ISG20, the functional consequences of the downregulated genes are nevertheless an interesting topic of study. Together, studies of both up- and down-regulated genes will provide a more complete understanding of how these factors are working together to suppress viral replication.

Another important area of future study is the mechanism by which ISG20 is stimulating IRF3 involvement, and what additional pathways may be involved, including other IRFs induced downstream or independently of IRF3, including IRF7 and IRF9, both of which are upregulated by ISG20. Importantly, IRF3 transcriptional activity is facilitated by polyphosphorylation and translocation to the nucleus, two biological activities that should be explored in further detail in our ISG20 overexpression model. We hypothesize the involvement of a signaling pathway where ISG20 is producing a second messenger as a degradation product of cellular RNAs, similar to the RIG-I-mediated enhancement of IFN observed from active RNase L (239). The primary focus of such work should define the targets of ISG20 degradation, whether degradation products may function as second messengers, and what cellular factors are necessary for signal transduction. Such a pathway would involve the mitochondrial adapter MAVS as well as the cytosolic RNA sensors RIG-I or MDA5. Studies should address this pathway through overexpression of ISG20 in either *Mavs*$^{-/-}$, *Ddx58*$^{-/-}$ (RIG-I) or *Mda5*$^{-/-}$ cells. While there is no clearly defined target for potential ISG20 degradation, the U6 snRNA would be a promising candidate for follow-up study due to its RNA structure and the predicted resulting degradation products.

Additionally, ISG20-stimulated feedback of IFN appears to occur *in vivo*, and may contribute to the overall phenotypic differences observed between *Isg20*$^{-/-}$ and WT mice. Thus it

is necessary to determine whether low-level IFN production, below the limits of detection with our current methods, may be contributing to the antiviral gene pathways regulated by overexpressed ISG20 *in vitro* as our model would predict. While type I IFNs, particularly IFN-β, have been the focus of our work with ISG20, IFN-λ may account for a similar induction profile as we've observed with ISG20-overexpression, and should be the focus of additional studies as a mediator of antiviral gene upregulation. Combined with our current understanding of ISG20 as a regulator of antiviral gene transcription, a more complete understanding of ISG20 activity may lead to targeted antiviral therapies and serve as a foundation for rational vaccine design against the alphaviruses and other cytoplasmic-replicating viruses.

5.0   MATERIALS AND METHODS

VIRUSES AND STOCKS

Generation of the wild type La Réunion CHIKV-LR clone (467), a gift from Dr. Stephen Higgs, Kansas State University, and the non-structural reporter CHIKV-nsP3-(GFP/nLuc) clone or structural reporter CHIKV-TaV-(GFP/nLuc) (56) are previously described. The WT VEEV (ZPC738) and VEEV-G3A clones are described (468, 469). The WT EEEV (FL93-939) clone is described (470). EEEV-nt4&6 (FL93-939-G4A/G6A) was generated by QuickChange site-directed mutagenesis of FL93-939 parental strain (Trobaugh, unpublished manuscript). Viruses were generated from *in vitro* transcribed infectious clones (mMessage mMachine, Ambion) and electroporated in BHK-21 cells. Supernatants were collected at 24 hours and centrifuged to remove cell debris prior to freezing individual use aliquots of each virus at -80ºC. All viral titers were determined by BHK-21 plaque assay and are expressed in PFU/mL.

MICE AND INFECTIONS

Male or pregnant female C57Bl/6J mice were purchased from the Jackson Laboratory. *Isg20*^{-/-} mice were generated at Washington University after receiving heterozygous sperm from C57BL/6 mice containing a promoter knockout (Isg20[tm1a(KOMP)Wtsi]) from the Knockout Mouse Project Repository (KOMP; University of California, Davis). Sperm was used for *in vitro* fertilization of eggs from C57BL/6 recipient female mice. Heterozygous *Isg20*^{+/−} mice were backcrossed to

establish the *Isg20*^{-/-} colony. *Isg20*^{-/-} mice produced normal litter sizes of expected Mendelian ratios, with all progeny appearing healthy. Mice were used at ages 1 day or 3 weeks for CHIKV infection and an age of 6 weeks for VEEV infection. CHIKV (10^3 plaque forming units, PFU) was inoculated subcutaneously (sc) in the left rear footpad in 10 μL of OptiMEM. VEEV was inoculated sc in each rear footpad with 10^3 PFU for a total of 2×10^3 PFU per animal. Disease was monitored by changes in weight and clinical scoring specific to the disease manifestations of each virus every 12 to 24 h. For virus titration, RNA isolation and IFN bioassay, serum was collected from submandibular vein, and mice were euthanized and perfused with 10 mL of PBS before tissue collection. Tissues were collected in 100 uL of PBS with 1% bovine serum per gram of tissue, mechanically dissociated, and virus titers were determined by BHK-21 plaque assay on the resulting supernatants. Serum was assayed for functional type I IFN using a bioassay as previously described (208). All animal experiments were conducted under the guidance of approved protocols by the institutional animal care and use committee of the University of Pittsburgh.

TET-OFF MEF CELL CULTURE

Tet-off murine embryonic fibroblasts (MEFs) overexpressing ISG20 and eGFP control proteins were previously described and tet-off MEFs overexpressing ISG20[D94G] (ExoII) cells were generated in the same fashion (340). The ExoII gene was made by aligning the human sequence with the mouse sequence and mutation the active site of the exonuclease to match the human ExoII nuclease deficient mutant (405). Tet-off MEFs were maintained in complete media consisting of Dulbecco's modified Eagle's medium (DMEM) supplemented with 10% heat-inactivated fetal bovine serum (FBS), 200 mM L-glutamine, 10,000 units/mL penicillin, 10 mg/mL streptomycin, 100 μg/mL G418 sulfate, and 100 μg/mL hygromycin sulfate. Gene overexpression was

suppressed with the addition of 2 µg/mL doxycycline hyclate (Sigma) for cell expansion prior to experiments.

OVEREXPRESSION OF TARGET GENES

For overexpression experiments, tet-off MEFs were trypsinized and washed in sterile phosphate buffered saline three times and plated and induced in doxycycline-free, complete tet-off MEF media for 72 hours prior to use. Gene overexpression was confirmed by both qRT-PCR and Western blot for these conditions. All cells were grown to approximately 80% confluence for optimal infection and transfection conditions in subsequent experiments.

GENERATION OF PRIMARY CELLS

Osteoblasts were prepared by dissecting calvaria from 4 day-old pups and manually removing surrounding tissue. Calvaria were washed in PBS and digested in two 20-minute and one 90-minute digests in AMEM with 96 µg/mL collagenase P and 0.01% trypsin-EDTA on a shaking 37°C incubator. Digested calvaria were washed in PBS and suspended in AMEM supplemented with 10% FBS, 10,000 units/mL penicillin, and 10 mg/mL streptomycin for 5 days undisturbed on 100 mm cell culture dishes. Osteoblasts were trypsinized and expanded for two passages on T-75 flasks prior to infections.

Primary MEFs were prepared from pregnant mice at 14 days gestation. The head and liver was removed from individual embryos and specimens were rinsed in PBS. Embryos were minced in ice cold 0.25% trypsin-EDTA solution then heated to 37°C for 30 minutes in a water bath. MEFs were homogenized by serial passage through 18 and 23 gauge needles. Cells were washed and

resuspended in DMEM supplemented with 10% heat-inactivated FBS, 10,000 units/mL penicillin, and 10 mg/mL streptomycin. MEFs were expanded to passage 2 for individual experiments.

VIRUS GROWTH ASSAYS

50 µL of WT, non-reporter virus supernatant was drawn from infected cells at various times post infection and virus titer was determined by BHK-21 plaque assay. Nano luciferase reporter-virus infected cells were washed 3 times in PBS and lysed in luciferase passive lysis buffer then frozen to aid in complete disruption of cellular membranes. 25 µL of each sample lysate was combined with 25 µL of prepared NanoGLO chemiluminescent reagent and incubated for 6 minutes at room temperature. Chemiluminescent signal was detected on a luminometer as relative light units and normalized to individual sample protein concentrations determined by BCA protein assay.

INTERFERON BIOASSAY

Cleared serum or cell culture supernatant was acidified to pH=2.0 with 1M HCl and incubated for 24 hours at 4°C. Samples were neutralized to pH=7.4 and serially diluted in 2-fold intervals in RPMI media supplemented with 10% FBS, 10% tryptose phosphate broth, 200 mM L-glutamine, 10,000 units/mL penicillin, and 10 mg/mL streptomycin. Diluted samples were added to confluent L929 murine mesenchymal cells on 96-well cluster plates and incubated for 24 hours at 37°C with 4% atmospheric CO_2. Cells were infected with EMCV at MOI=0.5 added directly to the IFN sample-treated cells and incubated for an additional 24 hours. Cells were fixed and stained with 1% crystal violet in 10% methanol for 15 minutes and washed to remove residual counterstain. IFN concentration was determined empirically against a standard dilution series of murine IFN-α4/β (1:1) of known concentration based on protection from cytopathic effect.

TRANSLATION REPORTERS

 The non-replicating host, EMCV and CHIKV virus-mimic translation reporters were described, or produced as described (127, 339). The CrPV translation reporter, a gift from Dr. Martin Bushell, Medical Research Council, UK, was described (471). Tet-off MEFs were induced on 150mm dishes as described above for overexpression of the contained gene of interest. Induced cells were trypsinized and washed once in OptiMEM. Approximately $3x10^7$ cells were resuspended in 1 mL of OptiMEM per reaction and electroporated with 7.5 µg of indicated reporter RNA and 750 ng of renilla luciferase mRNA. Electroporated cells were diluted in doxycycline-free MEF complete media and divided on 96-well cluster plates. Cells were collected at the indicated time points by centrifugation, washed once in PBS, and lysed in luciferase passive lysis buffer 0.25 µL of collected lysates were assayed by Dual Luciferase Assay (Promega) and normalized to protein concentration as determined by BCA protein assay (Thermo Scientific).

PROMOTER ACTIVATION REPORTERS

 Construction of promoter luciferase plasmids pRL-SV40, pβLUX, a gift form Dr. Barbara Sherry, North Carolina State University, (472), PRDI/III or PRDII, gifts form Dr. Tom Maniatis, Harvard University (245), were described previously. MEFs were induced in 24-well cluster plates for overexpression of the target protein for 3 days as described above. 0.5 µg/well of promoter luciferase plasmid and 0.25 µg/well of Renilla luciferase control plasmid were transfected into MEFs using TransIT-LT1 reagent (Mirus) for 24 hours. Cells were treated 16 hours prior to harvest with 0.3 µg poly-(I:C) in TransIT-LT1 reagent or transfection reagent alone. Lysates were collected in passive lysis buffer and measured by dual luciferase assay (Promega) and results given as a ratio of firefly to renilla luciferase signal.

RNA SEQUENCING

Total cellular RNA from two separately derived clones of tet-off MEFs overexpressing eGFP, ISG20 or ISG20^{D94G} was isolated and depleted of ribosomal RNA with the Ambion RiboMinus Eukaryote Kit v2 (Life Technologies). Directional sequencing libraries were generated using the NEBNext Ultra Directional RNA Library Prep Kit for Illumina with NEBNext Primer Set 1 (New England Biolabs). Multiplexed libraries were sequenced with 100bp paired end reads on the Illumina HiSeq2000 platform (Axeq Technologies). Reads were aligned to the iGenome indexed Mus musculus genome UCSC mm9 (Illumina) using Tophat and differential gene expression was determined using Cufflinks (473). Pathway analysis of differentially-regulated genes was performed using Ingenuity Pathway Analysis (Qiagen) with a minimum read threshold of 10 counts.

QRT-PCR

Forward and reverse primers for qRT-PCR were designed as follows: Isg20-F 5'-AAC ATC CAG AAC AAC TGG CGG-3'; Isg20-R 5'-GTC TGA CGT CCC AGG GCA-3'; Irgm2-F 5'-GCG ATA GAG ATT CGG AAA GC-3'; Irgm2-R 5'-CAG CAC CCA GTC ATC TTG TT-3'; Usp18-F 5'-AGG AGT CCC TGA TTT GCG TG-3'; Usp18-R 5'-GGG TTT TCA GAG GCT TTG CG-3'; Ifit3-F 5'-AGA TTT CTG AAC TGC TCA GCC C-3'; Ifit3-R 5'-CAG AGA TTC CCG GTT GAC CTC-3'; Irf7-F 5'-ATT CGG TCG TAG GGA TCT G-3'; Irf7-R 5'-GTT GGT CTT CCA GCC TCT TC-3'; Ifi44-F 5'-ACT CGT TTG ACA TGG CAG CA-3'; Ifi44-R 5'-TCT GCA CAC TCG CCT TGT AA-3'; Ifit1-F 5'-GTG GCT CAC ATA GAG CAG GA-3'; Ifit1-R 5'-AGT TTC CTC CAA GCA AAG GA-3'; Oas1a-F 5'-TCC ACA GTA CGC CCT AGA GT-3'; Oas1a-R 5'-GAC CAG TTC CAA GAC GGT CC-3'; Igtp-F 5'-TCT GAG CAG GTT CTG AAG GA-3'; Igtp-

R 5'-TCC TCG GCT TCT TTC TTC TC-3'; Isg15-F 5'-TCC ATG ACG GTG TCA GAA CT-3';

Isg15-R 5'-GAC CCA GAC TGG AAA GGG TA-3'; Ifit2-F 5'-AGA ATT CAC CTC TGG ATG

GG-3'; Ifit2-R 5'-GTC AAG CTT CAG TGC CAA GA-3'; Irf3-F 5'-GCG GTT AGC TGC TGA

CAA TA-3'; Irf3-R 5'-AGG CCA TCA AAT AAC TTC GG-3'; CHIKV-3'NTR-F 5'-ATA ATT

GGC AAA CGG AAG AGA T-3'; CHIKV-3'NTR-R 5'-ACA AAA TAA CAT CTC CTA CGT

CC-3'. qRT-PCR primers for CHIKV positive strand detection were previously described (474).

cDNA was reverse transcribed with specific reverse primers from 100 ng of tri-reagent-extracted

RNA and detected by qPCR with SYBR green on a MiniOpticon thermal cycler and detection unit

(Bio Rad). Fold-induction was determined for genes of interest using the $\Delta\Delta C_t$ method.

WESTERN BLOT

MEFs were induced for 72 hours as described above then lysed completely in radio

immunoprecipitation assay buffer with protease and phosphatase inhibitors. Cell wall debris was

cleared by centrifugation and 20ng of protein were electrophoresed on 5%/10% SDS poly-

acrylamide discontinuous gels. Gels were transferred to polyvinylidene difluoride (PVDF)

immunoblotting membrane by semi-dry transfer and blocked with 5% non-fat milk in tris-buffered

saline with 0.1% Tween-20 (TBS-T) for 1 hour. Anti-FLAG M2-Peroxidase conjugate (1:2000)

was applied for 2 hours at room temperature, or rabbit anti-mIFIT1 (1:1000) was applied overnight

at 4ºC with shaking. Secondary detection of IFIT1 was performed by thoroughly washing in TBS-

T followed by goat anti-rabbit-HRP conjugate (1:2000) for 1 hour at room temperature. Blots were

thoroughly washed prior to detection with Pierce ECL detection reagent (Thermo Scientific) and

chemiluminescence film exposure (GE Healthcare).

IMMUNOFLUORESCENCE

Cells grown on glass coverslips were fixed in 4% paraformaldehyde for 15 minutes and permeablized with 0.1% Triton X-100 in PBS for 15 minutes. Fixed cells were rehydrated in PBS with 0.5% BSA (PBS-B) and blocked for 45 minutes in 20% serum in PBS-B, corresponding to the secondary detection antibody species. Primary and secondary detection antibodies were applied for 1 hour each at room temperature in PBS-B. Immunofluorescence was preserved with SlowFade Gold antifade reagent with DAPI (Invitrogen) and mounded on glass slides for confocal microscopy. M2 anti-FLAG FITC conjugate antibody (Sigma) was used for detection of both FLAG-tagged murine ISG20 and ISG20^{D94G}.

STATISTICS

All statistics were calculated in GraphPad PRISM with $\alpha = 0.05$. Hypotheses for mRNA expression levels were calculated by two-tailed Mann-Whitney test on $\log_{10}$-transformed fold-change values. Parametric hypotheses with assumed standard deviations were calculated by multiple Student's t tests. Hypotheses for virus growth curves, reporter expression ratios, and percent of starting value were calculated on $\log_{10}$-transformed datasets by two-way ANOVA, correcting for multiple comparisons using the Holm-Sidak method, or ANOVA, correcting for multiple comparisons using Dunnett's method. Survival hypotheses were tested by log-rank test. The statistical model for differential gene expression by RNA-seq is described in detail (475). The Cuffdiff 2 gene expression model was determined for a false discovery rate of 5%.

APPENDIX A

DEFINITIONS

ATF-2	Activating transcription factor 2
BHK-21	Baby hamster kidney cell [clone C-13]
c-Jun	Early response transcription factor
CARD	Caspase activation and recruitment domain
CB	Cajal body
CBP	CREB-binding protein
cGAMP	Cyclic guanosine/adenosine monophosphate
cGAS	Cytosolic GAMP synthase
CHIKV	Chikungunya virus
CrPV	Cricket paralysis virus
DBS	Donor bovine serum
DMEM	Dulbecco's Modified Eagle Medium
DNA	Deoxyribonucleic acid
EEEV	Eastern equine encephalitis virus
eGFP	Enhanced green fluorescent protein
EMCV	Encephalomyocarditis virus
ExoII	ISG20 aspartic acid 94 to glycine mutation of exonuclease active site domain 2
FBS	Fetal Bovine Serum
IFIT	Interferon induced protein with tetratricopeptide repeats
IFN	Interferon
IFNAR	Interferon alpha receptor
IKKε	IκB kinase-ε
IRAK	Interleukin-1 receptor-associated kinase

112

IRF	Interferon regulatory factor
ISG	Interferon-stimulated gene
Isg20	Murine 20 kilodalton interferon-stimulated gene (gene)
ISG20	Human or mouse 20 kilodalton interferon-stimulated gene (protein)
Isg20$^{-/-}$	Homozygous *Isg20*-null genotype
ISGF	Interferon-stimulated gene factor complex
JAK	Janus kinase
kDa	kilodalton
L-929	NCTC clone 929 subcutaneous connective cell derived from strain L
lncRNA	Long non-coding RNA
MAVS	Mitochondrial antiviral signaling protein
MDA5	Melanoma differentiation-associated gene 5
MEF	Murine embryonic fibroblast cell
MyD88	Myeloid differentiation primary response protein 88
NFκB	Nuclear factor-κB
NLR	NOD-like receptors
nLuc	Nano-luciferase
NOD	Nucleotide-binding oligomerization domain-containing protein
nsP	non-structural protein
NTR	Non-translated region
p300	E1A binding protein
PAMP	Pathogen associated molecular pattern
Pol	RNA polymerase (I, II, or III)
PRR	Pattern recognition receptor
qRT-PCR	Quantitative reverse-transcription polymerase chain reaction
RIG-I	Retinoic acid inducible gene 1 (also *Ddx58*)
RLR	RIG-I-like receptor
RNA	Ribonucleic acid
RPMI	Roswell Park Memorial Institute 1640 Media
scaRNA	Small Cajal body associated RNA
SINV	Sindbis virus
siRNA	Small-interference ribonucleic acid
snoRNA	Small nucleolar RNA
snRNA	Small nuclear RNA
snRNP	Small nuclear ribonucleoprotein particle

ssRNA	Single-stranded ribonucleic acid
STAT	Signal transducer and activator of transcription
STING	Stimulator of IFN genes
SV	Sendai virus
TaV	Thosea assigna virus 2A-like cleavage signal peptide
TBK1	TANK-binding kinase 1
Tet	Tetracycline
Tet-off	Tetracycline removal-induction system
TLR	Toll-like receptor
TRAF	(Tumor Necrosis Factor) receptor-associated factor
TRIF	TIR domain-containing adapter protein inducing IFN-β
TYK-2	Tyrosine kinase 2
VEEV	Venezuelan equine encephalitis virus
VSG	Virus Stimulated Gene
WT	Wild type

APPENDIX B

ISG20-UPREGULATED GENES

Gene Name	Gene ID	Gene Description	Protein Class	log(ISG20/GFP)	log(ISG20/ExoII)
Apol9b	71898	Apolipoprotein 9b	apolipoprotein	1.131	1.908
Apol9a	223672	Apolipoprotein 9a	apolipoprotein	0.894	1.573
Apol10b	328561	Apolipoprotein 10b	apolipoprotein	0.691	0.871
Ccl7	20306	C-C motif chemokine 7	chemokine	0.669	0.775
Ccl2	20296	C-C motif chemokine 2	chemokine	0.628	0.964
Ddx58	230073	ATP-dependent RNA helicase RIG-I	cytoplasmic RNA sensor	0.834	0.763
Has2	15117	Hyaluronan synthase 2	glycosyltransferase	0.707	0.477
Irgm2	54396	Interferon-gamma induced GTPase	GTPase	1.697	1.367
Igtp	16145	Interferon-gamma induced GTPase	GTPase	1.119	1.189
Irgm1	15944	Immunity-related GTPase family M protein 1	GTPase	0.663	0.375
Ifit3b	667370	Interferon-induced protein with tetratricopeptide repeats 3B	IFIT protein	1.451	1.100
Ifit1	15957	Interferon-induced protein with tetratricopeptide repeats 1	IFIT protein	1.440	1.540
Ifit3	15959	Interferon-induced protein with tetratricopeptide repeats 3	IFIT protein	1.256	0.956
Xaf1	327959	XIAP-associated factor 1	metal ion binding	0.825	0.815

Trim30a	20128	Tripartite motif-containing protein 30A	nucleic acid binding	1.465	1.557
Trim12c	319236	Tripartite motif-containing 12C	nucleic acid binding	1.118	0.702
Parp14	547253	Poly [ADP-ribose] polymerase 14	nucleotidyltransferase	1.297	1.031
Oasl2	23962	2'-5'-oligoadenylate synthase-like protein 2	nucleotidyltransferase	1.165	1.926
Parp9	80285	Poly [ADP-ribose] polymerase 9	nucleotidyltransferase	0.946	0.668
Pde1b	18574	Calcium/calmodulin-dependent 3',5'-cyclic nucleotide phosphodiesterase 1B	phosphodiesterase	1.156	0.846
Samd9l	209086	Sterile alpha motif domain containing 9-like	protein binding	1.381	0.849
Lgals3bp	19039	Galectin-3-binding protein	protein binding	0.789	0.792
Lncenc1	100039691	Long non-coding RNA, embryonic stem cells expressed 1	regulator of gene expression	0.920	0.712
Irf7	54123	Interferon regulatory factor 7	transcription factor	1.343	1.354
Stat1	20846	Signal transducer and activator of transcription 1	transcription factor	0.596	0.570
Stat2	20847	Signal transducer and activator of transcription 2	transcription factor	0.574	0.522
Irf9	16391	Interferon regulatory factor 9	transcription factor	0.486	0.575
Tap1	21354	Antigen peptide transporter 1	transport protein	0.531	0.536
Isg15	100038882	Ubiquitin-like protein ISG15	ubiquitin-like protein	0.925	1.645
Dtx3l	209200	E3 ubiquitin-protein ligase DTX3L	ubiquitin-protein ligase	0.979	0.621
Herc6	67138	E3 ISG15--protein ligase Herc6	ubiquitin-protein ligase	0.789	0.434
Ifi44	99899	Interferon-induced protein 44	unassigned	1.483	1.673
Xlr	22441	X-linked lymphocyte-regulated protein PM1	unassigned	1.296	0.648
Sp140	434484	Sp140 nuclear body protein	unassigned	0.930	0.688
Bst2	69550	Bone marrow stromal antigen 2	unassigned	0.798	1.082
Ifi35	70110	Interferon-induced 35 kDa protein	unassigned	0.503	0.620

Illumina directional libraries were generated from ribosomal RNA-depleting total cellular RNA from MEFs overexpressing eGFP, ISG20, and ExoII mutant. 100 bp paired-end deep sequencing was performed on HighSeq 2000 (Illumina). Differential gene expression was determined by Tuxedo Suite pipeline and genes significantly upregulated by ISG20 overexpression versus both eGFP and ExoII controls. Common gene names were matched to mm9 genome loci and RefSeq gene IDs, gene descriptions and protein classes were determined by PANTHER classification system with additional manual curation.

APPENDIX C

ISG20-DOWNREGULATED GENES

Gene Name	Gene ID	Gene Description	Protein Class	log(ISG20/GFP)	log(ISG20/ExoII)
Sorbs2	234214	Sorbin and SH3 domain-containing protein 2	cytoskeletal protein	-1.190	-0.936
Col2a1	12824	Collagen alpha-1(II) chain	extracellular matrix linker protein	-1.298	-1.590
Lama2	16773	Laminin subunit alpha-2	extracellular matrix linker protein	-1.498	-1.860
Bmp4	12159	Bone morphogenetic protein 4	growth factor	-0.769	-0.824
Peg10	170676	Retrotransposon-derived paternally expressed 10	nucleic acid binding	-0.692	-0.735
Pde8a	18584	High affinity cAMP-specific and IBMX-insensitive 3',5'-cyclic phosphodiesterase 8A	phosphodiesterase	-0.737	-0.920
Xist	213742	Inactive X specific transcripts	ribonucleoprotein complex binding	-0.896	-1.204

Table 3: ISG20-Downregulated Genes

Illumina directional libraries were generated from ribosomal RNA-depleting total cellular RNA from MEFs overexpressing eGFP, ISG20, and ExoII mutant. 100 bp paired-end deep sequencing was performed on HighSeq 2000 (Illumina). Differential gene expression was determined by Tuxedo Suite pipeline and genes significantly downregulated by ISG20 overexpression versus both eGFP and ExoII controls. Common gene names were matched to mm9 genome loci and RefSeq gene IDs, gene descriptions and protein classes were determined by PANTHER classification system with additional manual curation.

APPENDIX D

PREDICTED UPSTREAM EFFECTORS OF ISG20 GENE-REGULATION PATHWAY

Upstream Regulator	Molecule Type	Predicted Activation State	Activation z-score	p-value of overlap	Target molecules in dataset	Mechanistic Network
IFNAR	group	Activated	4.305	1.34E-23	Bst2, Ccl2, CCL5, CXCL10, DDX58, EIF2AK2, IFI35, IFIH1, IFIT1B, IFIT2, IFIT3, Irgm1, ISG20, OAS1, PNPT1, STAT1, STAT2, USP18, XAF1	53 (18)
IRF7	transcription regulator	Activated	4.666	1.73E-23	ADAR, CCL5, CXCL10, DDX58, IFI35, IFI44, IFIH1, IFIT1B, IFIT2, IFIT3, Igtp, Irgm1, ISG15, ISG20, OAS1, Oasl2, RTP4, SAMD9L, STAT1, STAT2, Trim30a/Trim30d, USP18, XAF1	43 (13)
RIG-I	enzyme	Activated	3.243	4.31E-22	Ccl2, CCL5, CXCL10, DDX58, EIF2AK2, IFI35, IFI44, IFIH1, IFIT1B, IFIT2, IFIT3, ISG15, ISG20, OAS1, STAT1, STAT2	42 (13)
IRF3	transcription regulator	Activated	4.044	5.54E-19	Ccl2, CCL5, CXCL10, DDX58, IFI44, IFIH1, IFIT1B, IFIT2, IFIT3, Igtp, Irgm1, ISG15, ISG20, OAS1, Oasl2, SAMD9L, STAT1, STAT2, Trim30a/Trim30d, USP18	39 (14)

MAVS	other	Activated	3.395	7.62E-17	ADAR, CCL5, CXCL10, DDX58, IFIT1B, IFIT2, IFIT3, ISG15, ISG20, OAS1, Oasl2, STAT1, STAT2	42 (11)
IFN-λ1	cytokine	Activated	3.719	1.40E-16	CXCL10, DDX58, EIF2AK2, IFI35, IFI44, IFIH1, IFIT2,IFIT3, ISG15, ISG20, LGALS3BP, OAS1, STAT1, USP18	47 (12)
IFN-β	group	Activated	3.781	1.83E-15	CXCL10, DDX58, EIF2AK2, IFI35, IFI44, IFIH1, IFIT1B, IFIT2, IFIT3, ISG15, OAS1, PNPT1, STAT1, STAT2, USP18, XAF1	59 (17)
IRF5	transcription regulator	Activated	3.539	1.86E-15	CCL5, CXCL10, DDX58, IFI44, IFIH1, IFIT2, IFIT3, ISG15, ISG20, OAS1, Oasl2, STAT1, STAT2	44 (18)
TLR3	transmembrane receptor	Activated	2.634	9.60E-15	Ccl2, CCL5, Ccl7, CXCL10,DDX58, EIF2AK2, Ifi202b, IFI44, IFIH1, IFIT2, IFIT3, ISG15, ISG20, OAS1, Oasl2, PTX3, STAT1, TNC, USP18	47 (14)
IFN-α	group	Activated	4.253	5.48E-14	ADAR, BMP4, Bst2, CCL5, CXCL10, DDX58, EIF2AK2, F3, IFI35, IFIH1, IFIT1B, IFIT2, IFIT3, ISG15, ISG20, OAS1, PNPT1, SREBF2, STAT1, STAT2, USP18	49 (15)

Table 4: Predicted Upstream Effectors of ISG20 Gene-Regulation Pathway

ISG20-upregulated genes determined by RNA sequencing were imported to Ingenuity Pathway Analysis and analyzed for probable upstream effectors in an activated state. Predicted effectors include both individual transcription factors, defined signaling pathways, and receptors.

BIBLIOGRAPHY

1.   Strauss JH, Strauss EG (1994) The alphaviruses: gene expression, replication, and evolution. *Microbiol Rev* 58(3):491–562.

2.   Dubin DT, Stollar V (1975) Methylation of Sindbis virus "26S" messenger RNA. *Biochemical and Biophysical Research Communications* 66(4):1373–1379.

3.   Hyde JL, et al. (2014) A Viral RNA Structural Element Alters Host Recognition of Nonself RNA. *Science* 343(6172):783–787.

4.   Hefti E, Bishop DH, Dubin DT, Stollar V (1975) 5' nucleotide sequence of sindbis viral RNA. *Journal of Virology* 17(1):149–159.

5.   Frolov I, Hardy R, Rice CM (2001) Cis-acting RNA elements at the 5' end of Sindbis virus genome RNA regulate minus- and plus-strand RNA synthesis. *RNA* 7(11):1638–1651.

6.   Ou J-H, Strauss EG, Strauss JH, Simons K (1983) The 5′-terminal sequences of the genomic RNAs of several alphaviruses. *J Mol Biol* 168(1):1–15.

7.   Daffis S, et al. (2011) 2′-O methylation of the viral mRNA cap evades host restriction by IFIT family members. *Nature* 468(7322):452–456.

8.   Ou JH, Strauss EG, Strauss JH (1981) Comparative studies of the 3'-terminal sequences of several alpha virus RNAs. *Virology* 109(2):281–289.

9.   Niesters HG, Strauss JH (1990) Defined mutations in the 5' nontranslated sequence of Sindbis virus RNA. *Journal of Virology* 64(9):4162–4168.

10.   Strauss EG, Rice CM, Strauss JH (1984) Complete nucleotide sequence of the genomic RNA of Sindbis virus. *Virology* 133(1):92–110.

11.   Strauss EG, Rice CM, Strauss JH (1983) Sequence coding for the alphavirus nonstructural proteins is interrupted by an opal termination codon. *Proc Natl Acad Sci U S A* 80(17):5271–5275.

12.   Strauss EG, Levinson R, Rice CM, Dalrymple J, Strauss JH (1988) Nonstructural proteins nsP3 and nsP4 of Ross River and O'Nyong-nyong viruses: sequence and

comparison with those of other alphaviruses. *Virology* 164(1):265–274.

13. Takkinen K (1986) Complete nucleotide sequence of the nonstructural protein genes of Semliki Forest virus. *Nucleic Acids Res* 14(14):5667–5682.

14. Ryman KD, Klimstra WB (2008) Host responses to alphavirus infection. *Immunol Rev* 225:27–45.

15. Li G, Rice CM (1993) The signal for translational readthrough of a UGA codon in Sindbis virus RNA involves a single cytidine residue immediately downstream of the termination codon. *Journal of Virology* 67(8):5062–5067.

16. Shirako Y, Strauss JH (1994) Regulation of Sindbis virus RNA replication: uncleaved P123 and nsP4 function in minus-strand RNA synthesis, whereas cleaved products from P123 are required for efficient plus-strand RNA synthesis. *Journal of Virology* 68(3):1874–1885.

17. Lemm JA, Rice CM (1993) Assembly of functional Sindbis virus RNA replication complexes: requirement for coexpression of P123 and P34. *Journal of Virology* 67(4):1905–1915.

18. Lemm JA, Rümenapf T, Strauss EG, Strauss JH, Rice CM (1994) Polypeptide requirements for assembly of functional Sindbis virus replication complexes: a model for the temporal regulation of minus- and plus-strand RNA synthesis. *EMBO J* 13(12):2925–2934.

19. Martin JL, McMillan FM (2002) SAM (dependent) I AM: the S-adenosylmethionine-dependent methyltransferase fold. *Current Opinion in Structural Biology* 12(6):783–793.

20. Rozanov MN, Koonin EV, Gorbalenya AE (1992) Conservation of the putative methyltransferase domain: a hallmark of the "Sindbis-like" supergroup of positive-strand RNA viruses. *J Gen Virol* 73(8):2129–2134.

21. Schluckebier G, O'Gara M, Saenger W, Cheng X (1995) Universal catalytic domain structure of AdoMet-dependent methyltransferases. *J Mol Biol* 247(1):16–20.

22. Cross RK (1983) Identification of a unique guanine-7-methyltransferase in Semliki Forest virus (SFV) infected cell extracts. *Virology* 130(2):452–463.

23. Mi S, Stollar V (1991) Expression of Sindbis virus nsP1 and methyltransferase activity in Escherichia coli. *Virology* 184(1):423–427.

24. Laakkonen P, Ahola T, Kaariainen L (1996) The effects of palmitoylation on membrane association of Semliki forest virus RNA capping enzyme. *Journal of Biological Chemistry* 271(45):28567–28571.

25. Ahola T, Lampio A, Auvinen P, Kaariainen L (1999) Semliki Forest virus mRNA capping enzyme requires association with anionic membrane phospholipids for activity.

EMBO J 18(11):3164–3172.

26.   Lampio A, et al. (2000) Membrane binding mechanism of an RNA virus-capping enzyme. *Journal of Biological Chemistry* 275(48):37853–37859.

27.   Spuul P, et al. (2007) Role of the amphipathic peptide of Semliki forest virus replicase protein nsP1 in membrane association and virus replication. *Journal of Virology* 81(2):872–883.

28.   Gomatos PJ, Kaariainen L, Keränen S, Ranki M, Sawicki DL (1980) Semliki Forest virus replication complex capable of synthesizing 42S and 26S nascent RNA chains. *J Gen Virol* 49(1):61–69.

29.   Gomez de Cedrón M, Ehsani N, Mikkola ML, García JA, Kaariainen L (1999) RNA helicase activity of Semliki Forest virus replicase protein NSP2. *FEBS Letters* 448(1):19–22.

30.   Rikkonen M (1996) Functional significance of the nuclear-targeting and NTP-binding motifs of Semliki Forest virus nonstructural protein nsP2. *Virology* 218(2):352–361.

31.   Vasiljeva L, Merits A, Auvinen P, Kaariainen L (2000) Identification of a novel function of the alphavirus capping apparatus. RNA 5'-triphosphatase activity of Nsp2. *Journal of Biological Chemistry* 275(23):17281–17287.

32.   Hahn YS, Strauss EG, Strauss JH (1989) Mapping of RNA- temperature-sensitive mutants of Sindbis virus: assignment of complementation groups A, B, and G to nonstructural proteins. *Journal of Virology* 63(7):3142–3150.

33.   Hardy WR, Strauss JH (1989) Processing the nonstructural polyproteins of sindbis virus: nonstructural proteinase is in the C-terminal half of nsP2 and functions both in cis and in trans. *Journal of Virology* 63(11):4653–4664.

34.   Vasiljeva L, et al. (2003) Regulation of the sequential processing of Semliki Forest virus replicase polyprotein. *Journal of Biological Chemistry* 278(43):41636–41645.

35.   Sawicki DL, Kaariainen L, Lambek C, Gomatos PJ (1978) Mechanism for control of synthesis of Semliki Forest virus 26S and 42s RNA. *Journal of Virology* 25(1):19–27.

36.   Suopanki J, Sawicki DL, Sawicki SG, Kaariainen L (1998) Regulation of alphavirus 26S mRNA transcription by replicase component nsP2. *J Gen Virol* 79 (Pt 2)(2):309–319.

37.   Wang X, Ding M (1993) Nuclear localization of Sindbis virus nonstructural protein nsP2. *Cell Research* 3(1):27–37.

38.   Rikkonen M, Peranen J, Kaariainen L (1992) Nuclear and nucleolar targeting signals of semliki forest virus nonstructural protein nsP2. *Virology* 189(2):462–473.

39.   Peränen J, Rikkonen M, Liljeström P, Kaariainen L (1990) Nuclear localization of

Semliki Forest virus-specific nonstructural protein nsP2. *Journal of Virology* 64(5):1888–1896.

40. Bhalla N, et al. (2016) Host translation shutoff mediated by non-structural protein 2 is a critical factor in the antiviral state resistance of Venezuelan equine encephalitis virus. *Virology* 496:147–165.

41. Frolov I, et al. (1999) Selection of RNA replicons capable of persistent noncytopathic replication in mammalian cells. *Journal of Virology* 73(5):3854–3865.

42. Garmashova N, Gorchakov R, Frolova E, Frolov I (2006) Sindbis virus nonstructural protein nsP2 is cytotoxic and inhibits cellular transcription. *Journal of Virology* 80(12):5686–5696.

43. Garmashova N, et al. (2007) The Old World and New World alphaviruses use different virus-specific proteins for induction of transcriptional shutoff. *Journal of Virology* 81(5):2472–2484.

44. Gorchakov R, Frolova E, Frolov I (2005) Inhibition of transcription and translation in Sindbis virus-infected cells. *Journal of Virology* 79(15):9397–9409.

45. Kim KH, Rümenapf T, Strauss EG, Strauss JH (2004) Regulation of Semliki Forest virus RNA replication: a model for the control of alphavirus pathogenesis in invertebrate hosts. *Virology* 323(1):153–163.

46. LaStarza MW, Lemm JA, Rice CM (1994) Genetic analysis of the nsP3 region of Sindbis virus: evidence for roles in minus-strand and subgenomic RNA synthesis. *Journal of Virology* 68(9):5781–5791.

47. Allen MD, Buckle AM, Cordell SC, Löwe J, Bycroft M (2003) The crystal structure of AF1521 a protein from Archaeoglobus fulgidus with homology to the non-histone domain of macroH2A. *J Mol Biol* 330(3):503–511.

48. Park E, Griffin DE (2009) The nsP3 macro domain is important for Sindbis virus replication in neurons and neurovirulence in mice. *Virology* 388(2):305–314.

49. Pehrson JR, Fuji RN (1998) Evolutionary conservation of histone macroH2A subtypes and domains. *Nucleic Acids Res* 26(12):2837–2842.

50. Malet H, et al. (2009) The crystal structures of Chikungunya and Venezuelan equine encephalitis virus nsP3 macro domains define a conserved adenosine binding pocket. *Journal of Virology* 83(13):6534–6545.

51. Egloff M-P, et al. (2006) Structural and functional basis for ADP-ribose and poly(ADP-ribose) binding by viral macro domains. *Journal of Virology* 80(17):8493–8502.

52. Aaskov J, Jones A, Choi W, Lowry K, Stewart E (2011) Lineage replacement accompanying duplication and rapid fixation of an RNA element in the nsP3 gene in a

species of alphavirus. *Virology* 410(2):353–359.

53. Oberste MS, Parker MD, Smith JF (1996) Complete sequence of Venezuelan equine encephalitis virus subtype IE reveals conserved and hypervariable domains within the C terminus of nsP3. *Virology* 219(1):314–320.

54. Li GP, La Starza MW, Hardy WR, Strauss JH, Rice CM (1990) Phosphorylation of Sindbis virus nsP3 in vivo and in vitro. *Virology* 179(1):416–427.

55. Peränen J, Takkinen K, Kalkkinen N, Kaariainen L (1988) Semliki Forest virus-specific non-structural protein nsP3 is a phosphoprotein. *J Gen Virol* 69 (Pt 9)(9):2165–2178.

56. Sun C, Gardner CL, Watson AM, Ryman KD, Klimstra WB (2014) Stable, high-level expression of reporter proteins from improved alphavirus expression vectors to track replication and dissemination during encephalitic and arthritogenic disease. *Journal of Virology* 88(4):2035–2046.

57. Davis NL, Willis LV, Smith JF, Johnston RE (1989) In vitro synthesis of infectious venezuelan equine encephalitis virus RNA from a cDNA clone: analysis of a viable deletion mutant. *Virology* 171(1):189–204.

58. Galbraith SE, Sheahan BJ, Atkins GJ (2006) Deletions in the hypervariable domain of the nsP3 gene attenuate Semliki Forest virus virulence. *J Gen Virol* 87(Pt 4):937–947.

59. Lastarza MW, Grakoui A, Rice CM (1994) Deletion and Duplication Mutations in the C-Terminal Nonconserved Region of Sindbis Virus nsP3: Effects on Phosphorylation and on Virus Replication in Vertebrate and Invertebrate Cells. *Virology* 202(1):224–232.

60. Tuittila M, Hinkkanen AE (2003) Amino acid mutations in the replicase protein nsP3 of Semliki Forest virus cumulatively affect neurovirulence. *J Gen Virol* 84(Pt 6):1525–1533.

61. Rubach JK, et al. (2009) Characterization of purified Sindbis virus nsP4 RNA-dependent RNA polymerase activity in vitro. *Virology* 384(1):201–208.

62. de Groot RJ, Rümenapf T, Kuhn RJ, Strauss EG, Strauss JH (1991) Sindbis virus RNA polymerase is degraded by the N-end rule pathway. *Proc Natl Acad Sci U S A* 88(20):8967–8971.

63. Shirako Y, Strauss JH (1998) Requirement for an aromatic amino acid or histidine at the N terminus of Sindbis virus RNA polymerase. *Journal of Virology* 72(3):2310–2315.

64. Ding MX, Schlesinger MJ (1989) Evidence that Sindbis virus NSP2 is an autoprotease which processes the virus nonstructural polyprotein. *Virology* 171(1):280–284.

65. Atasheva S, Fish A, Fornerod M, Frolova EI (2010) Venezuelan equine Encephalitis virus capsid protein forms a tetrameric complex with CRM1 and importin alpha/beta that obstructs nuclear pore complex function. *Journal of Virology* 84(9):4158–4171.

66. Garmashova N, et al. (2007) Analysis of Venezuelan equine encephalitis virus capsid protein function in the inhibition of cellular transcription. *Journal of Virology* 81(24):13552–13565.

67. Atasheva S, Garmashova N, Frolov I, Frolova E (2008) Venezuelan equine encephalitis virus capsid protein inhibits nuclear import in Mammalian but not in mosquito cells. *Journal of Virology* 82(8):4028–4041.

68. Aguilar PV, Weaver SC, Basler CF (2007) Capsid protein of eastern equine encephalitis virus inhibits host cell gene expression. *Journal of Virology* 81(8):3866–3876.

69. Wu S-R, Haag L, Sjöberg M, Garoff H, Hammar L (2008) The dynamic envelope of a fusion class II virus. E3 domain of glycoprotein E2 precursor in Semliki Forest virus provides a unique contact with the fusion protein E1. *Journal of Biological Chemistry* 283(39):26452–26460.

70. Lobigs M, Zhao HX, Garoff H (1990) Function of Semliki Forest virus E3 peptide in virus assembly: replacement of E3 with an artificial signal peptide abolishes spike heterodimerization and surface expression of E1. *Journal of Virology* 64(9):4346–4355.

71. Wahlberg JM, Boere WA, Garoff H (1989) The heterodimeric association between the membrane proteins of Semliki Forest virus changes its sensitivity to low pH during virus maturation. *Journal of Virology* 63(12):4991–4997.

72. Navaratnarajah CK, Kuhn RJ (2007) Functional characterization of the Sindbis virus E2 glycoprotein by transposon linker-insertion mutagenesis. *Virology* 363(1):134–147.

73. Schlesinger S, Schlesinger MJ (1972) Formation of Sindbis virus proteins: identification of a precursor for one of the envelope proteins. *Journal of Virology* 10(5):925–932.

74. Smith JF, Brown DT (1977) Envelopments of Sindbis virus: synthesis and organization of proteins in cells infected with wild type and maturation-defective mutants. *Journal of Virology* 22(3):662–678.

75. Lescar J, et al. (2001) The Fusion glycoprotein shell of Semliki Forest virus: an icosahedral assembly primed for fusogenic activation at endosomal pH. *Cell* 105(1):137–148.

76. Wengler G, Koschinski A, Wengler G, Dreyer F (2003) Entry of alphaviruses at the plasma membrane converts the viral surface proteins into an ion-permeable pore that can be detected by electrophysiological analyses of whole-cell membrane currents. *J Gen Virol* 84(Pt 1):173–181.

77. Gibbons DL, et al. (2003) Visualization of the target-membrane-inserted fusion protein of Semliki Forest virus by combined electron microscopy and crystallography. *Cell* 114(5):573–583.

78. McInerney GM, Smit JM, Liljeström P, Wilschut J (2004) Semliki Forest virus produced

in the absence of the 6K protein has an altered spike structure as revealed by decreased membrane fusion capacity. *Virology* 325(2):200–206.

79. Yao JS, Strauss EG, Strauss JH (1996) Interactions between PE2, E1, and 6K required for assembly of alphaviruses studied with chimeric viruses. *Journal of Virology* 70(11):7910–7920.

80. Sanz MA, Madan V, Carrasco L, Nieva JL (2003) Interfacial domains in Sindbis virus 6K protein. Detection and functional characterization. *Journal of Biological Chemistry* 278(3):2051–2057.

81. Gaedigk-Nitschko K, Ding MX, Levy MA, Schlesinger MJ (1990) Site-directed mutations in the Sindbis virus 6K protein reveal sites for fatty acylation and the underacylated protein affects virus release and virion structure. *Virology* 175(1):282–291.

82. Snyder JE, et al. (2013) Functional characterization of the alphavirus TF protein. *Journal of Virology* 87(15):8511–8523.

83. Tsvetkova IB, Dragnea BG (2015) Encapsulation of nanoparticles in virus protein shells. *Methods Mol Biol* 1252(Chapter 1):1–15.

84. Rice CM, Strauss JH (1982) Association of sindbis virion glycoproteins and their precursors. *J Mol Biol* 154(2):325–348.

85. Ziemiecki A, Garofff H (1978) Subunit composition of the membrane glycoprotein complex of Semliki Forest virus. *J Mol Biol* 122(3):259–269.

86. Liljeström P, Garoff H (1991) Internally located cleavable signal sequences direct the formation of Semliki Forest virus membrane proteins from a polyprotein precursor. *Journal of Virology* 65(1):147–154.

87. Liu N, Brown DT (1993) Transient translocation of the cytoplasmic (endo) domain of a type I membrane glycoprotein into cellular membranes. *J Cell Biol* 120(4):877–883.

88. Paredes AM, Simon MN, Brown DT (1992) The mass of the Sindbis virus nucleocapsid suggests it has T = 4 icosahedral symmetry. *Virology* 187(1):329–332.

89. Cheng RH, et al. (1995) Nucleocapsid and glycoprotein organization in an enveloped virus. *Cell* 80(4):621–630.

90. Zhang W, et al. (2002) Placement of the structural proteins in Sindbis virus. *Journal of Virology* 76(22):11645–11658.

91. Leung JY-S, Ng MML, Chu JJH (2011) Replication of alphaviruses: a review on the entry process of alphaviruses into cells. *Adv Virol* 2011(3):249640–9.

92. Martín CS-S, Liu CY, Kielian M (2009) Dealing with low pH: entry and exit of

alphaviruses and flaviviruses. *Trends Microbiol* 17(11):514–521.

93.   Wahlberg JM, Bron R, Wilschut J, Garoff H (1992) Membrane fusion of Semliki Forest virus involves homotrimers of the fusion protein. *Journal of Virology* 66(12):7309–7318.

94.   Singh I, Helenius A (1992) Role of ribosomes in Semliki Forest virus nucleocapsid uncoating. *Journal of Virology* 66(12):7049–7058.

95.   Wengler G (1984) Identification of a transfer of viral core protein to cellular ribosomes during the early stages of alphavirus infection. *Virology* 134(2):435–442.

96.   Wengler G, Wengler G (2002) In vitro analysis of factors involved in the disassembly of Sindbis virus cores by 60S ribosomal subunits identifies a possible role of low pH. *J Gen Virol* 83(Pt 10):2417–2426.

97.   Lemm JA, Bergqvist A, Read CM, Rice CM (1998) Template-dependent initiation of Sindbis virus RNA replication in vitro. *Journal of Virology* 72(8):6546–6553.

98.   Sawicki DL, Sawicki SG (1980) Short-lived minus-strand polymerase for Semliki Forest virus. *Journal of Virology* 34(1):108–118.

99.   Sawicki DL, Sawicki SG (1994) Alphavirus positive and negative strand RNA synthesis and the role of polyproteins in formation of viral replication complexes. *Arch Virol Suppl* 9:393–405.

100.   Reef Hardy W, Hahn YS, de Groot RJ, Strauss EG, Strauss JH (1990) Synthesis and processing of the nonstructural polyproteins of several temperature-sensitive mutants of sindbis virus. *Virology* 177(1):199–208.

101.   Li M-L, Stollar V (2004) Identification of the amino acid sequence in Sindbis virus nsP4 that binds to the promoter for the synthesis of the subgenomic RNA. *Proc Natl Acad Sci U S A* 101(25):9429–9434.

102.   Li M-L, Wang H, Stollar V (2010) In vitro synthesis of Sindbis virus genomic and subgenomic RNAs: influence of nsP4 mutations and nucleoside triphosphate concentrations. *Journal of Virology* 84(6):2732–2739.

103.   Barton DJ, Sawicki SG, Sawicki DL (1991) Solubilization and immunoprecipitation of alphavirus replication complexes. *Journal of Virology* 65(3):1496–1506.

104.   Pardigon N, Strauss JH (1992) Cellular proteins bind to the 3' end of Sindbis virus minus-strand RNA. *Journal of Virology* 66(2):1007–1015.

105.   Pardigon N, Strauss JH (1996) Mosquito homolog of the La autoantigen binds to Sindbis virus RNA. *Journal of Virology* 70(2):1173–1181.

106.   Sawicki DL, Silverman RH, Williams BR, Sawicki SG (2003) Alphavirus minus-strand

synthesis and persistence in mouse embryo fibroblasts derived from mice lacking RNase L and protein kinase R. *Journal of Virology* 77(3):1801–1811.

107.   Cristea IM, et al. (2006) Tracking and elucidating alphavirus-host protein interactions. *Journal of Biological Chemistry* 281(40):30269–30278.

108.   Cristea IM, et al. (2010) Host factors associated with the Sindbis virus RNA-dependent RNA polymerase: role for G3BP1 and G3BP2 in virus replication. *Journal of Virology* 84(13):6720–6732.

109.   Frolova E, et al. (2006) Formation of nsP3-specific protein complexes during Sindbis virus replication. *Journal of Virology* 80(8):4122–4134.

110.   Burnham AJ, Gong L, Hardy RW (2007) Heterogeneous nuclear ribonuclear protein K interacts with Sindbis virus nonstructural proteins and viral subgenomic mRNA. *Virology* 367(1):212–221.

111.   Gui H, Lu CW, Adams S (2010) hnRNP A1 interacts with the genomic and subgenomic RNA promoters of Sindbis virus and is required for the synthesis of G and SG RNA. *Journal of …*.

112.   Lin J-Y, et al. (2009) hnRNP A1 interacts with the 5' untranslated regions of enterovirus 71 and Sindbis virus RNA and is required for viral replication. *Journal of Virology* 83(12):6106–6114.

113.   Varjak M, et al. (2013) Magnetic fractionation and proteomic dissection of cellular organelles occupied by the late replication complexes of Semliki Forest virus. *Journal of Virology* 87(18):10295–10312.

114.   Bonatti S, Cancedda R, Blobel G (1979) Membrane biogenesis. In vitro cleavage, core glycosylation, and integration into microsomal membranes of sindbis virus glycoproteins. *J Cell Biol* 80(1):219–224.

115.   Garoff H, Simons K, Dobberstein B (1978) Assembly of the Semliki Forest virus membrane glycoproteins in the membrane of the endoplasmic reticulum in vitro. *J Mol Biol* 124(4):587–600.

116.   de Curtis I, Simons K (1988) Dissection of Semliki Forest virus glycoprotein delivery from the trans-Golgi network to the cell surface in permeabilized BHK cells. *Proc Natl Acad Sci U S A* 85(21):8052–8056.

117.   Lusa S, Garoff H, Liljeström P (1991) Fate of the 6K membrane protein of Semliki Forest virus during virus assembly. *Virology* 185(2):843–846.

118.   Kim DY, Firth AE, Atasheva S, Frolova EI, Frolov I (2011) Conservation of a packaging signal and the viral genome RNA packaging mechanism in alphavirus evolution. *Journal of Virology* 85(16):8022–8036.

119. Lee S, et al. (1996) Identification of a protein binding site on the surface of the alphavirus nucleocapsid and its implication in virus assembly. *Structure* 4(5):531–541.

120. Skoging U, Vihinen M, Nilsson L, Liljeström P (1996) Aromatic interactions define the binding of the alphavirus spike to its nucleocapsid. *Structure* 4(5):519–529.

121. Wilkinson TA, Tellinghuisen TL, Kuhn RJ, Post CB (2005) Association of sindbis virus capsid protein with phospholipid membranes and the E2 glycoprotein: implications for alphavirus assembly. *Biochemistry* 44(8):2800–2810.

122. Xiong C, et al. (1989) Sindbis virus: an efficient, broad host range vector for gene expression in animal cells.

123. Huang HV, Rice CM, Xiong C, Schlesinger S (1989) RNA viruses as gene expression vectors. *Virus Genes*.

124. Kümmerer BM, Grywna K, Gläsker S, Wieseler J, Drosten C (2012) Construction of an infectious Chikungunya virus cDNA clone and stable insertion of mCherry reporter genes at two different sites. *Journal of General Virology* 93(9):1991–1995.

125. Gardner CL, et al. (2008) Eastern and Venezuelan equine encephalitis viruses differ in their ability to infect dendritic cells and macrophages: impact of altered cell tropism on pathogenesis. *Journal of Virology* 82(21):10634–10646.

126. Bick MJ, et al. (2003) Expression of the zinc-finger antiviral protein inhibits alphavirus replication. *Journal of Virology* 77(21):11555–11562.

127. Trobaugh DW, et al. (2013) RNA viruses can hijack vertebrate microRNAs to suppress innate immunity. *Nature* 506(7487):245–248.

128. Tesfay MZ, et al. (2008) Alpha/Beta Interferon Inhibits Cap-Dependent Translation of Viral but Not Cellular mRNA by a PKR-Independent Mechanism. *Journal of Virology* 82(6):2620–2630.

129. Frolov I, et al. (1996) Alphavirus-based expression vectors: strategies and applications. *Proc Natl Acad Sci U S A* 93(21):11371–11377.

130. Taylor RM, Hurlbut HS, Work TH, Kingston JR, Frothingham TE (1955) Sindbis Virus: A Newly Recognized Arthropod-Transmitted Virus. *Am J Trop Med Hyg* 4(5):844–862.

131. Gérardin P, et al. (2008) Estimating Chikungunya prevalence in La Réunion Island outbreak by serosurveys: two methods for two critical times of the epidemic. *BMC Infect Dis* 8(1):99.

132. Moro ML, et al. (2010) Chikungunya virus in North-Eastern Italy: a seroprevalence survey. *Am J Trop Med Hyg* 82(3):508–511.

133. Cassadou S, et al. (2014) Emergence of chikungunya fever on the French side of Saint

Martin island, October to December 2013. *Euro Surveill* 19(13).

134. Kuehn BM (2014) Chikungunya virus transmission found in the United States: US health authorities brace for wider spread. *JAMA* 312(8):776–777.

135. Silverman MA, et al. (2013) Eastern equine encephalitis in children, Massachusetts and New Hampshire,USA, 1970-2010. *Emerg Infect Dis* 19(2):194–201– quiz 352.

136. Casals J, Curnen EC, Thomas L (1943) VENEZUELAN EQUINE ENCEPHALOMYELITIS IN MAN. *J Exp Med* 77(6):521–530.

137. Robinson MC (1955) An epidemic of virus disease in Southern Province, Tanganyika Territory, in 1952–53. *Trans R Soc Trop Med Hyg*.

138. LUMSDEN WH (1955) An epidemic of virus disease in Southern Province, Tanganyika Territory, in 1952-53. II. General description and epidemiology. *Trans R Soc Trop Med Hyg* 49(1):33–57.

139. ROSS RW (1956) The Newala epidemic. III. The virus: isolation, pathogenic properties and relationship to the epidemic. *J Hyg (Lond)* 54(2):177–191.

140. Gilotra SK, Bhattacharya NC (1968) Mosquito vectors of dengue--chikungunya viruses in a rural area near Calcutta. *Bull Calcutta Sch Trop Med* 16(2):41–42.

141. Gilotra SK, Shah KV (1967) Laboratory studies on transmission of chikun-gunya virus by mosquitoes. *Am J Epidemiol*.

142. MCINTOSH BM, HARWIN RM, PATERSON HE, WESTWATER ML (1963) AN EPIDEMIC OF CHIKUNGUNYA IN SOUTH-EASTERN SOUTHERN RHODESIA. *Cent Afr J Med* 9:351–359.

143. PATERSON HE, MCINTOSH BM (1964) FURTHER STUDIES ON THE CHIKUNGUNYA OUTBREAK IN SOUTHERN RHODESIA IN 1962. II. TRANSMISSION EXPERIMENTS WITH THE AEDES FURCIFER-TAYLORI GROUP OF MOSQUITOES AND WITH A MEMBER OF THE ANOPHELES GAMBIAE COMPLEX. *Ann Trop Med Parasitol* 58:52–55.

144. Sarkar JK (1967) Calcutta's experience and findings in haemorrhagic fever and Chikungunya fever epidemic. *Jpn J Med Sci Biol* 20 Suppl:88–90.

145. Shah KV, Gilotra SK, GIBBS CJ, ROZEBOOM LE (1964) LABORATORY STUDIES OF TRANSMISSION OF CHIKUNGUNYA VIRUS BY MOSQUITOES: A PRELIMINARY REPORT. *Indian J Med Res* 52:703–709.

146. WEINBREN MP, HADDOW AJ, WILLIAMS MC (1958) The occurrence of Chikungunya virus in Uganda. I. Isolation from mosquitoes. *Trans R Soc Trop Med Hyg* 52(3):253–257.

147.   Tsetsarkin KA, Vanlandingham DL, McGee CE, Higgs S (2007) A single mutation in chikungunya virus affects vector specificity and epidemic potential. *PLoS Pathog* 3(12):e201.

148.   Chastel C (2005) [Chikungunya virus: its recent spread to the southern Indian Ocean and Reunion Island (2005-2006)]. *Bull Acad Natl Med* 189(8):1827–1835.

149.   Consigny PH, Lecuit M, Lortholary O (2006) [Chikungunya virus: a reemerging alphavirus]. *Med Sci (Paris)* 22(4):444–446.

150.   Higgs S (2006) The 2005-2006 Chikungunya epidemic in the Indian Ocean. *Vector Borne Zoonotic Dis* 6(2):115–116.

151.   Ravi V (2006) Re-emergence of chikungunya virus in India. *Indian J Med Microbiol* 24(2):83–84.

152.   Leparc-Goffart I, Nougairede A, Cassadou S, Prat C, de Lamballerie X (2014) Chikungunya in the Americas. *Lancet* 383(9916):514.

153.   Costa-da-Silva AL, et al. (2017) First report of naturally infected Aedes aegypti with chikungunya virus genotype ECSA in the Americas. *PLoS Negl Trop Dis* 11(6):e0005630.

154.   Borgherini G, et al. (2007) Outbreak of Chikungunya on Reunion Island: Early Clinical and Laboratory Features in 157 Adult Patients. *Clin Infect Dis* 44(11):1401–1407.

155.   Taubitz W, et al. (2007) Chikungunya Fever in Travelers: Clinical Presentation and Course. *Clin Infect Dis* 45(1):e1–e4.

156.   Staikowsky F, et al. (2009) Prospective Study of Chikungunya Virus Acute Infection in the Island of La Réunion during the 2005–2006 Outbreak. *PLoS ONE* 4(10):e7603.

157.   Nkoghe D, et al. (2012) Clinical Forms of Chikungunya in Gabon, 2010. *PLoS Negl Trop Dis* 6(2):e1517.

158.   Thiberville S-D, et al. (2013) Chikungunya Fever: A Clinical and Virological Investigation of Outpatients on Reunion Island, South-West Indian Ocean. *PLoS Negl Trop Dis* 7(1):e2004.

159.   Thiberville S-D, et al. (2013) Antiviral Research. *ANTIVIRAL RESEARCH*:1–26.

160.   Sissoko D, et al. (2009) Post-Epidemic Chikungunya Disease on Reunion Island: Course of Rheumatic Manifestations and Associated Factors over a 15-Month Period. *PLoS Negl Trop Dis* 3(3):e389.

161.   Borgherini G, et al. (2008) Persistent Arthralgia Associated with Chikungunya Virus: A Study of 88 Adult Patients on Reunion Island. *Clin Infect Dis* 47(4):469–475.

162.   Marimoutou C, Vivier E, Oliver M, Boutin J-P, Simon F (2012) Morbidity and Impaired Quality of Life 30 Months After Chikungunya Infection: Comparative Cohort of Infected and Uninfected French Military Policemen in Reunion Island. *Medicine* 91(4):212–219.

163.   Couturier E, et al. (2012) Impaired quality of life after chikungunya virus infection: a 2-year follow-up study. *Rheumatology (Oxford)* 51(7):1315–1322.

164.   Chow A, et al. (2010) Persistent Arthralgia Induced by Chikungunya Virus Infection is Associated with Interleukin-6 and Granulocyte Macrophage Colony-Stimulating Factor. *Journal of Infectious Diseases* 203(2):149–157.

165.   Gérardin P, et al. (2013) Predictors of Chikungunya rheumatism: a prognostic survey ancillary to the TELECHIK cohort study. *Arthritis Research & Therapy 2013 15:1* 15(1):R9.

166.   Moro ML, et al. (2012) Long-term chikungunya infection clinical manifestations after an outbreak in Italy: A prognostic cohort study. *Journal of Infection* 65(2):165–172.

167.   Couderc T, et al. (2008) A Mouse Model for Chikungunya: Young Age and Inefficient Type-I Interferon Signaling Are Risk Factors for Severe Disease. *PLoS Pathog* 4(2):e29.

168.   Gardner J, et al. (2010) Chikungunya virus arthritis in adult wild-type mice. *Journal of Virology* 84(16):8021–8032.

169.   Gardner CL, Burke CW, Higgs ST, Klimstra WB, Ryman KD (2012) Interferon-alpha/beta deficiency greatly exacerbates arthritogenic disease in mice infected with wild-type chikungunya virus but not with the cell culture-adapted live-attenuated 181/25 vaccine candidate. *Virology* 425(2):103–112.

170.   Sourisseau M, et al. (2007) Characterization of reemerging chikungunya virus. *PLoS Pathog* 3(6):e89–e89.

171.   Kubes V, Ríos F (1938) *Datos preliminares sobre el agente etiológico de la encefalitis infecciosa de los equinos en Venezuela* (Publicación de la Dirección de Ganadería. Ministerio …).

172.   Beck CE, Wyckoff RW (1938) VENEZUELAN EQUINE ENCEPHALOMYELITIS. *Science* 88(2292):530–530.

173.   Lord RD (1974) History and geographic distribution of Venezuelan equine encephalitis. *Bull Pan Am Health Organ* 8(2):100–110.

174.   Walton TE, Grayson M (1988) *Venezuelan equine encepha lomyelitis. Monath TP, ed. The Arboviruses: Epidemiology and Ecology. Volume IV.*

175.   Oberste MS, et al. (1998) Association of Venezuelan equine encephalitis virus subtype IE with two equine epizootics in Mexico. *Am J Trop Med Hyg* 59(1):100–107.

176.   Rico-Hesse R, Weaver SC, de Siger J, Medina G, Salas RA (1995) Emergence of a new epidemic/epizootic Venezuelan equine encephalitis virus in South America. *Proc Natl Acad Sci U S A* 92(12):5278–5281.

177.   Weaver SC, et al. (1996) Re-emergence of epidemic Venezuelan equine encephalomyelitis in South America. *The Lancet* 348(9025):436–440.

178.   Johnson KM, Martin DH (1974) Venezuelan equine encephalitis. *Adv Vet Sci Comp Med* 18(0):79–116.

179.   Grayson MA, Galindo P (1969) Ecology of Venezuelan equine encephalitis virus in Panama. *J Am Vet Med Assoc* 155(12):2141–2145.

180.   Barrera R, et al. (2002) Contrasting sylvatic foci of Venezuelan equine encephalitis virus in northern South America. *Am J Trop Med Hyg* 67(3):324–334.

181.   Hawley RJ, Eitzen EM Jr (2003) Biological Weapons—a Primer for Microbiologists1. *http://dxdoiorg/101146/annurevmicro551235* 55(1):235–253.

182.   Franck PT, Johnson KM (1970) An outbreak of Venezuelan encephalitis in man in the Panama Canal Zone. *… Journal of Tropical Medicine and Hygiene.*

183.   Johnson KM, Shelokov A, Peralta PH (1968) Recovery of Venezuelan equine encephalomyelitis virus in Panama. A fatal case in man. *American Journal of ….*

184.   Zarate ML, Scherer WF, Dickerman RW (1970) [Venezuelan equine encephalitis virus as a human infection determinant. Description of a fatal case occurring in Jaltipan, Ver., in 1965]. *Rev Invest Salud Publica* 30(4):296–302.

185.   la Monte de S, Castro F, Bonilla NJ, Gaskin de Urdaneta A, Hutchins GM (1985) The systemic pathology of Venezuelan equine encephalitis virus infection in humans. *Am J Trop Med Hyg* 34(1):194–202.

186.   Weaver SC, Ferro C, Barrera R, Boshell J, Navarro J-C (2004) Venezuelan equine encephalitis. *Annu Rev Entomol* 49(1):141–174.

187.   Jackson AC, SenGupta SK, Smith JF (1991) Pathogenesis of Venezuelan equine encephalitis virus infection in mice and hamsters. *Vet Pathol* 28(5):410–418.

188.   Aronson JF, et al. (2000) A single-site mutant and revertants arising in vivo define early steps in the pathogenesis of Venezuelan equine encephalitis virus. *Virology* 270(1):111–123.

189.   Fothergill LD, DlnGLE JH, Farber S (1938) Human encephalitis caused by the virus of the eastern variety of equine encephalomyelitis. *New England Journal ….*

190.   Feemster RF (1938) Outbreak of encephalitis in man due to the eastern virus of equine encephalomyelitis. *American Journal of Public Health and the ….*

191.	FARBER S, HILL A, CONNERLY ML, DINGLE JH (1940) ENCEPHALITIS IN INFANTS AND CHILDREN: CAUSED BY THE VIRUS OF THE EASTERN VARIETY OF EQUINE ENCEPHALITIS. *JAMA* 114(18):1725–1731.

192.	McGOWAN JE, BRYAN JA, GREGG MB (1973) SURVEILLANCE OF ARBOVIRAL ENCEPHALITIS IN THE UNITED STATES, 1955-1971. *Am J Epidemiol* 97(3):199–207.

193.	Armstrong PM, Andreadis TG (2010) Eastern Equine Encephalitis Virus in Mosquitoes and Their Role as Bridge Vectors. *Emerg Infect Dis* 16(12):1869–1874.

194.	Bingham AM, et al. (2012) Detection of eastern equine encephalomyelitis virus RNA in North American snakes. *Am J Trop Med Hyg* 87(6):1140–1144.

195.	White G, Ottendorfer C, Graham S, Unnasch TR (2011) Competency of reptiles and amphibians for eastern equine encephalitis virus. *Am J Trop Med Hyg* 85(3):421–425.

196.	Scott TW, Weaver SC (1989) Eastern equine encephalomyelitis virus: epidemiology and evolution of mosquito transmission. *Adv Virus Res* 37:277–328.

197.	Mitchell CJ, et al. (1992) Isolation of eastern equine encephalitis virus from Aedes albopictus in Florida. *Science* 257(5069):526–528.

198.	Deresiewicz RL, Thaler SJ, Hsu L, Zamani AA (1997) Clinical and neuroradiographic manifestations of eastern equine encephalitis. *N Engl J Med* 336(26):1867–1874.

199.	Przelomski MM, O'Rourke E, Grady GF, Berardi VP, Markley HG (1988) Eastern equine encephalitis in Massachusetts: a report of 16 cases, 1970-1984. *Neurology* 38(5):736–739.

200.	Vogel P, Kell WM, Fritz DL, Parker MD, Schoepp RJ (2005) Early events in the pathogenesis of eastern equine encephalitis virus in mice. *Am J Pathol* 166(1):159–171.

201.	Liu C, Voth DW, Rodina P, Shauf LR, Gonzalez G (1970) A comparative study of the pathogenesis of western equine and eastern equine encephalomyelitis viral infections in mice by intracerebral and subcutaneous inoculations. *J Infect Dis* 122(1):53–63.

202.	Gardner CLC, Ebel GDG, Ryman KDK, Klimstra WBW (2011) Heparan sulfate binding by natural eastern equine encephalitis viruses promotes neurovirulence. *Proc Natl Acad Sci U S A* 108(38):16026–16031.

203.	Isaacs A, Lindenmann J (1957) Virus interference. I. The interferon. *... of the Royal ...*.

204.	Samarajiwa SA, Wilson W, Hertzog PJ (2006) *Type I Interferons: Genetics and Structure* (Wiley-VCH Verlag GmbH & Co. KGaA, Weinheim, FRG).

205.	Lasfar A (2006) Characterization of the Mouse IFN- Ligand-Receptor System: IFN- s Exhibit Antitumor Activity against B16 Melanoma. *Cancer Research* 66(8):4468–4477.

206.   Sommereyns C, Paul S, Staeheli P, Michiels T (2008) IFN-lambda (IFN-lambda) is expressed in a tissue-dependent fashion and primarily acts on epithelial cells in vivo. *PLoS Pathog* 4(3):e1000017.

207.   Witte K, et al. (2009) Despite IFN-lambda receptor expression, blood immune cells, but not keratinocytes or melanocytes, have an impaired response to type III interferons: implications for therapeutic applications of these cytokines. *Genes Immun* 10(8):702–714.

208.   Burke CW, Gardner CL, Steffan JJ, Ryman KD, Klimstra WB (2009) Characteristics of alpha/beta interferon induction after infection of murine fibroblasts with wild-type and mutant alphaviruses. *Virology* 395(1):121–132.

209.   Seth RB, Sun L, Ea C-K, Chen ZJ (2005) Identification and characterization of MAVS, a mitochondrial antiviral signaling protein that activates NF-kappaB and IRF 3. *Cell* 122(5):669–682.

210.   Akhrymuk I, Frolov I, Frolova EI (2016) Both RIG-I and MDA5 detect alphavirus replication in concentration-dependent mode. *Virology* 487:230–241.

211.   Hiscott J, Lacoste J, Lin R (2006) Recruitment of an interferon molecular signaling complex to the mitochondrial membrane: disruption by hepatitis C virus NS3-4A protease. *Biochem Pharmacol* 72(11):1477–1484.

212.   Lin R, et al. (2006) Dissociation of a MAVS/IPS-1/VISA/Cardif-IKKepsilon molecular complex from the mitochondrial outer membrane by hepatitis C virus NS3-4A proteolytic cleavage. *Journal of Virology* 80(12):6072–6083.

213.   Ohman T, Rintahaka J, Kalkkinen N, Matikainen S, Nyman TA (2009) Actin and RIG-I/MAVS signaling components translocate to mitochondria upon influenza A virus infection of human primary macrophages. *J Immunol* 182(9):5682–5692.

214.   Horner SM, Liu HM, Park HS, Briley J, Gale M (2011) Mitochondrial-associated endoplasmic reticulum membranes (MAM) form innate immune synapses and are targeted by hepatitis C virus. *Proceedings of the National Academy of Sciences* 108(35):14590–14595.

215.   Panne D (2008) The enhanceosome. *Current Opinion in Structural Biology* 18(2):236–242.

216.   McNab F, Mayer-Barber K, Sher A, Wack A, O'Garra A (2015) Type I interferons in infectious disease. *Nat Rev Immunol* 15(2):87–103.

217.   Marié I, Durbin JE, Levy DE (1998) Differential viral induction of distinct interferon-alpha genes by positive feedback through interferon regulatory factor-7. *EMBO J* 17(22):6660–6669.

218.   Sato M, et al. (1998) Positive feedback regulation of type I IFN genes by the IFN-

inducible transcription factor IRF-7. *FEBS Letters* 441(1):106–110.

219. Siegal FP, et al. (1999) The nature of the principal type 1 interferon-producing cells in human blood. *Science* 284(5421):1835–1837.

220. Honda K, et al. (2005) IRF-7 is the master regulator of type-I interferon-dependent immune responses. *Nature* 434(7034):772–777.

221. Jarrossay D, Napolitani G, Colonna M, Sallusto F, Lanzavecchia A (2001) Specialization and complementarity in microbial molecule recognition by human myeloid and plasmacytoid dendritic cells. *Eur J Immunol* 31(11):3388–3393.

222. Lund JM, et al. (2004) Recognition of single-stranded RNA viruses by Toll-like receptor 7. *Proc Natl Acad Sci U S A* 101(15):5598–5603.

223. Heil F, et al. (2004) Species-specific recognition of single-stranded RNA via toll-like receptor 7 and 8. *Science* 303(5663):1526–1529.

224. Diebold SS, Kaisho T, Hemmi H, Akira S, Reis e Sousa C (2004) Innate antiviral responses by means of TLR7-mediated recognition of single-stranded RNA. *Science* 303(5663):1529–1531.

225. Burke CW (2009) *The influence of cell type on alphavirus type I interferon induction.*

226. Nishimoto KP, et al. (2007) Restricted and Selective Tropism of a Venezuelan Equine Encephalitis Virus-Derived Replicon Vector for Human Dendritic Cells. *http://wwwliebertpubcom/vim* 20(1):88–104.

227. Yoneyama M, et al. (2004) The RNA helicase RIG-I has an essential function in double-stranded RNA-induced innate antiviral responses. *Nat Immunol* 5(7):730–737.

228. Yoneyama M, et al. (2005) Shared and unique functions of the DExD/H-box helicases RIG-I, MDA5, and LGP2 in antiviral innate immunity. *J Immunol* 175(5):2851–2858.

229. Saito T, et al. (2007) Regulation of innate antiviral defenses through a shared repressor domain in RIG-I and LGP2. *Proc Natl Acad Sci U S A* 104(2):582–587.

230. Kang D-C, et al. (2004) Expression analysis and genomic characterization of human melanoma differentiation associated gene-5, mda-5: a novel type I interferon-responsive apoptosis-inducing gene. *Oncogene* 23(9):1789–1800.

231. Cui S, et al. (2008) The C-terminal regulatory domain is the RNA 5'-triphosphate sensor of RIG-I. *Mol Cell* 29(2):169–179.

232. Kawai T, et al. (2005) IPS-1, an adaptor triggering RIG-I- and Mda5-mediated type I interferon induction. *Nat Immunol* 6(10):981–988.

233. Meylan E, et al. (2005) Cardif is an adaptor protein in the RIG-I antiviral pathway and is

targeted by hepatitis C virus. *Nature* 437(7062):1167–1172.

234. Xu L-G, et al. (2005) VISA is an adapter protein required for virus-triggered IFN-beta signaling. *Mol Cell* 19(6):727–740.

235. Saito T, Owen DM, Jiang F, Marcotrigiano J, Gale M (2008) Innate immunity induced by composition-dependent RIG-I recognition of hepatitis C virus RNA. *Nature* 454(7203):523–527.

236. Uzri D, Gehrke L (2009) Nucleotide sequences and modifications that determine RIG-I/RNA binding and signaling activities. *Journal of Virology* 83(9):4174–4184.

237. Hornung V, et al. (2006) 5'-Triphosphate RNA is the ligand for RIG-I. *Science* 314(5801):994–997.

238. Kim M-J, Hwang S-Y, Imaizumi T, Yoo J-Y (2008) Negative feedback regulation of RIG-I-mediated antiviral signaling by interferon-induced ISG15 conjugation. *Journal of Virology* 82(3):1474–1483.

239. Malathi K, Dong B, Gale M, Silverman RH (2007) Small self-RNA generated by RNase L amplifies antiviral innate immunity. *Nature* 448(7155):816–819.

240. Malathi K, et al. (2010) RNase L releases a small RNA from HCV RNA that refolds into a potent PAMP. *RNA* 16(11):2108–2119.

241. Devarkar SC, et al. (2016) Structural basis for m7G recognition and 2'-O-methyl discrimination in capped RNAs by the innate immune receptor RIG-I. *Proceedings of the National Academy of Sciences* 113(3):596–601.

242. Li X, et al. (2009) Structural basis of double-stranded RNA recognition by the RIG-I like receptor MDA5. *Arch Biochem Biophys* 488(1):23–33.

243. Kumar KP, McBride KM, Weaver BK, Dingwall C, Reich NC (2000) Regulated nuclear-cytoplasmic localization of interferon regulatory factor 3, a subunit of double-stranded RNA-activated factor 1. *Mol Cell Biol* 20(11):4159–4168.

244. Fitzgerald KA, et al. (2003) IKKepsilon and TBK1 are essential components of the IRF3 signaling pathway. *Nat Immunol* 4(5):491–496.

245. McWhirter SM, et al. (2004) IFN-regulatory factor 3-dependent gene expression is defective in Tbk1-deficient mouse embryonic fibroblasts. *Proc Natl Acad Sci U S A* 101(1):233–238.

246. Servant MJ, Grandvaux N, Hiscott J (2002) Multiple signaling pathways leading to the activation of interferon regulatory factor 3. *Biochem Pharmacol* 64(5-6):985–992.

247. Grandvaux N, et al. (2002) Transcriptional profiling of interferon regulatory factor 3 target genes: direct involvement in the regulation of interferon-stimulated genes. *Journal*

of Virology 76(11):5532–5539.

248.   Schulz O, et al. (2005) Toll-like receptor 3 promotes cross-priming to virus-infected cells. *Nature* 433(7028):887–892.

249.   Neighbours LM, Long K, Whitmore AC, Heise MT (2012) Myd88-dependent toll-like receptor 7 signaling mediates protection from severe Ross River virus-induced disease in mice. *Journal of Virology* 86(19):10675–10685.

250.   Lundberg AM, et al. (2007) Key differences in TLR3/poly I:C signaling and cytokine induction by human primary cells: a phenomenon absent from murine cell systems. *Blood* 110(9):3245–3252.

251.   Agudo J, et al. (2014) The miR-126-VEGFR2 axis controls the innate response to pathogen-associated nucleic acids. *Nat Immunol* 15(1):54–62.

252.   Roberts WK, Hovanessian A, Brown RE, Clemens MJ, Kerr IM (1976) Interferon-mediated protein kinase and low-molecular-weight inhibitor of protein synthesis. *Nature* 264(5585):477–480.

253.   Sen GC, Taira H, Lengyel P (1978) Interferon, double-stranded RNA, and protein phosphorylation. Characteristics of a double-stranded RNA-activated protein kinase system partially purified from interferon treated Ehrlich ascites tumor cells. *Journal of Biological Chemistry* 253(17):5915–5921.

254.   Bevilacqua PC, George CX, Samuel CE, Cech TR (1998) Binding of the protein kinase PKR to RNAs with secondary structure defects: role of the tandem A-G mismatch and noncontiguous helixes. *Biochemistry* 37(18):6303–6316.

255.   Kostura M, Mathews MB (1989) Purification and activation of the double-stranded RNA-dependent eIF-2 kinase DAI. *Mol Cell Biol* 9(4):1576–1586.

256.   Taylor DR, et al. (1996) Autophosphorylation sites participate in the activation of the double-stranded-RNA-activated protein kinase PKR. *Mol Cell Biol* 16(11):6295–6302.

257.   Colthurst DR, Campbell DG, Proud CG (1987) Structure and regulation of eukaryotic initiation factor eIF-2. Sequence of the site in the alpha subunit phosphorylated by the haem-controlled repressor and by the double-stranded RNA-activated inhibitor. *Eur J Biochem* 166(2):357–363.

258.   Cheshire JL, Williams BR, Baldwin AS (1999) Involvement of double-stranded RNA-activated protein kinase in the synergistic activation of nuclear factor-kappaB by tumor necrosis factor-alpha and gamma-interferon in preneuronal cells. *Journal of Biological Chemistry* 274(8):4801–4806.

259.   Gil J, et al. (2004) TRAF family proteins link PKR with NF-kappa B activation. *Mol Cell Biol* 24(10):4502–4512.

260. Bonnet MC, Weil R, Dam E, Hovanessian AG, Meurs EF (2000) PKR stimulates NF-kappaB irrespective of its kinase function by interacting with the IkappaB kinase complex. *Mol Cell Biol* 20(13):4532–4542.

261. Gil J, Alcamí J, Esteban M (2000) Activation of NF-kappa B by the dsRNA-dependent protein kinase, PKR involves the I kappa B kinase complex. *Oncogene* 19(11):1369–1378.

262. Schulz O, et al. (2010) Protein kinase R contributes to immunity against specific viruses by regulating interferon mRNA integrity. *Cell Host and Microbe* 7(5):354–361.

263. Pham AM, et al. (2016) PKR Transduces MDA5-Dependent Signals for Type I IFN Induction. *PLoS Pathog* 12(3):e1005489.

264. Barry G, et al. (2009) PKR acts early in infection to suppress Semliki Forest virus production and strongly enhances the type I interferon response. *J Gen Virol* 90(Pt 6):1382–1391.

265. Hovanessian AG, Brown RE, Kerr IM (1977) Synthesis of low molecular weight inhibitor of protein synthesis with enzyme from interferon-treated cells. *Nature* 268(5620):537–540.

266. Kerr IM, Brown RE (1978) pppA2'p5'A2"p5"A: an inhibitor of protein synthesis synthesized with an enzyme fraction from interferon-treated cells. *Proc Natl Acad Sci U S A* 75(1):256–260.

267. Floyd-Smith G, Slattery E, Lengyel P (1981) Interferon action: RNA cleavage pattern of a (2"-5")oligoadenylate--dependent endonuclease. *Science* 212(4498):1030–1032.

268. Ryman KDK, White LJL, Johnston RER, Klimstra WBW (2002) Effects of PKR/RNase L-dependent and alternative antiviral pathways on alphavirus replication and pathogenesis. *Viral Immunol* 15(1):53–76.

269. Zhou A, Paranjape JM, Der SD, Williams BR, Silverman RH (1999) Interferon action in triply deficient mice reveals the existence of alternative antiviral pathways. *Virology* 258(2):435–440.

270. Yamamoto M, et al. (2002) Cutting edge: a novel Toll/IL-1 receptor domain-containing adapter that preferentially activates the IFN-beta promoter in the Toll-like receptor signaling. *J Immunol* 169(12):6668–6672.

271. Hemmi H, et al. (2002) Small anti-viral compounds activate immune cells via the TLR7 MyD88-dependent signaling pathway. *Nat Immunol* 3(2):196–200.

272. Gohda J, Matsumura T, Inoue J-I (2004) Cutting edge: TNFR-associated factor (TRAF) 6 is essential for MyD88-dependent pathway but not toll/IL-1 receptor domain-containing adaptor-inducing IFN-beta (TRIF)-dependent pathway in TLR signaling. *J Immunol* 173(5):2913–2917.

273.   Medzhitov R, et al. (1998) MyD88 is an adaptor protein in the hToll/IL-1 receptor family signaling pathways. *Mol Cell* 2(2):253–258.

274.   Wesche H, Henzel WJ, Shillinglaw W, Li S, Cao Z (1997) MyD88: an adapter that recruits IRAK to the IL-1 receptor complex. *Immunity* 7(6):837–847.

275.   Jurk M, et al. (2002) Human TLR7 or TLR8 independently confer responsiveness to the antiviral compound R-848. *Nat Immunol* 3(6):499–499.

276.   Mercurio F, et al. (1997) IKK-1 and IKK-2: cytokine-activated IkappaB kinases essential for NF-kappaB activation. *Science* 278(5339):860–866.

277.   Régnier CH, et al. (1997) Identification and characterization of an IkappaB kinase. *Cell* 90(2):373–383.

278.   Woronicz JD, Gao X, Cao Z, Rothe M, Goeddel DV (1997) IkappaB kinase-beta: NF-kappaB activation and complex formation with IkappaB kinase-alpha and NIK. *Science* 278(5339):866–869.

279.   Zandi E, Rothwarf DM, Delhase M, Hayakawa M, Karin M (1997) The IkappaB kinase complex (IKK) contains two kinase subunits, IKKalpha and IKKbeta, necessary for IkappaB phosphorylation and NF-kappaB activation. *Cell* 91(2):243–252.

280.   Yamaoka S, et al. (1998) Complementation cloning of NEMO, a component of the IkappaB kinase complex essential for NF-kappaB activation. *Cell* 93(7):1231–1240.

281.   Rothwarf DM, Zandi E, Natoli G, Karin M (1998) IKK-gamma is an essential regulatory subunit of the IkappaB kinase complex. *Nature* 395(6699):297–300.

282.   Visvanathan KV, Goodbourn S (1989) Double-stranded RNA activates binding of NF-kappa B to an inducible element in the human beta-interferon promoter. *EMBO J* 8(4):1129–1138.

283.   Lutfalla G, et al. (1995) Mutant U5A cells are complemented by an interferon-alpha beta receptor subunit generated by alternative processing of a new member of a cytokine receptor gene cluster. *EMBO J* 14(20):5100–5108.

284.   Krishnan K, Yan H, Lim JT, Krolewski JJ (1996) Dimerization of a chimeric CD4-interferon-alpha receptor reconstitutes the signaling events preceding STAT phosphorylation. *Oncogene* 13(1):125–133.

285.   Li X, Leung S, Kerr IM, Stark GR (1997) Functional subdomains of STAT2 required for preassociation with the alpha interferon receptor and for signaling. *Mol Cell Biol* 17(4):2048–2056.

286.   Sakatsume M, et al. (1995) The Jak kinases differentially associate with the alpha and beta (accessory factor) chains of the interferon gamma receptor to form a functional receptor unit capable of activating STAT transcription factors. *Journal of Biological*

Chemistry 270(29):17528–17534.

287.   John J, et al. (1991) Isolation and characterization of a new mutant human cell line unresponsive to alpha and beta interferons. *Mol Cell Biol* 11(8):4189–4195.

288.   Fu XY, Kessler DS, Veals SA, Levy DE, Darnell JE (1990) ISGF3, the transcriptional activator induced by interferon alpha, consists of multiple interacting polypeptide chains. *Proc Natl Acad Sci U S A* 87(21):8555–8559.

289.   Kessler DS, Veals SA, Fu XY, Levy DE (1990) Interferon-alpha regulates nuclear translocation and DNA-binding affinity of ISGF3, a multimeric transcriptional activator. *Genes Dev* 4(10):1753–1765.

290.   Levy DE, Kessler DS, Pine R, Darnell JE (1989) Cytoplasmic activation of ISGF3, the positive regulator of interferon-alpha-stimulated transcription, reconstituted in vitro. *Genes Dev* 3(9):1362–1371.

291.   David M, et al. (1995) Requirement for MAP kinase (ERK2) activity in interferon alpha- and interferon beta-stimulated gene expression through STAT proteins. *Science* 269(5231):1721–1723.

292.   Chung CD, et al. (1997) Specific inhibition of Stat3 signal transduction by PIAS3. *Science* 278(5344):1803–1805.

293.   Pfeffer LM, et al. (1997) STAT3 as an adapter to couple phosphatidylinositol 3-kinase to the IFNAR1 chain of the type I interferon receptor. *Science* 276(5317):1418–1420.

294.   Nguyen KB, et al. (2002) Critical role for STAT4 activation by type 1 interferons in the interferon-gamma response to viral infection. *Science* 297(5589):2063–2066.

295.   Weinstein SL, et al. (2000) Phosphatidylinositol 3-kinase and mTOR mediate lipopolysaccharide-stimulated nitric oxide production in macrophages via interferon-beta. *J Leukoc Biol* 67(3):405–414.

296.   Kotenko SV, et al. (2003) IFN-lambdas mediate antiviral protection through a distinct class II cytokine receptor complex. *Nat Immunol* 4(1):69–77.

297.   Sheppard P, et al. (2003) IL-28, IL-29 and their class II cytokine receptor IL-28R. *Nat Immunol* 4(1):63–68.

298.   Dumoutier L, Tounsi A, Michiels T (2004) ... *Interleukin (IL)-28 Receptor Tyrosine Residues for Antiviral and Antiproliferative Activity of IL-29/Interferon-l1. SIMILARITIES WITH TYPE 1 INTERFERON* (Journal of Biological ...).

299.   Dumoutier L, Lejeune D, Hor S, Fickenscher H, Renauld J-C (2003) Cloning of a new type II cytokine receptor activating signal transducer and activator of transcription (STAT)1, STAT2 and STAT3. *Biochem J* 370(Pt 2):391–396.

300. Doyle SE, et al. (2006) Interleukin-29 uses a type 1 interferon-like program to promote antiviral responses in human hepatocytes. *Hepatology* 44(4):896–906.

301. Marcello T, et al. (2006) Interferons alpha and lambda inhibit hepatitis C virus replication with distinct signal transduction and gene regulation kinetics. *Gastroenterology* 131(6):1887–1898.

302. Velazquez L, Fellous M, Stark GR, Pellegrini S (1992) A protein tyrosine kinase in the interferon alpha/beta signaling pathway. *Cell* 70(2):313–322.

303. Watling D, et al. (1993) Complementation by the protein tyrosine kinase JAK2 of a mutant cell line defective in the interferon-gamma signal transduction pathway. *Nature* 366(6451):166–170.

304. Shuai K, Schindler C, Prezioso VR, Darnell JE (1992) Activation of transcription by IFN-gamma: tyrosine phosphorylation of a 91-kD DNA binding protein. *Science* 258(5089):1808–1812.

305. Shuai K, et al. (1994) Interferon activation of the transcription factor Stat91 involves dimerization through SH2-phosphotyrosyl peptide interactions. *Cell* 76(5):821–828.

306. Lew DJ, Decker T, Strehlow I, Darnell JE (1991) Overlapping elements in the guanylate-binding protein gene promoter mediate transcriptional induction by alpha and gamma interferons. *Mol Cell Biol* 11(1):182–191.

307. Papadopoulou AS, et al. (2011) The thymic epithelial microRNA network elevates the threshold for infection-associated thymic involution via miR-29a mediated suppression of the IFN-α receptor. *Nat Immunol* 13(2):181–187.

308. Lu L-F, et al. (2010) Function of miR-146a in controlling Treg cell-mediated regulation of Th1 responses. *Cell* 142(6):914–929.

309. Gracias DT, et al. (2013) The microRNA miR-155 controls CD8(+) T cell responses by regulating interferon signaling. *Nat Immunol* 14(6):593–602.

310. Gilchrist DA, et al. (2012) Regulating the regulators: the pervasive effects of Pol II pausing on stimulus-responsive gene networks. *Genes Dev* 26(9):933–944.

311. Endo TA, et al. (1997) A new protein containing an SH2 domain that inhibits JAK kinases. *Nature* 387(6636):921–924.

312. Yasukawa H, et al. (1999) The JAK-binding protein JAB inhibits Janus tyrosine kinase activity through binding in the activation loop. *EMBO J* 18(5):1309–1320.

313. Qing Y, Costa-Pereira AP, Watling D, Stark GR (2005) Role of tyrosine 441 of interferon-gamma receptor subunit 1 in SOCS-1-mediated attenuation of STAT1 activation. *Journal of Biological Chemistry* 280(3):1849–1853.

314. Fenner JE, et al. (2006) Suppressor of cytokine signaling 1 regulates the immune response to infection by a unique inhibition of type I interferon activity. *Nat Immunol* 7(1):33–39.

315. Kinjyo I, et al. (2002) SOCS1/JAB is a negative regulator of LPS-induced macrophage activation. *Immunity* 17(5):583–591.

316. Malakhov MP, Malakhova OA, Kim KI, Ritchie KJ, Zhang D-E (2002) UBP43 (USP18) specifically removes ISG15 from conjugated proteins. *Journal of Biological Chemistry* 277(12):9976–9981.

317. Malakhova OA, et al. (2006) UBP43 is a novel regulator of interferon signaling independent of its ISG15 isopeptidase activity. *EMBO J* 25(11):2358–2367.

318. Knobeloch K-P, Utermöhlen O, Kisser A, Prinz M, Horak I (2005) Reexamination of the role of ubiquitin-like modifier ISG15 in the phenotype of UBP43-deficient mice. *Mol Cell Biol* 25(24):11030–11034.

319. Osiak A, Utermöhlen O, Niendorf S, Horak I, Knobeloch K-P (2005) ISG15, an interferon-stimulated ubiquitin-like protein, is not essential for STAT1 signaling and responses against vesicular stomatitis and lymphocytic choriomeningitis virus. *Mol Cell Biol* 25(15):6338–6345.

320. Kim KI, et al. (2006) Ube1L and protein ISGylation are not essential for alpha/beta interferon signaling. *Mol Cell Biol* 26(2):472–479.

321. Atkins GJ (2012) The pathogenesis of alphaviruses. *ISRN Virology*.

322. Frolova EI, et al. (2002) Roles of nonstructural protein nsP2 and Alpha/Beta interferons in determining the outcome of Sindbis virus infection. *Journal of Virology* 76(22):11254–11264.

323. Yin JJ, Gardner CLC, Burke CWC, Ryman KDK, Klimstra WBW (2009) Similarities and differences in antagonism of neuron alpha/beta interferon responses by Venezuelan equine encephalitis and Sindbis alphaviruses. *Journal of Virology* 83(19):10036–10047.

324. Fros JJ, et al. (2010) Chikungunya virus nonstructural protein 2 inhibits type I/II interferon-stimulated JAK-STAT signaling. *Journal of Virology* 84(20):10877–10887.

325. Fros J, et al. (2010) Chikungunya virus nonstructural protein 2 is a potent inhibitor of JAK-STAT signaling. 128–128.

326. Simmons JD, et al. (2009) Venezuelan Equine Encephalitis Virus Disrupts STAT1 Signaling by Distinct Mechanisms Independent of Host Shutoff. *Journal of Virology* 83(20):10571–10581.

327. Simmons JD, Wollish AC, Heise MT (2010) A Determinant of Sindbis Virus Neurovirulence Enables Efficient Disruption of Jak/STAT Signaling. *Journal of*

Virology 84(21):11429–11439.

328. de Veer MJ, et al. (2001) Functional classification of interferon-stimulated genes identified using microarrays. *J Leukoc Biol* 69(6):912–920.

329. Schoggins JW, et al. (2012) A diverse range of gene products are effectors of the type I interferon antiviral response. *Nature* 472(7344):481–485.

330. Metz DH, Esteban M (1972) Interferon inhibits viral protein synthesis in L cells infected with vaccinia virus. *Nature* 238(5364):385–388.

331. Horisberger MA, Staeheli P, Haller O (1983) Interferon induces a unique protein in mouse cells bearing a gene for resistance to influenza virus. *Proc Natl Acad Sci U S A* 80(7):1910–1914.

332. Zürcher T, Pavlovic J, Staeheli P (1992) Mouse Mx2 protein inhibits vesicular stomatitis virus but not influenza virus. *Virology* 187(2):796–800.

333. Haller O, Frese M, Rost D, Nuttall PA, Kochs G (1995) Tick-borne thogoto virus infection in mice is inhibited by the orthomyxovirus resistance gene product Mx1. *Journal of Virology* 69(4):2596–2601.

334. Jin HK, et al. (2001) Mouse Mx2 protein inhibits hantavirus but not influenza virus replication. *Arch Virol* 146(1):41–49.

335. Lebleu B, Sen GC, Shaila S, Cabrer B, Lengyel P (1976) Interferon, double-stranded RNA, and protein phosphorylation. *Proc Natl Acad Sci U S A* 73(9):3107–3111.

336. Zilberstein A, Federman P, Shulman L, Revel M (1976) Specific phosphorylation in vitro of a protein associated with ribosomes of interferon-treated mouse L cells. *FEBS Letters* 68(1):119–124.

337. Clemens MJ, Williams BR (1978) Inhibition of cell-free protein synthesis by pppA2'p5'A2"p5"A: a novel oligonucleotide synthesized by interferon-treated L cell extracts. *Cell* 13(3):565–572.

338. Zhou A, Hassel BA, Silverman RH (1993) Expression cloning of 2-5A-dependent RNAase: a uniquely regulated mediator of interferon action. *Cell* 72(5):753–765.

339. Ryman KD, et al. (2005) Sindbis Virus Translation Is Inhibited by a PKR/RNase L-Independent Effector Induced by Alpha/Beta Interferon Priming of Dendritic Cells. *Journal of Virology* 79(3):1487–1499.

340. Zhang Y, Burke CW, Ryman KD, Klimstra WB (2007) Identification and Characterization of Interferon-Induced Proteins That Inhibit Alphavirus Replication. *Journal of Virology* 81(20):11246–11255.

341. Jiang DD, et al. (2008) Identification of three interferon-inducible cellular enzymes that

inhibit the replication of hepatitis C virus. *Journal of Virology* 82(4):1665–1678.

342. Jiang DD, et al. (2010) Identification of five interferon-induced cellular proteins that inhibit west nile virus and dengue virus infections. *Journal of Virology* 84(16):8332–8341.

343. Schoggins JW, et al. (2013) Pan-viral specificity of IFN-induced genes reveals new roles for cGAS in innate immunity. *Nature* 505(7485):691–695.

344. Gardner CLC, Yin JJ, Burke CWC, Klimstra WBW, Ryman KDK (2009) Type I interferon induction is correlated with attenuation of a South American eastern equine encephalitis virus strain in mice. *Virology* 390(2):338–347.

345. Gardner CL, Burke CW, Higgs ST, Klimstra WB, Ryman KD (2012) Interferon-alpha/beta deficiency greatly exacerbates arthritogenic disease in mice infected with wild-type chikungunya virus but not with the cell culture-adapted live-attenuated 181/25 vaccine candidate. *Virology* 425(2):103–112.

346. Ryman KD, Meier KC, Gardner CL, Adegboyega PA, Klimstra WB (2007) Non-pathogenic Sindbis virus causes hemorrhagic fever in the absence of alpha/beta and gamma interferons. *Virology* 368(2):13–13.

347. Schoggins JW, et al. (2013) Pan-viral specificity of IFN-induced genes reveals new roles for cGAS in innate immunity. *Nature*. doi:10.1038/nature12862.

348. Gao G, Guo X, Goff SP (2002) Inhibition of retroviral RNA production by ZAP, a CCCH-type zinc finger protein. *Science* 297(5587):1703–1706.

349. Guo X, Carroll JWN, MacDonald MR, Goff SP, Gao G (2004) The Zinc Finger Antiviral Protein Directly Binds to Specific Viral mRNAs through the CCCH Zinc Finger Motifs. *Journal of Virology* 78(23):12781–12787.

350. MacDonald MR, Machlin ES, Albin OR, Levy DE (2007) The zinc finger antiviral protein acts synergistically with an interferon-induced factor for maximal activity against alphaviruses. *Journal of Virology* 81(24):13509–13518.

351. Karki S, et al. (2012) Multiple interferon stimulated genes synergize with the zinc finger antiviral protein to mediate anti-alphavirus activity. *PLoS ONE* 7(5):e37398.

352. Teng T-S, et al. (2012) Viperin restricts chikungunya virus replication and pathology. *J Clin Invest* 122(12):4447–4460.

353. Lenschow DJ, et al. (2005) Identification of interferon-stimulated gene 15 as an antiviral molecule during Sindbis virus infection in vivo. *Journal of Virology* 79(22):13974–13983.

354. Werneke SW, et al. (2011) ISG15 is critical in the control of Chikungunya virus infection independent of UbE1L mediated conjugation. *PLoS Pathog* 7(10):e1002322.

355.   Zhao C, Denison C, Huibregtse JM, Gygi S, Krug RM (2005) Human ISG15 conjugation targets both IFN-induced and constitutively expressed proteins functioning in diverse cellular pathways. *Proc Natl Acad Sci U S A* 102(29):10200–10205.

356.   Lu G, et al. (2006) ISG15 enhances the innate antiviral response by inhibition of IRF-3 degradation. *Cell Mol Biol (Noisy-le-grand)* 52(1):29–41.

357.   Shi H-X, et al. (2010) Positive regulation of interferon regulatory factor 3 activation by Herc5 via ISG15 modification. *Mol Cell Biol* 30(10):2424–2436.

358.   Arimoto K-I, Konishi H, Shimotohno K (2008) UbcH8 regulates ubiquitin and ISG15 conjugation to RIG-I. *Mol Immunol* 45(4):1078–1084.

359.   Durfee LA, Lyon N, Seo K, Huibregtse JM (2010) The ISG15 conjugation system broadly targets newly synthesized proteins: implications for the antiviral function of ISG15. *Mol Cell* 38(5):722–732.

360.   Li MMH, et al. (2017) TRIM25 Enhances the Antiviral Action of Zinc-Finger Antiviral Protein (ZAP). *PLoS Pathog* 13(1):e1006145.

361.   Gack MU, et al. (2007) TRIM25 RING-finger E3 ubiquitin ligase is essential for RIG-I-mediated antiviral activity. *Nature* 446(7138):916–920.

362.   Atasheva S, Akhrymuk M, Frolova EI, Frolov I (2012) New PARP gene with an anti-alphavirus function. *Journal of Virology* 86(15):8147–8160.

363.   Atasheva S, Frolova EI, Frolov I (2014) Interferon-stimulated poly(ADP-Ribose) polymerases are potent inhibitors of cellular translation and virus replication. *Journal of Virology* 88(4):2116–2130.

364.   Reynaud JM, et al. (2015) IFIT1 Differentially Interferes with Translation and Replication of Alphavirus Genomes and Promotes Induction of Type I Interferon. *PLoS Pathog* 11(4):e1004863.

365.   Jones PH, et al. (2013) BST-2/tetherin-mediated restriction of chikungunya (CHIKV) VLP budding is counteracted by CHIKV non-structural protein 1 (nsP1). *Virology* 438(1):37–49.

366.   Poddar S, Hyde JL, Gorman MJ, Farzan M, Diamond MS (2016) The Interferon-Stimulated Gene IFITM3 Restricts Infection and Pathogenesis of Arthritogenic and Encephalitic Alphaviruses. *Journal of Virology* 90(19):8780–8794.

367.   Gad HH, et al. (2012) The E2-E166K substitution restores Chikungunya virus growth in OAS3 expressing cells by acting on viral entry. *Virology* 434(1):27–37.

368.   Chebath J, Merlin G, Metz R, Benech P, Revel M (1983) Interferon-induced 56,000 Mr protein and its mRNA in human cells: molecular cloning and partial sequence of the cDNA. *Nucleic Acids Res* 11(5):1213–1226.

369. Kusari J, Sen GC (1987) Transcriptional analyses of interferon-inducible mRNAs. *Mol Cell Biol* 7(1):528–531.

370. Levy D, Larner A, Chaudhuri A, Babiss LE, Darnell JE (1986) Interferon-stimulated transcription: isolation of an inducible gene and identification of its regulatory region. *Proc Natl Acad Sci U S A* 83(23):8929–8933.

371. Wathelet M, et al. (1986) Molecular cloning, full-length sequence and preliminary characterization of a 56-kDa protein induced by human interferons. *Eur J Biochem* 155(1):11–17.

372. Bluyssen HA, et al. (1994) Structure, chromosome localization, and regulation of expression of the interferon-regulated mouse Ifi54/Ifi56 gene family. *Genomics* 24(1):137–148.

373. Lee CG, Demarquoy J, Jackson MJ, O'Brien WE (1994) Molecular cloning and characterization of a murine LPS-inducible cDNA. *J Immunol* 152(12):5758–5767.

374. Niikura T, Hirata R, Weil SC (1997) A novel interferon-inducible gene expressed during myeloid differentiation. *Blood Cells Mol Dis* 23(3):337–349.

375. Yu M, et al. (1997) Cloning of a gene (RIG-G) associated with retinoic acid-induced differentiation of acute promyelocytic leukemia cells and representing a new member of a family of interferon-stimulated genes. *Proc Natl Acad Sci U S A* 94(14):7406–7411.

376. Zhu H, Cong JP, Shenk T (1997) Use of differential display analysis to assess the effect of human cytomegalovirus infection on the accumulation of cellular RNAs: induction of interferon-responsive RNAs. *Proc Natl Acad Sci U S A* 94(25):13985–13990.

377. de Veer MJ, Sim H, Whisstock JC, Devenish RJ, Ralph SJ (1998) IFI60/ISG60/IFIT4, a new member of the human IFI54/IFIT2 family of interferon-stimulated genes. *Genomics* 54(2):267–277.

378. Der SD, Zhou A, Williams BR, Silverman RH (1998) Identification of genes differentially regulated by interferon alpha, beta, or gamma using oligonucleotide arrays. *Proc Natl Acad Sci U S A* 95(26):15623–15628.

379. Darnell JE, Kerr IM, Stark GR (1994) Jak-STAT pathways and transcriptional activation in response to IFNs and other extracellular signaling proteins. *Science* 264(5164):1415–1421.

380. Bandyopadhyay SK, Leonard GT, Bandyopadhyay T, Stark GR, Sen GC (1995) Transcriptional induction by double-stranded RNA is mediated by interferon-stimulated response elements without activation of interferon-stimulated gene factor 3. *Journal of Biological Chemistry* 270(33):19624–19629.

381. Elco CP, Guenther JM, Williams BRG, Sen GC (2005) Analysis of genes induced by Sendai virus infection of mutant cell lines reveals essential roles of interferon regulatory

factor 3, NF-kappaB, and interferon but not toll-like receptor 3. *Journal of Virology* 79(7):3920–3929.

382. Sarkar SN, Sen GC (2004) Novel functions of proteins encoded by viral stress-inducible genes. *Pharmacology & Therapeutics* 103(3):245–259.

383. Grandvaux N, et al. (2002) Transcriptional profiling of interferon regulatory factor 3 target genes: direct involvement in the regulation of interferon-stimulated genes. *Journal of Virology* 76(11):5532–5539.

384. Sarkar SN, et al. (2004) Novel roles of TLR3 tyrosine phosphorylation and PI3 kinase in double-stranded RNA signaling. *Nat Struct Mol Biol* 11(11):1060–1067.

385. Ogawa S, et al. (2005) Molecular determinants of crosstalk between nuclear receptors and toll-like receptors. *Cell* 122(5):707–721.

386. Terenzi F, Hui DJ, Merrick WC, Sen GC (2006) Distinct induction patterns and functions of two closely related interferon-inducible human genes, ISG54 and ISG56. *Journal of Biological Chemistry* 281(45):34064–34071.

387. D'Andrea LD, Regan L (2003) TPR proteins: the versatile helix. *Trends in Biochemical Sciences* 28(12):655–662.

388. Fensterl V, Sen GC (2011) The ISG56/IFIT1 gene family. *Journal of Interferon & Cytokine Research* 31(1):71–78.

389. Fensterl V, Sen GC (2015) Interferon-induced Ifit proteins: their role in viral pathogenesis. *Journal of Virology* 89(5):2462–2468.

390. Hui DJ, Terenzi F, Merrick WC, Sen GC (2005) Mouse p56 blocks a distinct function of eukaryotic initiation factor 3 in translation initiation. *Journal of Biological Chemistry* 280(5):3433–3440.

391. Terenzi F, Pal S, Sen GC (2005) Induction and mode of action of the viral stress-inducible murine proteins, P56 and P54. *Virology* 340(1):116–124.

392. Wang C, et al. (2003) Alpha interferon induces distinct translational control programs to suppress hepatitis C virus RNA replication. *Journal of Virology* 77(7):3898–3912.

393. Terenzi F, Saikia P, Sen GC (2008) Interferon-inducible protein, P56, inhibits HPV DNA replication by binding to the viral protein E1. *EMBO J* 27(24):3311–3321.

394. Li Y, et al. (2009) ISG56 is a negative-feedback regulator of virus-triggered signaling and cellular antiviral response. *Proceedings of the National Academy of Sciences* 106(19):7945–7950.

395. Pichlmair A, et al. (2011) IFIT1 is an antiviral protein that recognizes 5′-triphosphate RNA. *Nature Publishing Group* 12(7):624–630.

396. Habjan M, et al. (2013) Sequestration by IFIT1 impairs translation of 2'O-unmethylated capped RNA. *PLoS Pathog* 9(10):e1003663.

397. Abbas YM, Pichlmair A, Górna MW, Superti-Furga G, Nagar B (2013) Structural basis for viral 5'-PPP-RNA recognition by human IFIT proteins. *Nature* 494(7435):60–64.

398. Kumar P, et al. (2014) Inhibition of translation by IFIT family members is determined by their ability to interact selectively with the 5"-terminal regions of cap0-, cap1- and 5"ppp- mRNAs. *Nucleic Acids Res* 42(5):3228–3245.

399. Gongora C, et al. (1997) Molecular cloning of a new interferon-induced PML nuclear body-associated protein. *Journal of Biological Chemistry* 272(31):19457–19463.

400. Nguyen LH, Espert L, Mechti N, Wilson DM (2001) The human interferon- and estrogen-regulated ISG20/HEM45 gene product degrades single-stranded RNA and DNA in vitro. *Biochemistry* 40(24):7174–7179.

401. Horio T, et al. (2004) Crystal structure of human ISG20, an interferon-induced antiviral ribonuclease. *FEBS Letters* 577(1-2):111–116.

402. Gongora C, Degols G, Espert L, Hua TD, Mechti N (2000) A unique ISRE, in the TATA-less human Isg20 promoter, confers IRF-1-mediated responsiveness to both interferon type I and type II. *Nucleic Acids Res* 28(12):2333–2341.

403. Espert L, et al. (2004) The exonuclease ISG20 is directly induced by synthetic dsRNA via NF-kappaB and IRF1 activation. *Oncogene* 23(26):4636–4640.

404. Espert L, et al. (2006) The exonuclease ISG20 mainly localizes in the nucleolus and the Cajal (Coiled) bodies and is associated with nuclear SMN protein-containing complexes. *J Cell Biochem* 98(5):1320–1333.

405. Espert L (2003) ISG20, a New Interferon-induced RNase Specific for Single-stranded RNA, Defines an Alternative Antiviral Pathway against RNA Genomic Viruses. *Journal of Biological Chemistry* 278(18):16151–16158.

406. Espert L, et al. (2005) Interferon-induced exonuclease ISG20 exhibits an antiviral activity against human immunodeficiency virus type 1. *J Gen Virol* 86(Pt 8):2221–2229.

407. Hao Y, Yang D (2008) Cloning, eukaryotic expression of human ISG20 and preliminary study on the effect of its anti-HBV. *J Huazhong Univ Sci Technolog Med Sci* 28(1):11–13.

408. Katsounas A, et al. (2014) Interferon stimulated exonuclease gene 20 kDa links psychiatric events to distinct hepatitis C virus responses in human immunodeficiency virus positive patients. *J Med Virol* 86(8):1323–1331.

409. Qu H, et al. (2016) Influenza A Virus-induced expression of ISG20 inhibits viral replication by interacting with nucleoprotein. *Virus Genes*:1–9.

410. Leong CR, et al. (2016) Interferon-stimulated gene of 20 kDa protein (ISG20) degrades RNA of Hepatitis B virus to impede the replication of HBV in vitro and in vivo. *Oncotarget* 5(0). doi:10.18632/oncotarget.11907.

411. Zhou Z, et al. (2011) Antiviral activities of ISG20 in positive-strand RNA virus infections. *Virology* 409(2):175–188.

412. Andersen J, VanScoy S, Cheng T-F, Gomez D, Reich NC (2007) IRF-3-dependent and augmented target genes during viral infection. *Genes Immun* 9(2):168–175.

413. Dai L, et al. (2016) Transcriptomic analysis of KSHV-infected primary oral fibroblasts: The role of interferon-induced genes in the latency of oncogenic virus. *Oncotarget* 7(30):47052–47060.

414. Taylor KL, et al. (2008) Identification of interferon-beta-stimulated genes that inhibit angiogenesis in vitro. *J Interferon Cytokine Res* 28(12):733–740.

415. Carmo-Fonseca M, Pepperkok R, Carvalho MT, Lamond AI (1992) Transcription-dependent colocalization of the U1, U2, U4/U6, and U5 snRNPs in coiled bodies. *J Cell Biol* 117(1):1–14.

416. Platani M, Goldberg I, Lamond AI, Swedlow JR (2002) Cajal body dynamics and association with chromatin are ATP-dependent. *Nat Cell Biol* 4(7):502–508.

417. Machyna M, Heyn P, Neugebauer KM (2013) Cajal bodies: where form meets function. *Wiley Interdiscip Rev RNA* 4(1):17–34.

418. Platani M, Goldberg I, Swedlow JR, Lamond AI (2000) In vivo analysis of Cajal body movement, separation, and joining in live human cells. *J Cell Biol* 151(7):1561–1574.

419. Jacobs EY, et al. (1999) Coiled bodies preferentially associate with U4, U11, and U12 small nuclear RNA genes in interphase HeLa cells but not with U6 and U7 genes. *Mol Biol Cell* 10(5):1653–1663.

420. Smith KP, Carter KC, Johnson CV, Lawrence JB (1995) U2 and U1 snRNA gene loci associate with coiled bodies. *J Cell Biochem* 59(4):473–485.

421. Gao L, Frey MR, Matera AG (1997) Human genes encoding U3 snRNA associate with coiled bodies in interphase cells and are clustered on chromosome 17p11.2 in a complex inverted repeat structure. *Nucleic Acids Res* 25(23):4740–4747.

422. Schul W, Adelaar B, van Driel R, de Jong L (1999) Coiled bodies are predisposed to a spatial association with genes that contain snoRNA sequences in their introns. *J Cell Biochem* 75(3):393–403.

423. Frey MR, Bailey AD, Weiner AM, Matera AG (1999) Association of snRNA genes with coiled bodies is mediated by nascent snRNA transcripts. *Curr Biol* 9(3):126–135.

424.   Smith KP, Lawrence JB (2000) Interactions of U2 gene loci and their nuclear transcripts with Cajal (coiled) bodies: evidence for PreU2 within Cajal bodies. *Mol Biol Cell* 11(9):2987–2998.

425.   Frey MR, Matera AG (2001) RNA-mediated interaction of Cajal bodies and U2 snRNA genes. *J Cell Biol* 154(3):499–509.

426.   Filipowicz W, Pogacić V (2002) Biogenesis of small nucleolar ribonucleoproteins. *Curr Opin Cell Biol* 14(3):319–327.

427.   Sleeman JE, Lamond AI (1999) Newly assembled snRNPs associate with coiled bodies before speckles, suggesting a nuclear snRNP maturation pathway. *Curr Biol* 9(19):1065–1074.

428.   Jády BEB, et al. (2003) Modification of Sm small nuclear RNAs occurs in the nucleoplasmic Cajal body following import from the cytoplasm. *EMBO J* 22(8):1878–1888.

429.   Nesic D, Tanackovic G, Krämer A (2004) A role for Cajal bodies in the final steps of U2 snRNP biogenesis. *Journal of Cell Science* 117(Pt 19):4423–4433.

430.   Stanek D, et al. (2008) Spliceosomal small nuclear ribonucleoprotein particles repeatedly cycle through Cajal bodies. *Mol Biol Cell* 19(6):2534–2543.

431.   Boulon S, et al. (2004) PHAX and CRM1 are required sequentially to transport U3 snoRNA to nucleoli. *Mol Cell* 16(5):777–787.

432.   Pradet-Balade B, et al. (2011) CRM1 controls the composition of nucleoplasmic pre-snoRNA complexes to licence them for nucleolar transport. *EMBO J* 30(11):2205–2218.

433.   Samarsky DA, Fournier MJ, Singer RH, Bertrand E (1998) The snoRNA box C/D motif directs nucleolar targeting and also couples snoRNA synthesis and localization. *EMBO J* 17(13):3747–3757.

434.   Richard P, et al. (2003) A common sequence motif determines the Cajal body-specific localization of box H/ACA scaRNAs. *EMBO J* 22(16):4283–4293.

435.   Narayanan A, Speckmann W, Terns R, Terns MP (1999) Role of the box C/D motif in localization of small nucleolar RNAs to coiled bodies and nucleoli. *Mol Biol Cell* 10(7):2131–2147.

436.   Jády BE, Bertrand E, Kiss T (2004) Human telomerase RNA and box H/ACA scaRNAs share a common Cajal body-specific localization signal. *J Cell Biol* 164(5):647–652.

437.   Venteicher AS, et al. (2009) A human telomerase holoenzyme protein required for Cajal body localization and telomere synthesis. *Science* 323(5914):644–648.

438.   Tomlinson RL, Li J, Culp BR, Terns RM, Terns MP (2010) A Cajal body-independent

pathway for telomerase trafficking in mice. *Exp Cell Res* 316(17):2797–2809.

439. Schneider WM, Chevillotte MD, Rice CM (2014) Interferon-stimulated genes: a complex web of host defenses. *Annu Rev Immunol* 32(1):513–545.

440. Ooi Y, Dubé M, Kielian M (2015) BST2/Tetherin Inhibition of Alphavirus Exit. *Viruses 2015, Vol 7, Pages 2147-2167* 7(4):2147–2167.

441. Weston S, et al. (2016) Alphavirus Restriction by IFITM Proteins. *Traffic* 17(9):997–1013.

442. Jackson RJ, Hellen CUT, Pestova TV (2010) The mechanism of eukaryotic translation initiation and principles of its regulation. 1–15.

443. Reis LF, Ho Lee T, Vilcek J (1989) Tumor necrosis factor acts synergistically with autocrine interferon-beta and increases interferon-beta mRNA levels in human fibroblasts. *Journal of Biological Chemistry* 264(28):16351–16354.

444. Liu Y, et al. (2017) Interferon-inducible ribonuclease ISG20 inhibits hepatitis B virus replication through directly binding to the epsilon stem-loop structure of viral RNA. *PLoS Pathog* 13(4):e1006296.

445. Stanek DD, Neugebauer KMK (2006) The Cajal body: a meeting place for spliceosomal snRNPs in the nuclear maze. *Chromosoma* 115(5):343–354.

446. Morris GE (2008) The Cajal body. *Biochimica et Biophysica Acta (BBA) - Molecular Cell Research* 1783(11):2108–2115.

447. Morrison TE, et al. (2011) A mouse model of chikungunya virus-induced musculoskeletal inflammatory disease: evidence of arthritis, tenosynovitis, myositis, and persistence. *Am J Pathol* 178(1):32–40.

448. WEISS HJ, HALSTEAD SB, RUSS SB (1965) HEMORRHAGIC DISEASE IN RODENTS CAUSED BY CHIKUNGUNYA VIRUS. 1. STUDIES OF HEMOSTASIS. *Proc Soc Exp Biol Med* 119:427–432.

449. Klimstra WB, Ryman KD, Johnston RE (1998) Adaptation of Sindbis virus to BHK cells selects for use of heparan sulfate as an attachment receptor. *Journal of Virology* 72(9):7357–7366.

450. Morrison TE (2014) Reemergence of chikungunya virus. *Journal of Virology* 88(20):11644–11647.

451. Bréhin A-C, et al. (2009) The large form of human 2′,5′-Oligoadenylate Synthetase (OAS3) exerts antiviral effect against Chikungunya virus. *Virology* 384(1):216–222.

452. Schilte C, et al. (2010) Type I IFN controls chikungunya virus via its action on nonhematopoietic cells. *Journal of Experimental Medicine* 207(2):429–442.

453. Rudd PA, et al. (2012) Interferon Response Factors 3 and 7 Protect against Chikungunya Virus Hemorrhagic Fever and Shock. *Journal of Virology* 86(18):9888–9898.

454. Kolb SJ, Battle DJ, Dreyfuss G (2007) Molecular Functions of the SMN Complex. *Journal of Child Neurology* 22(8):990–994.

455. Ro-Choi TS (1999) Nuclear snRNA and Nuclear Function (Discovery of 5′ Cap Structures in RNA). *CRE* 9(2):107–158.

456. Mroczek S, Dziembowski A (2013) U6 RNA biogenesis and disease association. *Wiley Interdiscip Rev RNA* 4(5):581–592.

457. Kunkel GR, Maser RL, Calvet JP, Pederson T (1986) U6 small nuclear RNA is transcribed by RNA polymerase III. *Proc Natl Acad Sci U S A* 83(22):8575–8579.

458. Dunn EA, Rader SD (2010) Secondary structure of U6 small nuclear RNA: implications for spliceosome assembly. *Biochem Soc Trans* 38(4):1099–1104.

459. Jiang F, et al. (2011) Structural basis of RNA recognition and activation by innate immune receptor RIG-I. *Nature* 479(7373):423–427.

460. Wang C, Marcotrigiano J, Miller M, Jiang F (2016) Crystal structure of RIG-I in complex with Cap-0 RNA. doi:10.2210/pdb5f98/pdb.

461. Sharma S, et al. (2003) Triggering the interferon antiviral response through an IKK-related pathway. *Science* 300(5622):1148–1151.

462. Lin R, Heylbroeck C, Pitha PM, Hiscott J (1998) Virus-dependent phosphorylation of the IRF-3 transcription factor regulates nuclear translocation, transactivation potential, and proteasome-mediated degradation. *Mol Cell Biol* 18(5):2986–2996.

463. Long L, et al. (2014) Recruitment of phosphatase PP2A by RACK1 adaptor protein deactivates transcription factor IRF3 and limits type I interferon signaling. *Immunity* 40(4):515–529.

464. Ponting CP, Oliver PL, Reik W (2009) Evolution and functions of long noncoding RNAs. *Cell* 136(4):629–641.

465. Hung T, Chang HY (2010) Long noncoding RNA in genome regulation: prospects and mechanisms. *RNA Biol* 7(5):582–585.

466. Keren H, Lev-Maor G, Ast G (2010) Alternative splicing and evolution: diversification, exon definition and function. *Nat Rev Genet* 11(5):345–355.

467. Tsetsarkin K, et al. (2006) Infectious clones of Chikungunya virus (La Réunion isolate) for vector competence studies. *Vector Borne Zoonotic Dis* 6(4):325–337.

468. Anishchenko M, et al. (2004) Generation and characterization of closely related

epizootic and enzootic infectious cDNA clones for studying interferon sensitivity and emergence mechanisms of Venezuelan equine encephalitis virus. *Journal of Virology* 78(1):1–8.

469.   White LJ, Wang JG, Davis NL, Johnston RE (2001) Role of alpha/beta interferon in Venezuelan equine encephalitis virus pathogenesis: effect of an attenuating mutation in the 5' untranslated region. *Journal of Virology* 75(8):3706–3718.

470.   Aguilar PV, et al. (2008) Structural and nonstructural protein genome regions of eastern equine encephalitis virus are determinants of interferon sensitivity and murine virulence. *Journal of Virology* 82(10):4920–4930.

471.   Meijer HA, et al. (2013) Translational Repression and eIF4A2 Activity Are Critical for MicroRNA-Mediated Gene Regulation. *Science* 340(6128):82–85.

472.   Noah DL, Blum MA, Sherry B (1999) Interferon regulatory factor 3 is required for viral induction of beta interferon in primary cardiac myocyte cultures. *Journal of Virology* 73(12):10208–10213.

473.   Trapnell C, et al. (2012) Differential gene and transcript expression analysis of RNA-seq experiments with TopHat and Cufflinks. *Nat Protoc* 7(3):562–578.

474.   Ho PS, Ng MML, Chu JJH (2010) Establishment of one-step SYBR green-based real time-PCR assay for rapid detection and quantification of chikungunya virus infection. *Virology Journal* 7(1):13.

475.   Trapnell C, et al. (2013) Differential analysis of gene regulation at transcript resolution with RNA-seq. *Nat Biotechnol* 31(1):46–53.